MAX-PLANCK-INSTITUT
FÜR MOLEKULARE PHYSIOLOGIE

technische universität
dortmund

Mass spectrometric analysis of small-molecule-induced ubiquitination and deubiquitination

Dissertation

zur Erlangung des akademischen Grades

Doktorin der Naturwissenschaften

(Dr. rer. nat.)

Der Fakultät der Chemie und Chemischen Biologie der
Technischen Universität Dortmund

vorgelegt von

Siska Führer, M.Sc.

Geboren am 29. Juni 1998 in Cuxhaven

Dortmund, den 4. November 2025

Die vorliegende Dissertation wurde im Zeitraum von April 2022 bis November 2025 unter der Anleitung von Prof. Dr. Dr. h.c. Herbert Waldmann und Dr. Malte Gersch an der Technischen Universität Dortmund, Fakultät für Chemie und Chemische Biologie, dem Chemical Genomics Centre der Max-Plack-Gesellschaft und dem Max-Plack-Institut für molekulare Physiologie Dortmund verfasst.

1. Gutachter: Prof. Dr. Dr. h. c. Herbert Waldmann
2. Gutachter: Dr. Malte Gersch

Die in dieser Dissertation enthaltenen Ergebnisse sind Teil der folgenden Publikationen:

S. Führer, K. Gallant, F. Kaschani, M. Kaiser, P. Janning, H. Waldmann, M. Gersch. Small Molecule-Induced Alterations of Protein Polyubiquitination Revealed by Mass-Spectrometric Ubiquitome Analysis. *Angew. Chem. Int. Ed.* 2025, 64, e202508916. https://doi.org/10.1002/anie.202508916[1]

K. Wendrich, K. Gallant, S. Recknagel, S. Petroulia, N. H. Kazi, J. A. Hane, **S. Führer**, K. Bezstarosti, R. O'Dea, J. Demmers, M. Gersch. Discovery and mechanism of K63-linkage-directed deubiquitinase activity in USP53. *Nat Chem Biol* (2024). https://doi.org/10.1038/s41589-024-01777-0[2]

Die in dieser Dissertation enthaltenen Ergebnisse sind außerdem Teil der Bachelorarbeit von Sarah Ballmann, deren Arbeit zum Kapitel 4.2.3.1 dieser Dissertation beigetragen haben:

Sarah Ballmann, „Validierung des Einflusses kleiner Moleküle auf die Polyubiquitinierung von Proteinen“, 2025, Technische Universität Dortmund

Daria Bezbakh hat durch Unterstützung der Experimente in Kapitel 4.2.2.1 und 4.2.2.2 im Rahmen ihres Forschungsmoduls zu dieser Dissertation beigetragen.

Celine Da Cruz Lopes Guita hat durch Unterstützung der Experimente in Kapitel 4.2.4 zu dieser Dissertation beigetragen.

> *„Die besten Doktoranden sind am Ende die, die sowieso machen, was sie wollen.“*
> Prof. Dr. Dr. h.c. Herbert Waldmann (2022)

Table of Contents

1. Summary

The therapeutic targeting of the ubiquitin system is a steadily growing field in chemical biology. As PROTACs, molecular glue degraders, and deubiquitinase inhibitors enter clinical applications, the need to reliably detect small molecules altering protein ubiquitination is emerging. At the same time, there is a lack of methods for the unbiased and broad screening of small molecules for their ability to target the ubiquitin system.

This thesis describes the establishment of a mass-spectrometric method to detect changes in the cellular polyubiquitome upon treatment of mammalian cells with different small molecules.

The envisioned assay design involves the enrichment of polyubiquitinated proteins from cell lysate using a tandem ubiquitin binding entity, followed by an acidic elution step, the digestion of the polyubiquitome, the labeling of the gained peptides using multiplexing by tandem mass tags, and their analysis by LC-MS/MS.

The identification of the optimal assay conditions involved the implementation of semi-denaturing lysis and washing conditions, the choice of biotin as the immobilization tag on streptavidin magnetic beads, and an acidic elution step to reduce background signals.

In a first application case, the resulting assay platform was used to show the enrichment of PROTAC target proteins from cells with inhibited proteasome. As this was successful, the method further demonstrated its versatility in the context of an intact proteasome and deubiquitinase inhibitors by displaying several literature-reported deubiquitinase substrates being changed in their polyubiquitination. Furthermore, UBE3A showed increased polyubiquitination upon USP7 inhibition, in a non-degradative manner.

Finally, applying the method to uncharacterized research compounds from a monovalent degrader derivative library against IDO1 and three members of a newly established proteasome cluster from a phenotypic screen showed the versatility and quality of the assay to recognize subtle changes in protein polyubiquitination. Collectively, the enrichment of polyubiquitinated proteins coupled to mass spectrometry provides a valuable addition to the repertoire of proteomics-based methods for the discovery and characterization of small molecules targeting the ubiquitin system.

Zusammenfassung

Die therapeutische Adressierung des Ubiquitin-Systems ist ein stetig wachsender Bereich in der chemischen Biologie. Da sich PROTACs, Molecular-Glue-Degrader und Deubiquitinase-Inhibitoren der klinischen Anwendung nähern, entsteht der Bedarf, kleine Moleküle, die die Protein-Ubiquitinierung beeinflussen, zuverlässig nachzuweisen. Gleichzeitig mangelt es an Methoden für ein unvoreingenommenes und umfassendes Screening kleiner Moleküle hinsichtlich ihrer Fähigkeit, das Ubiquitin-System zu beeinflussen.

Diese Arbeit beschreibt die Etablierung einer massenspektrometrischen Methode zum Nachweis von Veränderungen im zellulären Polyubiquitom nach Behandlung von Säugetierzellen mit verschiedenen kleinen Molekülen. Das vorgesehene Assay-Design beinhaltet die Anreicherung von polyubiquitinierten Proteinen aus Zelllysat unter Verwendung einer Tandem-Ubiquitin-Bindedomäne, gefolgt von einem sauren Elutionsschritt, der Verdauung des Polyubiquitoms, der Markierung der resultierenden Peptide mittels Multiplexing durch Tandem-Mass-Tags und ihrer Analyse durch LC-MS/MS. Die Identifizierung der optimalen Assay-Bedingungen umfasste die Implementierung von semi-denaturierenden Lyse- und Waschbedingungen, die Wahl von Biotin zur Immobilisierung auf magnetischen Streptavidin-Beads und einen sauren Elutionsschritt zur Reduzierung von Hintergrundsignalen durch unmodifizierte Proteine.

In einem ersten Anwendungs-Experiment wurde die Assay-Plattform verwendet, um die Anreicherung von PROTAC-Zielproteinen aus Zellen mit inhibiertem Proteasom nachzuweisen. Da dies erfolgreich war, wurde die Methode weitergehend auf ihre Vielseitigkeit im Zusammenhang mit einem intakten Proteasom und Deubiquitinase-Inhibitoren getestet, indem sie mehrere in der Literatur beschriebene Deubiquitinase-Substrate aufzeigte, deren Polyubiquitinierung verändert war. Darüber hinaus zeigte UBE3A bei USP7-Inhibition eine erhöhte Polyubiquitinierung, ohne dass es zu einem Abbau des Proteins kam.

Schließlich zeigte die Anwendung der Methode auf uncharakterisierte Forschungsverbindungen aus einer Bibliothek monovalenter Degrader-Derivate gegen IDO1 und drei Mitglieder eines neu etablierten Proteasom-Clusters aus einem phänotypischen Screening die Vielseitigkeit und Qualität des Assays, auch geringfügige Veränderungen in der Protein-Polyubiquitinierung zu erkennen. Insgesamt stellt die Anreicherung von polyubiquitinierten Proteinen in Verbindung mit Massenspektrometrie eine wertvolle Ergänzung des Repertoires proteomikbasierter Methoden zur Entdeckung und Charakterisierung kleiner Moleküle dar, die auf das Ubiquitin-System abzielen.

2. Introduction

2.1 The chemical biology of discovering bioactive small molecules

The persistent demand for effective treatments of human diseases has contributed to the steady development of new therapeutic agents. These molecules have substantiated their value through consistent innovation, as evidenced by the continuous emergence of novel discoveries and the approval of new applications in human medicine. A notable illustration of this significance is evidenced by the fact that 32 out of 50 (64%) of the FDA-approved drugs in 2024 were small molecules, underscoring their critical role in the pharmaceutical landscape[3].

There is no doubt that the discovery of novel small-molecule therapeutics relies on the chemical biology that enables these innovations with a variety of unbiased or targeted, phenotypic or activity-based methods. Traditionally, the pharmaceutical industry mainly follows a rational approach for preclinical drug discovery starting from the identification of a therapeutically relevant biological target, leading via great library screening campaigns to lead discovery and its optimization towards a safe and efficient drug[4]. On the other hand, there are also completely unbiased approaches, which start from phenotypically characterizing a small molecule's effect on human cells, which only then leads to the identification of the small molecule's target[5]. This Phenotypic Drug Discovery (PDD) has the advantage over Target-based Drug Discovery (TDD) that the underlying biological process does not need to be fully understood in order to demonstrate efficacy, which in turn may lead to new insights into the biological mechanisms and pathways affected by the drug. TDD however allows for an immediate connection between substance activity and biological function, which is based on a wide range of activity-based assays. However, the success of TDD in contrast to PDD is considerably low, with only around 9 % of approved drugs being discovered by TDD[6]. The compromise between the two approaches is to use both to maximize the efficiency of drug discovery[5]. For the finding of an enzyme inhibitor, a single phenotypic screen (e.g. the cell painting assay or a viability screen) may be sufficient to answer the question if the small molecule has biological relevance. From this starting point onwards, it might be beneficial for the further characterization of the small molecule to unravel its enzyme target by testing it in activity-based assays (e.g. in a respective enzyme product formation assay)[5]. Since the majority of approved small molecules work according to the so-called occupancy-based mode of action (e.g. enzyme inhibitors), a huge pipeline of these activity-based discovery methods has co-evolved[4]. However, this tailoring excludes a large fraction of the proteome from being

druggable because the potential targets in this group often lack active centers, substrate binding domains, or ordered cavities[4]. In order to surmount this limitation, the field of medicinal chemistry has recently undergone significant advancements, leading to the exploration of alternative modes of action. These include the interruption of protein-protein interactions[7], the development of covalent inhibitors[8] and the hijacking of the ubiquitination machinery within cells for the purpose of targeted protein degradation and beyond, irrespective of their biological function[9,10]. Given the ubiquitin system's substantial capacity to expand the druggable proteome, in conjunction with the lack of methodologies for identifying small molecules that interfere with it, this thesis will concentrate on investigating the influence of small molecules on the ubiquitin system.

2.2 Ubiquitin and the ubiquitin proteasome system

Ubiquitin (Ub) is a small protein (76 amino acids) with a molecular weight of approximately 8 kDa. Four human genes - namely, *UBB, UBC, UBA52*, and *RPS27A/UBA80* - encode ubiquitin[11]. It is notable that *UBB* and *UBC* contain three and nine ubiquitin units in sequential order; conversely, *UBA52* and *RPS27A/UBA80* encode a single ubiquitin-bound ribosomal subunit[11]. Ub contains a C-terminal glycine that enables covalent attachment to protein lysine residues via an isopeptide bond and is one of the largest posttranslational modifications that proteins can bear[12]. Despite the simplicity of this transfer, the process of ubiquitination is precisely tuned and reversible. This is achieved by the ubiquitination cascade consisting of three different classes of enzymes, namely the E1 (ubiquitin activating), E2 (ubiquitin conjugating) and E3 (ubiquitin ligating) families of enzymes[13]. In humans, eight E1s are responsible for the initiation of conjugation of ubiquitin-like modifiers (UBL), with two of them (UBA1 and UBA6) being specialized, canonical E1s for ubiquitin[14]. Their catalysis is initiated by the binding of the respective E1 enzyme to ATP, Mg^{2+} and ubiquitin, which subsequently leads to the C-terminal acyl adenylation of the small protein. The catalytic cysteine of the E1 then forms an activated complex with ubiquitin via a thioester bond[14]. Afterwards, the charged E1 is then transferring ubiquitin onto one of the at least 38 human E2 enzymes, which finally synergize with E3 enzymes to transfer ubiquitin onto the target protein (see Figure 1A)[15]. It is noteworthy that, compared to the few members of E1 and E2 enzymes that are encoded by the human genome, E3 enzymes feature more than 600 members, which lays the basis for the huge precision and variety of ubiquitin conjugation[14-16]. The two biggest groups

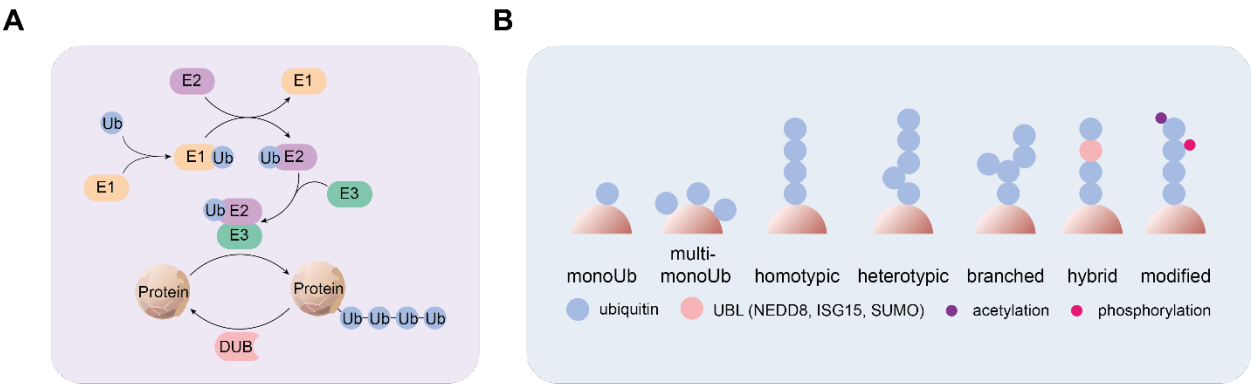

Figure 1: *Creation and architecture of ubiquitination.* ***A.*** *Schematic representation of the ubiquitination machinery.* ***B.*** *Ubiquitination and ubiquitin chain composition. Panel* ***B*** *is inspired by Swatek, K. N. & Komander, D. Cell Res (2016).*

within the E3 ligase family are built by HECT and RING ligases[15,16]. HECT E3s receive ubiquitin from E2s and build up thioester intermediates with the Ub itself, whereas RING ligases work rather modular and bind E2s via their name-giving domain, which finally allows for a supramolecular assembly of multiple proteins including the ubiquitin target, enabling its ubiquitination[15,16]. This fine-tuned system allows for a complex signaling language build-up on ubiquitin, starting from mono- to multi-mono-ubiquitination, via linear homotypic, to heterotypic or even branched chains (see Figure 1B)[12,13]. This variety of chain architecture is not only derived from the diverse conjugating machineries, but also by ubiquitin's ability to become conjugated onto its own siblings via its seven surface-accessible lysines (K6, K11, K27, K29, K33, K48, K63) or its N-terminus (M1, see Figure 2A)[13]. Recently, even hybrid chains were introduced, which can contain other UBLs such as NEDD8, SUMO or ISG15 alongside ubiquitin[17]. Finally, as for other proteins, ubiquitin's lysine residues can be further modified by acetylation, giving even more complexity to the ubiquitin code[13]. This multifaceted language does not come without a purpose. Ubiquitination plays a role in almost every process of a eukaryotic cell. The best-studied one is the mediation of protein degradation. Polyubiquitination of a target protein, mainly linked via K48, leads to the shuttling of the target to the proteasome, where the polypeptide is unfolded and chopped into smaller peptides, whereas ubiquitin is recycled[18]. Although this responsibility of ubiquitin is the most prominent and abundant, given that many proteins become degraded via this pathway after reaching the end of their lifetime, it is not the sole function (see Figure 2B). Monoubiquitination alone is enough to trigger the internalization of cell-surface receptors or to control transcription via histone ubiquitination[19,20]. Linear M1 chains positively affect NF-κB-signaling and serve as scaffolding chains in innate immune response, whereas K6-ubiquitin play an important role in mitophagy[13,21]. K11 and K29 ubiquitination is connected to cell cycle control, with K29 also playing a role in epigenetic regulation and proteotoxic stress[13,22]. K27 and K63 ubiquitination are involved

in DNA damage response and K33- and K63-linked ubiquitin chains facilitate intracellular trafficking[13,23,24]. As soon as these diverse codes are written, it needs readers to decipher them. This function is taken by ubiquitin-binding proteins, which themselves mediate the downstream effects of the individual ubiquitin chains[24]. All so-called ubiquitin receptors have in common that they possess distinct ubiquitin binding domains (UBDs), which can be divided into different classes e.g. alpha-helices, zinc fingers or PH-folds[24]. Although single UBDs possess only weak

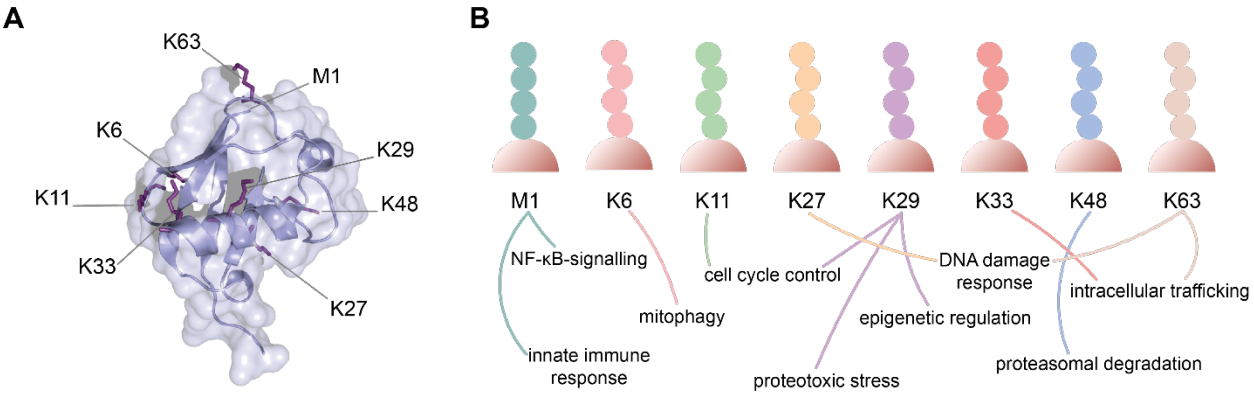

Figure 2: *Ubiquitin chains have different topologies linked to their physiological function.* ***A****. Structure of Ubiquitin with its seven Lysines and Methionine residues being highlighted. Structure is based on PDB entry 5GOI.* ***B****. The different homotypically linked ubiquitin chains and examples of their function in cells. This scheme was inspired by Swatek, K. N. & Komander, D. Cell Res (2016).*

affinity to ubiquitin, their interaction with poly-Ub, oligomerization, or simultaneous interactions with other PTMs create tightly controlled, high-affinity interactions with ubiquitinated proteins under physiological conditions[25]. With their UBDs, the reader proteins enable all known functions of ubiquitin signaling[26]. This includes, for example, the transport of ubiquitinated proteins to the proteasome[26]. In yeast, this role is taken over by proteins such as Dsk2p and Rap23p, whereas in humans, proteins like ZNF216 perform this function[26]. Furthermore, UBD proteins such as EPS15, TSG10 or HRS facilitate the sorting of ubiquitinated proteins in endocytosis[26]. In DNA repair mechanisms involving ubiquitinated proteins, such as PCNA, the recruitment of DNA polymerases, such as POLH, is enabled by their UBDs[26]. This emphasizes the importance of UBDs in maintaining complex Ub signaling beyond degradation. Like ubiquitination itself, the function of UBD proteins has to be regulated in order to maintain cellular homeostasis[27]. Early studies in 2007 investigating UBD-containing proteins revealed that Ub receptors are capable of regulating themselves by recruiting E2 enzymes and undergoing monoubiquitination independently of E3 ligases[27]. The resulting modifications influence the activity and localization of the respective UBD protein[27].

Apart from their physiological function, ubiquitin reader proteins and their UBDs are utilized in recombinantly expressed fusion proteins to facilitate ubiquitin enrichment. Quite commonly used for ubiquitin enrichment tools are alpha-helices, which themselves are divided into the two groups of ubiquitin-associated domains (UBA) and ubiquitin-interacting motifs (UIM)[24]. An example for a protein containing a UBA is the Alzheimer-associated protein Ubiquilin-1, which has a role in trafficking to the proteasome and clearance of misfolded proteins[28,29]. Chapter 2.5.1 discusses the specific advantages of UBDs in terms of ubiquitin enrichment further.

The specific and complex system of ubiquitin architecture and readers would soon be rendered ineffective if the modification on target proteins were to remain permanent. It is therefore essential to cell homeostasis that ubiquitination is a reversible modification. This is achieved by the so-called "erasers of the ubiquitin code": the deubiquitinases (DUBs).

2.3 Deubiquitinases (DUBs)

Similar to ubiquitin ligases and ubiquitin reader proteins, deubiquitinases consist of multiple classes and families[30]. The majority of DUBs have been identified as members of the family of cysteine proteases, though some have been found to be metalloproteases[30]. The classification system for human DUBs has been further subdivided into seven families, including Josefins, ubiquitin-specific proteases (USPs), ubiquitin C-terminal hydrolases (UCHs), Ovarian tumor proteases (OTUs), MINDYs, ZUP1 and JAMMs, whereby only the last are zinc metalloproteases (see Figure 3A)[30,31]. Despite the structural diversity observed among these enzymes, all have

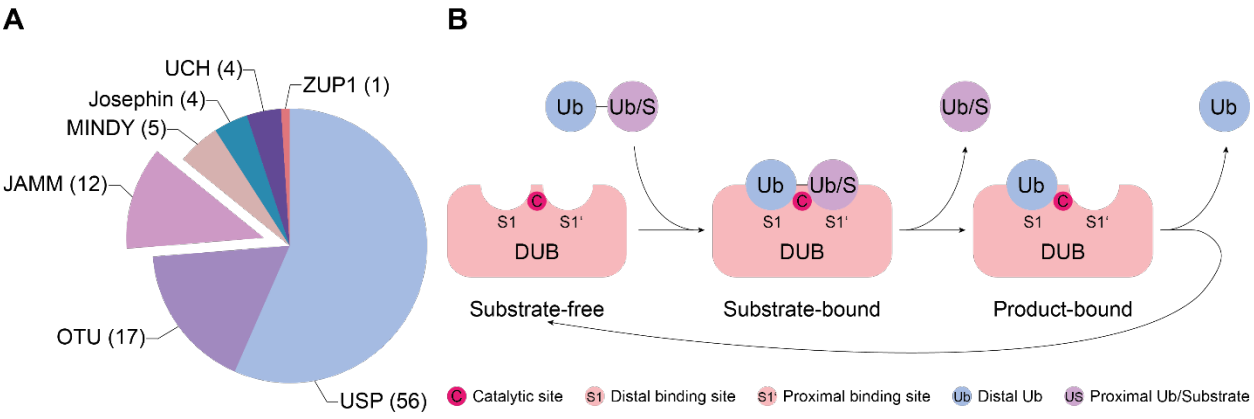

***Figure 3**: The class of deubiquitinating enzymes contains different families with distinct catalytic function. **A**. Pie chart of different families of DUBs with the number of members indicated in brackets. **B**. Schematic representation of the catalytic mechanism of ubiquitin cleavage of cysteine deubiquitinases. Panel **B** was adapted from Lange, S. M., Armstrong, L. A. & Kulathu, Y., Mol Cell (2022).*

been shown to interact with ubiquitin via a common hydrophobic patch, ensuring their substrate recognition[30].

Though their structure may drastically vary in length and domain composition, all DUBs catalyze the hydrolysis of the Ub-Ub/substrate isopeptide bond by coordinating the ubiquitinated protein via an S1 and, in many cases, an S1' binding pockets on each site of their catalytic center[30,32]. During the transition from its substrate-free to its substrate-bound state, the DUB binds the so-called distal ubiquitin in S1, whereas the proximal ubiquitin (the one that is conjugated to the distal ubiquitin via one of its lysine residues) or the ubiquitinated protein get bound in the S1' site (see Figure 3B)[32]. Following the hydrolysis catalyzed by the DUB, the S1'-bound proteins dissociate and the DUB transitions to its third state, the product-bound state, in which ubiquitin is bound in S1 alone[32]. This process subsequently leads to the attainment of the substrate-free state through the dissociation of Ub, thereby resuming the catalytic cycle[32]. This seemingly common catalysis cycle should not distract from the high degree of specialization towards different protein substrates or chain types DUBs have. While some DUBs are specifically removing mono-Ub from defined substrates (e.g. USP3 and USP22 from histones), other deubiquitinases exert high selectivity towards certain chain types and lengths[31]. Examples are the DUBs Cezanne and USP30, which selectively cleave K11- and K6-Ub chains respectively[31]. TRABID can cleave K29 and K33 chains, while USP14 is able to remove complete chains from substrates *en bloc*[31,33].

Given the many roles that ubiquitin fulfils in the cell, it is crucial that ubiquitin signaling is tightly controlled and stopped when no longer required. It is thus not surprising that also deubiquitinases are involved in many cellular pathways, that exceed the simple counteraction of E3-ligases[31]. An examination of the most fundamental functions of deubiquitinases reveals their role in the stabilization of polyubiquitinated proteins. This stabilization process involves the rescue of these proteins from proteasomal degradation[31]. In contrast, they are essential for an economical degradation of proteins by the proteasome, as DUBs such as RPN11, USP14 and UCHL5, which are bound to the proteasome ensure that ubiquitin is cut off from their target proteins, before they get unfolded and degraded[31,34]. DUBs such as USP5 are essential to generate a free ubiquitin pool, firstly enabling Ub-conjugation after its expression in repeats from *UBB* and *UBC*[31]. As ubiquitin is involved in DNA damage response, DUBs as USP22, USP48 and OTUB1 act as crucial counterparts in these pathways to regulate the repair of double-strand breaks[31]. Apart from their role in Ub signaling, deubiquitinases can also act on other UBLs such as NEDD8, whose conjugation on neddylation-dependent E3 ligases is a key regulator of these enzymes[35]. Consequently, COPS5, which is a member of the JAMM metallo-DUBs, removes NEDD8 from

these Cullin-RING E3s, finely regulating their activity[35]. Finally, DUBs are involved in pathways related to innate immune response, mitophagy, protein trafficking, cell proliferation and many more[31].

Upon elucidating the stringent regulation of the ubiquitin system by deubiquitinases, the sensitivity of these networks to manipulation or abnormalities becomes evident. Thus, mutations or dysregulations of DUBs are connected to severe diseases.

One of the most evident and well-studied relevancies of deubiquitinases in malign contexts is their role in cancer[36]. Where DUBs fail to regulate cancer targets, whether through dysregulation of their activity or mutations, cancer patients often face poor prognosis[36]. As such, USP22 is encoded by one of the "death-from-cancer" genes, regulating cancer-driving proteins such as MYC and FBP1[36]. It is also part of the SAGA complex, which regulates transcription by histone H2A and H2B deubiquitination[36]. USP7, on the other hand, is known to be involved in cancer progression through deubiquitination of MDM2, thereby affecting p53 tumor suppression[37]. One example of a mutation in DUBs that cause cancer is the UCH-member BRCA1-associated protein 1 (BAP1), which has been connected to multiple cancer types like mesothelioma and cutaneous melanoma[36,38,39]. Apart from their relevance in tumor development, DUBs could play a role in cardiac diseases, as USP10 was found to be connected to heart fibrosis in a diabetes mouse model[40]. Finally, DUBs are also relevant in the context of infectious diseases and parasites[41-43]. Specifically, DUBs from invading species, such as *Legionella pneumophila* bacteria can stabilize their own injected proteins, which become ubiquitinated by the host organism, consequently counteracting the innate immune system of the human cell [41,42]. The multifaceted roles that deubiquitinases fulfil in malignant processes have led to several clinical trials investigating the therapeutic potential of inhibiting DUBs. At the moment, three DUBs are under clinical investigation to study their inhibition by small molecules. The role of USP1 in DNA damage response is exploited by its inhibitor, KSQ-4279, which is in phase 1 trials for the treatment of solid tumors with mutations in the homologous recombination repair mechanisms[44]. Inhibiting USP28 has shown promise in the treatment of Burkitt lymphoma, resulting in the preclinical trial of CT1113, an inhibitor targeting the deubiquitinase[45]. Finally, USP30 inhibition by the small molecule MTX652 is under clinical investigation for the treatment of acute kidney injury[46].

The presented examples underscore the significance of deubiquitinases and the intricate functions of the ubiquitin system in health and disease. This emphasizes the appeal of targeting these enzymes, thereby expanding the druggable proteome to encompass E3 ligases, deubiquitinases, and their downstream effector proteins[37,47].

2.4 Small molecules as modulators of the ubiquitin system

Due to their complexity in structure and regulation, the exploration of the druggable proteome in the ubiquitin system and the UPS offers many possibilities to interfere with them at different stages. Until today, medicinal chemistry brought up several small molecules targeting the proteasome, E3-ligases and deubiquitinases (see Figure 4)[48]. One of the most broad and drastic interference with the UPS is given by the inhibition of the proteasome by small molecules, leading to the persistence of proteins, which would otherwise be degraded by the big protease complex[49]. Consequently, polyubiquitinated proteins accumulate inside of the cell, which not only stops the steady degradation of the targets, but also decreases the size of the cellular free ubiquitin pool due to the lacking recycling of ubiquitin by proteasomal deubiquitinases[50]. Overall, proteasomal inhibition was found to lead to apoptosis of cancer cells, which paved the way for the first generation of proteasome inhibitors to be used as anti-cancer therapeutics[49]. The first-in-class example of this small molecule family is bortezomib, a boronic acid peptide analog that reversibly binds to the 20S subunit of the proteasome, primarily the chymotrypsin-like protease (see Figure 5)[49]. The effect of bortezomib on multiple myeloma and mantle cell lymphoma cells was so effective that it led to the approval of bortezomib for the salvage treatment of these cancers in 2003[49,51]. Following this success, proteasomal inhibitors became established for further cancers treatments. Another approved member of this mode-of-action family is carfilzomib, which is a chemical analogue of the natural product proteasome inhibitor epoxomicin and binds irreversibly to the 20S proteasome[52]. With the optimization of the epoxyketone epoxomicin to an epoxyketo-morpholine, Craig Crews and colleagues established carfilzomib, which was approved for multiple myeloma treatment, even of bortezomib-resistant patients in 2012[49,52].

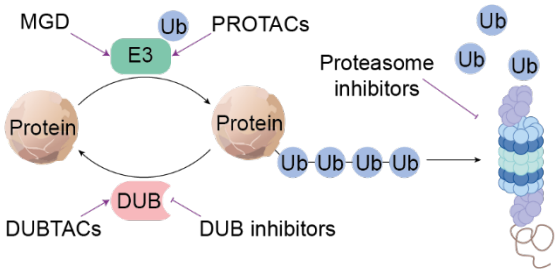

Figure 4: *Different strategies to interfere with the ubiquitin system therapeutically and their respective target point of action.*

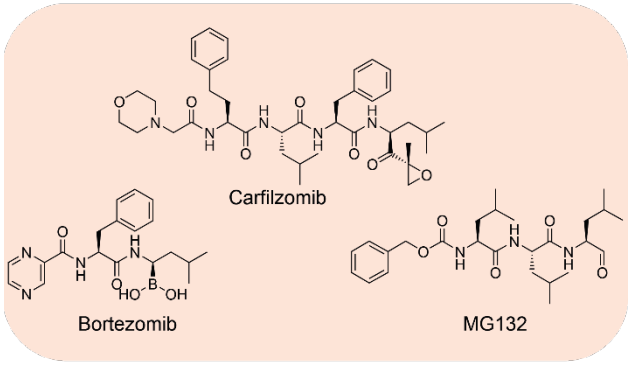

Figure 5: *Structures of representative examples of proteasome inhibitors.*

Apart from their clinical use, proteasome inhibitors also serve as tool compounds for cell biology[53]. In addition to rather unspecific inhibitors of the proteasome such as 3,4-dichloroisocoumarin or the more specific lactacystins, peptide-boronates and -vinyl sulfones, peptide aldehydes such as MG132 (see Figure 5) are highly-selective molecules to study the influence of proteasomal inhibition on eukaryotic cells[53]. MG132 is an reversible inhibitor, primarily binding to the chymotrypsin-like active site of the 20S proteasome with nanomolar potency[53].

In general, proteasome inhibitors have proven to be effective agents in targeting the ubiquitin-proteasome system (UPS), albeit as a rather drastic approach. Beyond their initial application in clinical settings and *in vitro* studies, there has been a growing trend in the utilization of these molecules in combination with other treatments, particularly in dual therapeutic regimens[49]. In the clinic, the use of bortezomib and carfilzomib together with so-called molecular glue degraders (MGDs) such as lenalidomide and pomalidomide emerges for the treatment of myeloma (see Figure 7)[49]. Simultaneously, proteasomal inhibition is crucial for the identification of novel degrader molecules and the investigation of their underlying mechanisms of degradation in rescue experiments, whether they are PROTACs or MGDs.

2.4.1 Molecular glue degraders

One of the most significant scandals in the annals of pharmaceuticals was precipitated by the sedative drug "Contergan," which was introduced by Grünenthal in 1956[54]. The biologically active component of this drug, thalidomide, was found to induce severe developmental defects in newborns, resulting in tragic consequences for numerous families[54-56]. It was not until 2010, several decades later, that the off target of the drug was identified and it took until 2013 to elucidate the underlying mechanism responsible for these severe side effects[57,58]. Lenalidomide, a derivative of thalidomide, was found to cause a *de novo* interaction between the transcription factors IKZF1/2 and CRBN, which is part of an E3 ligase[57,59,60]. This

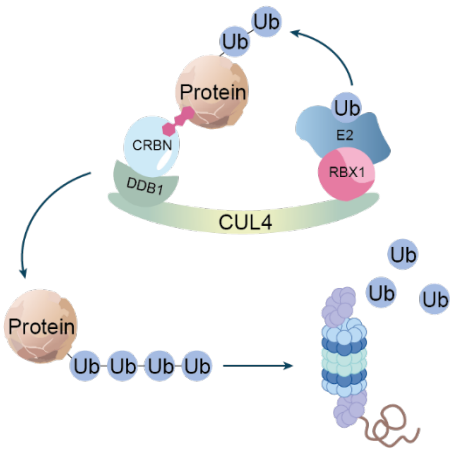

Figure 6: *Schematic representation of the mechanism of induced ubiquitination of* de novo *targets by molecular glue degraders utilizing the CRBN E3 ligase.*

lenalidomide-induced proximity between the two components results in a polyubiquitination of the transcription factors and their downstream degradation (see Figure 6)[57]. Until that point, the concept had only been described in the context of natural regulation of plant hormone degradation[61,62]. Together with this finding, thalidomide and its derivatives, the so-called immunomodulatory imide drugs (IMiDs) led to the establishment of the field of molecular glue degraders, which, despite their unfortunate history, holds significant promise for therapeutic applications[62]. In contrast to classical inhibitors, which are limited to catalytically active proteins, molecular glue degraders (MGDs) cause the removal of their target proteins by hijacking the UPS, without the need of impeding target protein activity or catalytic function, therefore expanding the druggable proteome[62]. At the same time, a sole MGD molecule has the capacity to induce the degradation of multiple target proteins, thereby giving them catalytic activity[57,60,62]. This phenomenon stands in contrast to the action of the majority of classical inhibitors, which necessitate the attainment of at least equimolar concentrations to adequately inhibit protein function[63]. It is therefore no surprise that lenalidomide and its derivatives soon became rebranded as an effective therapeutic for the treatment of cancers such as multiple myeloma[59,62]. Fueled by this success, novel small molecules with the same mode of action (MoA) were discovered. One structurally different MGD subclass are sulfonamides, such as indisulam, which was found to effectively degrade RBM39 (see Figure 7)[64,65]. Other approaches utilized the identification of the glutarimide moiety of IMiDs as the CRBN-binding entity for further derivatization towards degradation of other target proteins[59,66]. One of the most prominent glutarimide-containing MGDs targeting beyond the classical IMiD-related proteins is FPFT-2216, which is inducing the depletion of the small phosphodiesterase PDE6D next to the typical IMiD targets (see Figure 7)[66,67]. Until today, the discovery of molecular glue degraders has undergone a transition from coincidence towards rational drug discovery, mainly by utilizing glutarimids as a lead starting point[66]. This “degradation by design” concept is even more common for another class of small molecules causing targeted protein degradation, which emerged in parallel to MGDs and has several structural overlaps with them: the so-called proteolysis-targeting chimeras (PROTACs).

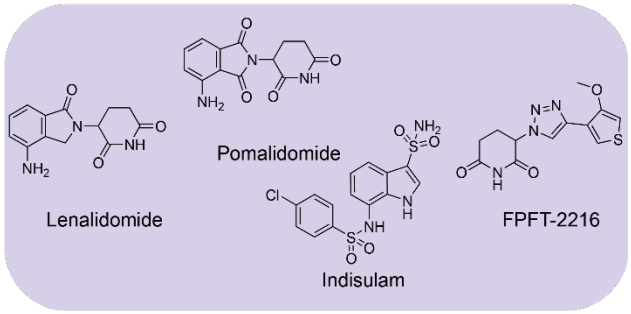

Figure 7: *Structures of representative examples of molecular glue degraders (MGDs).*

2.4.2 PROTACs

The approach of a chemical knockdown of proteins did not emerge with the discovery of molecular glue degraders. The concept of proximity induction between E3 ligases and yet targetable proteins was introduced in 2001 by a bivalent linkage of a protein binder to a peptidic Skp1-Cullin1 E3 ligase recruiter[68]. Seven years later, scientists at Yale university introduced the first small-molecule PROTAC[69]. Their idea involved a heterobifunctional molecule which, on one side, recruits the androgen receptor via a selective androgen receptor modulator (SARM) and, on the other side, binds to the E3 ligase MDM2 via a nutlin-moiety (imidazole), causing the ubiquitination and downstream degradation of the androgen receptor[69]. Both active parts of the molecule were linked via a PEG3-linker, yielding the first-in-class androgen receptor PROTAC SARM-nutlin (see Figure 8)[69]. With this innovation, novel small-molecules with the same MoA emerged. Soon, the recruitment of other E3 ligases became possible, with the most prominent ones being the ligases von Hippel-Lindau (VHL) and, in parallel to the discovery of IMiD MGDs, cereblon (CRBN)[70]. One extensively studied PROTAC is MZ1 (see Figure 8), which recruits VHL on its thiazole side, and Bromodomain-containing proteins (BRDs) 2, 3, and 4 on its diazepine side, causing their selective degradation with the result of a chemical knockdown[71]. dBET1, a PROTAC causing the same cellular effect, on the other hand utilizes CRBN via a pomalidomide derivative for ubiquitination, while having the same target BRD proteins[72]. The basis for the target protein recruitment in these PROTACs is the same inhibitor of BRDs, JQ1, which was published before and became a scaffold for the conjugation to the different E3-binders (see Figure 8)[71,72]. Until the present day, the majority of PROTAC development is based on rational design, commencing from these VHL and CRBN ligase binders[73,74]. However, it should be noted that these binders only cover a minute portion of the approximately 600 human E3 ligases that remain to be targeted by PROTACs[73,74]. Compared to molecular glue degraders, PROTACs can be much more easily designed and synthesized due

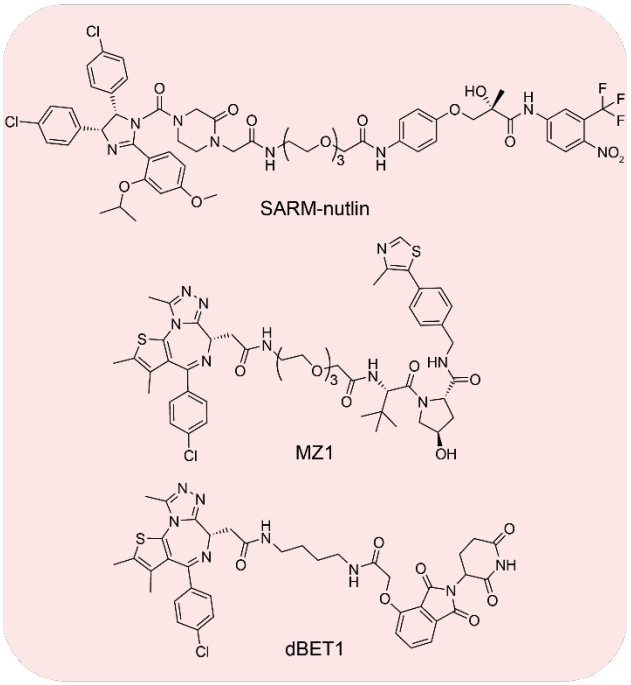

Figure 8: *Structures of representative examples of Proteolysis targeting chimeras (PROTACs).*

to their modular structure[62]. However, they suffer from the so-called *hook effect*, which is described as the oversaturation of bound protein partners by the small molecule, preventing the bivalent induction of proximity between target protein and E3 ligase[74]. Another crucial aspect of the design of PROTACs is the linker connecting the E3 ligase binding moiety with the substrate recruiter[75]. Since the linker length and polarity of PROTAC linkers is crucial for their degradation efficiency, past approaches mainly empirically solved the so-called “linkerology”-problem[75]. Latest chemical approaches however tried to rationalize the design of PROTACs further by introducing increased-throughput methods, such as solid phase synthesis, copper-catalyzed click reactions or Staudinger ligations[75]. Together with the generally bivalent structure of the resulting molecules, PROTACs are, compared to molecular glues, a rather modular assembly of available components from the medicinal chemistry toolbox and way easier to establish, resulting in more candidates with a broader variety of target proteins being under clinical investigation compared to MGDs[62]. This perk, however, comes at the price of a higher molecular weight and permeability issues, which usually are less critical for MGDs[62,75,76]. Another aspect that differentiates PROTACs from molecular glue degraders is their binding kinetics[62]. While MGDs modify the molecular surface of their target proteins (either degraded protein or E3 ligase), facilitating the *de novo* interaction between both, PROTACs form a rather equal bivalent interaction [62,76]. A prerequisite for this MoA is the existence of a target protein binder, which itself requires the presence of ligandable pockets or surfaces on the protein, which in many cases is based on existing inhibitors[62]. Although this can be seen as a drawback in terms of expanding the druggable proteome, it also offers the possibility of therapeutic benefits between degradation and target inhibition, as many PROTACs retain the inhibitory activity of their parent molecules[62]. Taken together, PROTACs and MGDs offer complementary concepts in targeted protein degradation, but with this exert a synergistic effect for efficient targeting of the ubiquitin proteasome system for therapeutic applications. While these two classes of therapeutics share the same point of interference with the UPS, a completely different MoA was emerging with the idea of targeting the counterpart of E3 ligases, the deubiquitinases (DUBs).

2.4.3 DUB inhibitors and DUB-targeting chimeras

Deubiquitinases regulate many cellular mechanisms and act as erasing enzymes for the ubiquitin code written by the ubiquitin ligase machinery (see section 2.3). As an inhibition of one DUB can lead to the affection of many (disease relevant) target proteins, it is therefore intuitive to target them therapeutically. This endeavor, however, can be challenging, since many DUBs, especially the cysteine proteases among them, share high structural homology, which could affect the selectivity of the developed inhibitors[32,77]. It was therefore necessary to address DUBs at different structural elements, which enabled a sorting of DUB inhibitors into different classes[32]. This classification divides DUB inhibitors into catalytic site-binding (either in active or inactive conformation), Ub binding site-binding (either S1, S1' or other), Co-factor-competitive binding or bivalent inhibitors[32]. One of the pioneering compounds in the class of DUB inhibitors, the aryl-thiocyanate PR-619, addressed many DUBs by catalytic site-binding and thus serves as a tool compound to suppress general DUB activity (see Figure 9)[78]. Only some years later, inhibition of deubiquitinases flourished and several USP-specific inhibitors were established, including candidates for the family members USP7, USP25/28 and USP30[79-82]. Today, the discovery of novel DUB inhibitors and the determination of their selectivity is increasingly facilitated by several high-throughput screening methods and activity-based assays[82-84]. This coevolution has led to the emergence of DUB inhibitors as attractive targets also for the pharmaceutical industry, which developed bioactive substances for members of the USP family, e.g. USP21[85]. One of the best-characterized compounds in this field is FT671, which targets USP7 with sub-µM potency and outstanding selectivity among other DUBs (see Figure 9)[86]. Other attempts addressed deubiquitinases, whose central functions are so broad that their inhibition leads to global changes in the UPS, as it is the case for IU1-47, which is targeting the proteasome-bound USP14 (see Figure 9)[87]. IU1-47 increases proteasome activity and consequently was found to induce Alzheimer-disease-relevant tau-protein degradation in neurons[87,88]. Finally, also members of other DUB families could successfully be targeted by small molecules. One example is the UCHL1 inhibitor GK13S (see Figure 9), which was the tool and parent compound for the further optimization towards UCHL1-selective inhibitors[89,90].

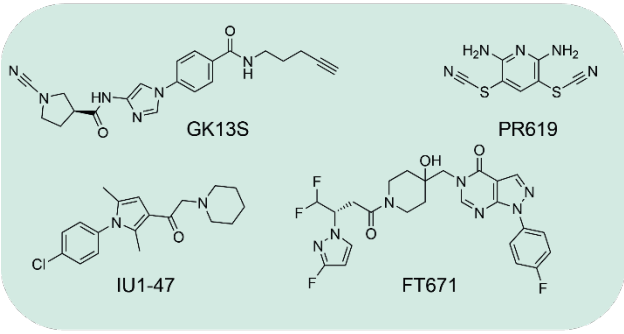

***Figure 9**: Structures of representative examples of deubiquitinase inhibitors.*

With the emergence of the PROTAC technology, it also became desirable to degrade DUBs in order to interfere not only with their target deubiquitination, but also with their non-enzymatic functions, such as complex formation[32]. One of the first successful implications of DUB PROTACs was achieved for USP7 by recruiting CRBN towards the deubiquitinating enzyme[91]. Since this recruitment was performed by using a well-established USP7 inhibitor core scaffold, a prevalent concern of DUB targeted protein degradation (TPD) could be circumvented, namely that the DUB can deubiquitinate itself once processed by the E3 ligase[32,91].

In the context of the application of chimeric molecules to the recruitment of deubiquitinases, an orthogonal approach to the induced ubiquitination by E3 ligases becomes evident. This approach involves the recruitment of proteins to DUBs with the objective of removing their ubiquitin chains and thereby stabilizing them or, in general, silencing their Ub-signaling. The results of this methodology are so-called deubiquitinase-targeting chimeras (DUBTACs)[92]. Similar to the PROTAC approach, DUBTACs do not require an inhibiting molecule of the targeted deubiquitinase to successfully recruit another protein. Instead, for the successful stabilization of a ubiquitinated protein by a deubiquitinase, it is essential that DUB-function is not impaired, which is why pioneering studies in this field focused on identifying allosteric DUB-binders first[92]. This yielded the discovery of a DUBTAC recruiting the deubiquitinase OTUB1 towards a mutant of the cystic fibrosis-linked ion channel CFTR, improving the ion channel conductance and thus proving therapeutic relevance of the DUBTAC approach[92]. Further elaborations of the concept expanded towards the recruitment of OTUB1 to other disease-relevant proteins such as the tumor suppressor p53[93]. Recently, it became possible to also engage other DUBs into the ternary complex without losing their catalytic activity, which was demonstrated by the non-covalent DUBTACs targeting USP7 and CFTR or AMPK[93].

All these examples show the impressive therapeutic potential that lies in targeting deubiquitinases, either by impeding their catalytic function using small molecule inhibitors or by hijacking their catalytic activity for impairing their Ub-signaling in a complementary approach using DUBTACs. Addressing DUBs with small molecules provides another addition to the attractiveness of the ubiquitin system for therapeutic applications or even the fundamental understanding of cellular processes. It is therefore inherent that the investigation of the UPS requires solid methodologies, which are versatile in their application scope.

2.5 Strategies to probe the ubiquitin system

With the complexity of the ubiquitin system involving E1-3 enzymes, ubiquitin reading and binding proteins and deubiquitinases comes the need for a variety of methods that allow for the investigation of the related processes at all of their stages. The basis of the UPS, the creation of ubiquitination can be reconstituted *in vitro* by combining the protein of interest (POI) with all necessary components of the ubiquitination machinery in order to show a potential connection between an E3-ligase and a hypothetical target[94]. Furthermore, this approach has also proven to be a powerful tool to show the neddylation-dependency of E3 ligases[95]. However, it is only a limited indication for the actual ubiquitination happening natively in cells. Complementary approaches involving proximity labeling of E3 ligase substrates by expressing the respective E3 as fusion protein with the ligase BirA for biotinylation allowed for a more unbiased identification of the interaction landscape of the Ub-conjugating machineries by mass spectrometry[96].

To answer the fundamental question, if a protein acts catalytically on ubiquitin, the system of activity-based probes (ABPs) became well-established[97,98]. This involves the semi-synthetic equipment of ubiquitin with a reactive group, such as a vinyl-sulfone (VS) or a halogen-substituted alkyl chain in order to covalently capture the DUB or E-enzyme while acting on it[99]. While these approaches mainly cover proteins equipped with a catalytic cysteine, they become versatile in not only an observed size-shift in SDS-PAGE or a visualization with fluorophore-labeled ubiquitin, but also are suitable tools to compete with potential inhibitors of Ub-catalytic activity, e.g. in deubiquitinases[97-99]. Further evolution of Ub probes involved the linkage to fluorophores like TAMRA via an isopeptide bond, allowing for the monitoring of Ub-cleavage kinetics of DUBs via a fluorescence-polarization-based read-out[100].

The proteasome plays a distinct role in UPS investigations, as it lacks catalytic activity towards Ub itself apart from its removal from target proteins by the metallo-DUB RPN11 as part of the 19S assembly[101]. Nevertheless, it still performs the most prevalent function of the UPS: protein degradation. While Ub-ABPs are not suitable for the investigation of proteasome function, several methods were designed based on proteasome reactivity against substrates[98]. The well-established default method for measuring 26S proteasome activity is the utilization of short peptides, which are linked to fluorophores like 7-amino-4-methylcoumarin (AMC)[98]. These peptides have the ability to diffuse into the proteasome, where they can be cleaved if the proteasome is catalytically active[98]. This process increases the AMC fluorescence, enabling precise quantification of proteasomal activity[98]. More advances for the development of

proteasome ABPs involved the establishment of subunit-specific peptide analogues, which covalently bind to different β-subunits of the 20S core and are linked to fluorophores like Cy5, permitting discrete quantification of catalytic subunits[98]. Finally, model PROTACs such as dBET1 also allow for indirect conclusions on the intactness of the proteasome activity via the abundance of the degrader target protein BRD4[98].

For the discovery of small molecules which cause an alteration of a protein's ubiquitination state, either by induced proximity or by inhibition of a UPS-component or a DUB, the presence or absence of Ub on the respective protein is of particular interest and essential to prove the suspected mode of action in the ubiquitin system. It thus is one of the most straightforward and well-established approaches to enrich ubiquitinated proteins for their downstream analysis using different ubiquitin enrichment handles.

2.5.1 Ubiquitin enrichment handles

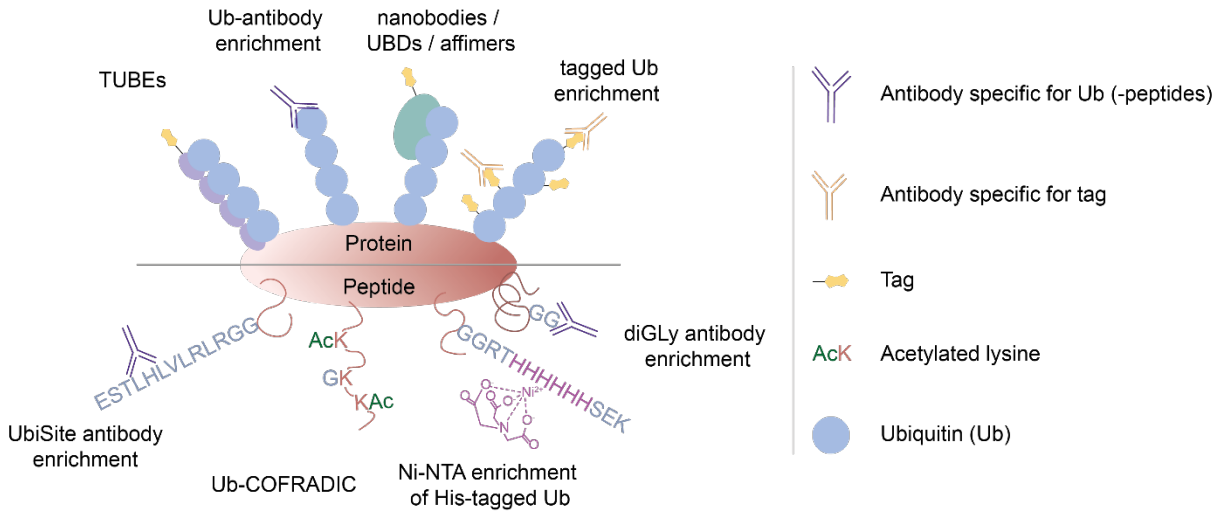

Figure 10: *Different strategies to identify ubiquitinated proteins by ubiquitin enrichment on the protein (top) and on the peptide level (bottom). Figure is partially inspired by Mattern, M. et al, M. S. Trends Biochem Sci (2019) and Sun, M. & Zhang, X. Cell Biosci (2022).*

Ubiquitin site-occupancy is very low compared to other PTMs[102]. Therefore, specific enrichment of ubiquitinated proteins is often crucial to show the presence of the PTM on the protein of interest, whether in a targeted approach via immunoblotting, or in an unbiased way by mass-spectrometry (see Figure 10). This enrichment can occur at the protein or peptide level, respectively before or after the digestion of ubiquitinated proteins. One traditional way of enrichment for different POIs on the protein level, the immunoprecipitation, is also used for the enrichment of ubiquitinated

proteins[103]. This is either achieved by using antibodies which directly bind native ubiquitin, or tagged-Ub, which is fused to a Flag or comparable tag and allows for tag-specific binding[103]. The application of the principle of enrichment was not only confined to the whole protein level, which offers the advantage of compatibility with an immunoblotting readout, but it could also be used on the peptide level following protein digestion, primarily for the purpose of proteomics analyses[103,104]. One of the most prominent examples is the usage of an antibody, which is selectively binding the two C-terminal di-glycine residues remaining on a formerly ubiquitinated protein via an isopeptide bond after its digestion with trypsin[105]. This so-called diGly-enrichment allows the identification of modified proteins carrying either an Ub, ISG15 or NEDD8 as UBLs, but cannot differentiate between the three[102,105]. This drawback is overcome by another antibody-based enrichment strategy targeting Ub-derived peptides using the UbiSite antibody after digestions of proteins with the LysC enzyme, which is leaving a longer Ub-peptide on the POI and allows for discrimination between UBLs (see Figure 10)[104]. Additionally, tagged and overexpressed Ub is also used for enrichments on the peptide level, mainly by using 6xHis-tagged ubiquitin in combination with an NTA purification[104]. Another antibody-free, but synthetically more challenging approach is followed in the Combined Fractional Diagonal Chromatography (COFRADIC) method for ubiquitination[104,106]. This strategy involves the protection of unmodified amines with an acetyl-group, which leaves Ub-sites untouched[106]. After a removal of Ub using a DUB, unmodified lysines are further derivatized with a Boc-glycine, followed by two sequential HPLC analyses, interrupted by a TFA-induced removal of the Boc group[106]. This process causes a retention time shift of the peptide peaks in the chromatogram, enabling the identification of Ub sites[104,106].

All of these peptide-based approaches allow for selective enrichment of formerly ubiquitinated proteins, but are hampered by the fact that they only allow identification of proteins which carry Ub on a unique peptide. This drawback is circumvented when Ub binding happens on the protein level prior to digestion and analysis by mass spectrometry and also allows for orthogonal read out methods such as immunoblotting and fluorescence microscopy[103]. Besides the common immunoprecipitation techniques, Ub enrichment on the protein level can be achieved either with nanobodies, single UBDs, or so-called tandem ubiquitin binding entities (TUBEs)[103]. Both classes of tools allow for coupling to different affinity elements such as biotin or GST for immobilization, e.g. onto beads, allowing separation of ubiquitinated proteins[103].

Ub affimers or single UBD-based enrichment handles are mainly small proteins derived from ubiquitin binding proteins, whether readers, writers, or erasers[103]. One example of a versatile and

potent UBD tool is OtUBD, which is derived from a deubiquitinase in *Orientia tsutsugamushi*[107]. This domain was engineered to bind ubiquitin irrespective of its chain length and linkage type and is thus also able to enrich mono-ubiquitinated substrates and free ubiquitin[107,108]. In *in vitro* studies, OtUBD has shown to reliably enrich the ubiquitome from yeast extract, both in immunoblotting- and proteomics-based readouts[108]. In the same study, the authors also demonstrated that they could face one bottleneck of Ub enrichment on the protein level, the co-purification of non-ubiquitinated proteins, by applying semi-denaturing conditions in the cell lysis and the washing steps of the enriched fractions[108]. Still, one drawback of this global enrichment of Ub could be that the background of free Ub in the eluates is overshadowing signals of low-abundant Ub proteins, especially in mass-spectrometry-based experiments.

This potential effect is less of a concern when TUBE reagents are used, even though their enrichment selectivity may still depend on the applied washing conditions. Tandem ubiquitin binding entities are repeats of UBAs or UIMs that selectively bind longer Ub chains and can be specific for certain Ub linkage types (see Figure 11)[103,109]. One of the first and most widely used TUBEs is a reagent derived from Ubiquilin-1, whose UBA was arranged in tandem repeats of four and, by this, is able to bind Ub chains independently of their linkage type[110]. At the same time, another non-selective TUBE was engineered from the UBA of the RAD23A ubiquitin-binding protein (see chapter 2.2)[110]. Since then, variety of TUBEs were engineered from other Ub binding proteins and several of these tool show selectivity for defined chain linkages, such as K63, which is demonstrated by a Rap80-derived TUBE[111]. The DUB Mindy-1 contains a tandem repeat of a

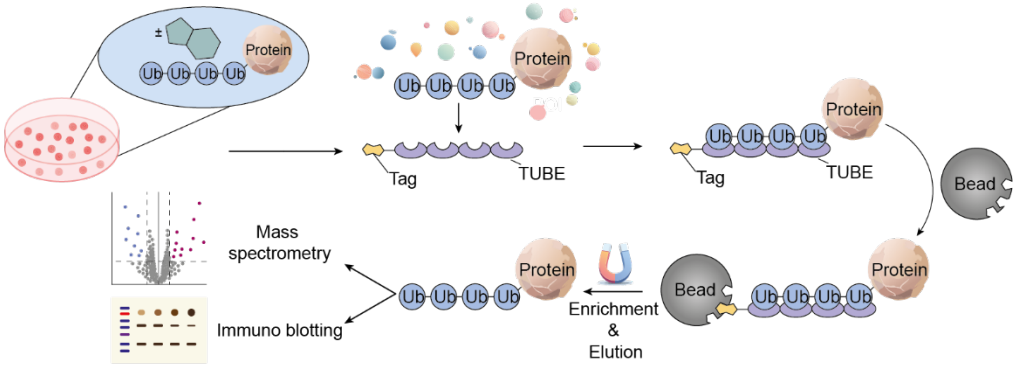

Figure 11: *Schematic representation of poly-ubiquitin enrichment from whole cell lysate after treatment with small molecules using Tandem ubiquitin binding entities (TUBEs). TUBEs are immobilized onto a solid phase followed by binding of ubiquitinated proteins from cell extracts. Bound proteins are washed and eluted off the beads, allowing for analysis of eluates either by immunoblotting or mass spectrometry.*

motif interacting with Ub (MIU) natively, which was successfully utilized to establish a K48-selective TUBE[112]. By modifying the original Ubiquilin-1 pan-Ub TUBE by mutations, a trypsin-resistant TUBE was designed, which not only can be utilized to protect Ub chains from decay,

which was already the case for the parental protein, but allowed for the cleavage off the Ub-modified protein in order to investigate Ub chain architecture globally[113]. All these examples show the potential that TUBEs have for the characterization of ubiquitination, irrespective of the biological question that lies behind it. However, their use in drug discovery is not established until today. For the investigation of small molecules altering ubiquitination on proteins, different methods were implemented.

2.5.2 Methods to discover small molecules altering protein ubiquitination

An elementary bottleneck in the discovery and design of DUB inhibitors, DUBTACs, degraders, and molecular glues in particular is the efficient detection of targeted degradation[114]. Whereas classical inhibitor-based drug discovery can rely on a large portfolio of structure-activity related assays and *in vitro* detection methods, the systematic discovery and characterization of small

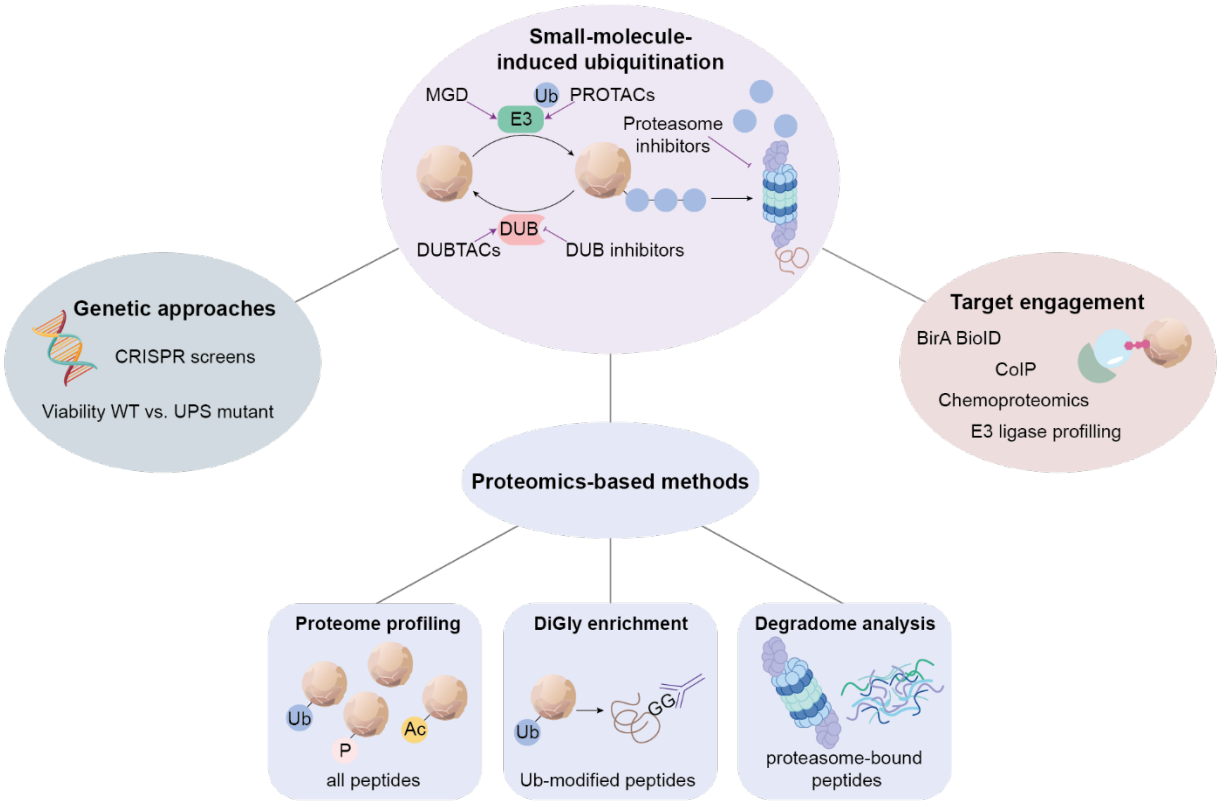

Figure 12: *Methods for the discovery and characterization of small molecules that alter protein ubiquitination can be divided into three main classes. Genetic approaches involve techniques such as CRISPR screens, while target engagement can be investigated by immunoprecipitation or proximity labeling. Proteomics-based methods allow for an unbiased characterization of small molecule effects on global protein abundance, ubiquitin modification or processing by the proteasome. This figure is partially inspired by Scholes, N. S., Mayor-Ruiz, C. & Winter, G. E. Cell Chem Biol. (2021).*

molecule-induced ubiquitination is mainly based on three different methodological fields (see Figure 12)[114]. Firstly, genetic approaches such as CRISPR-screens can be used to identify the MoA of a biologically active compound[114,115]. With creating a cell line in which the NEDD8-conjugating E2 enzyme UBE2M is mutated, which impairs neddylation-dependent ubiquitination, Christina Mayor-Ruiz and colleagues identified several molecular glue degrader candidates by comparing the cell viability of the mutated cells upon compound treatment with the viability of WT cells[115]. While this method is promising in identifying degrader-induced lethality in cells, the system is limited to the identification of neddylation-dependent MoAs and does not recognize small molecules altering ubiquitination in a non-cytotoxic way.

The second methodological field which is used to characterize compounds affecting the UPS, is to show their target engagement within the Ub machinery[114]. In this context, methods from the traditional drug discovery pipeline were successfully adapted[114]. Besides the well-established setups of Co-IP experiments, which show the enrichment of UPS-components together with the POI upon compound treatment or vice versa, chemoproteomics were implemented to identify the binding UPS components and the target protein of a degrader molecule[114]. In addition to these methods, the profiling of E3-ligase interactors by the biotinylation of their formed Ub-chains by an BirA fusion to the respective E3 enzyme (see section 2.5 above) was already successfully used in the context of the identification of degrader molecules[96].

However, all these methods are usually follow-ups on rationally designed small-molecules and thus contain a certain bias towards well-established scaffolds, previously explored E3-ligases or other components of the UPS.

2.5.2.1 Using mass spectrometry to unravel the influence of small molecules on protein ubiquitination

The most unbiased way to discover small molecules altering ubiquitination irrespective of the affected parts of the ubiquitination machinery is proteomics. In this context, three main methods were established[1].

First and foremost, whole proteome analysis is used to identify a decrease in protein levels in response to compound treatment[114,116,117]. As a novelty in this workflow, *Jochem et al.* recently introduced an innovative approach of detecting degrader-induced protein decay by pulsed-SILAC joined to translatome labeling with enrichment handles[118]. This approach is capable to notice the influence of one compound on multiple targets at once, but is at the same time neither able to distinguish between compound-associated primary and downstream effects, nor to identify non-

degradative ubiquitination[1,114]. Nevertheless, whole proteome profiling was already successfully implied in drug discovery as a follow-up on phenotypic screens[115,119].

As an orthogonal approach, ubiquitinated proteins can be enriched by pulling down proteins with the characteristic diGly-peptide which remains on the protein after trypsin digestion (see section 2.5.1)[105,114]. This procedure shows actual ubiquitination of target proteins which is not possible with a whole proteome analysis[114]. Nevertheless, this workflow cannot display the formation of ubiquitin chains, which are essential for degradation[114]. Furthermore, it cannot identify proteins beyond the ubiquitinated peptide itself, which is crucial for achieving high identification rates given the very low global occupancy of ubiquitination sites in the proteome[102,114].

Finally, proteasome-bound peptides can be captured while they are processed in the degrading machine and identified by proteomics analysis, allowing for an immediate conclusion on proteasome-processed proteins[120]. The utilization of this method in the context of small molecules that modify ubiquitination is yet to be investigated; however, it will be constrained to degradative ubiquitination.

Conclusively, drug discovery in the ubiquitin system can already profit from a broad variety of methods that facilitate the identification of small molecule candidates[114]. Nonetheless, a methodological discrepancy emerges in the context of unbiased identification of small molecules that modulate protein ubiquitination, independent of their point of interference with the Ub machinery, be it the writing of the ubiquitin code by E1-3 enzymes or its erasure by deubiquitinases. A suitable method to fill this gap that would also be able to recognize non-degradative ubiquitination could be the entailing integration of a tandem ubiquitin binding entity (TUBE)-based enrichment with an unbiased mass spectrometry-based readout.

The potential of this approach has already been demonstrated by others in contexts other than those involving small molecules. Ubiquitin enrichment connected to mass-spectrometry has been previously adopted in the analysis of plants[121], yeast lysate[122,123] and parasite infections in erythrocytes[124]. In plant seedlings, overexpression of a GFP-tagged, K63-selective enrichment handle derived from the yeast VPS27 UIM allowed for the identification of 100 proteins carrying K63-linked ubiquitin using a label-free quantification approach[121]. Another K63-tailored approach utilized multiplexing by SILAC to identify over 100 K63-ubiquitinated proteins from yeast lysate using a commercial Flag-tagged K63-TUBE[123]. For the simultaneous analysis of red blood cell and malaria-causing parasite lysate ubiquitomes, GST-TUBEs were cross-linked onto agarose resins in a column-based setup, followed by a ten-step elution procedure and in-gel digestion[124].

This approach allowed for the identification of 12 human and parasite proteins after filtering for DiGly-modified peptides in the search results[124].

These first attempts of TUBE-enrichments coupled to mass spectrometry were promising, but often lacked sufficient protein identification rates to give a representative picture of the ubiquitome or were not able to quantify differences in polyubiquitination rates[125]. Furthermore, these methods repeatedly relied on low-throughput protein digestion strategies, such as in-gel digestion, which are not compatible with the required throughput for a possibly unbiased screening[122,124,126]. It thus remains a challenge to adapt this workflow towards a first-in-line method for an unbiased screening of substances with known or unknown mode of action in the ubiquitin system.

3. Motivation and Aim

The field of small molecules that target the ubiquitin system is steadily gaining ground. However, the new modes of action that these therapeutics bring are often challenging to directly detect by established assays, which are tailored towards compounds inhibiting enzymatic activity. With this development, the need for methods which can reliably sense the effects of altered protein ubiquitination is rising. The field of proteomics has achieved great advances lately. As an unbiased detection method with high throughput and broad coverage, proteomics is a valuable tool for studying post-translational modifications of proteins. Still, a mass spectrometric method that can discover and characterize altered polyubiquitination at the point of modification while being sensitive and broadly applicable to different fates of polyubiquitination is lacking.

The utilization of TUBE enrichment coupled to mass spectrometry for the characterization of small molecules bears a huge potential for the emerging field of targeted protein degradation as well as the characterization of small molecules targeting the ubiquitin system in general. This potential in the context of PROTACS was already postulated, but data proving this is lacking until today[127].

This thesis aims to develop an assay which combines the effective enrichment of ubiquitinated proteins using tandem ubiquitin binding entities with a sensitive, mass-spectrometric readout in order to investigate compound-induced changes in protein ubiquitination. Furthermore, and in contrast to other proteomics-based methods, it should recognize also non-degradative polyubiquitination, as this consequence of small molecule treatment is fairly understudied until today. The envisioned assay setup should be cell-based and will involve the enrichment of (poly)ubiquitinated proteins from mammalian cell lysate after treatment of intact cells with the respective small molecule. After the successful enrichment, the protein eluates should be transformed into peptides using a MS-compatible Trypsin/LysC digest, followed by an LC-MS/MS analysis and appropriate interpretation of the data. In this context, the method should reliably detect the influences of well-characterized bioactive molecules on the ubiquitome at different points of interference as a proof of principle. Namely, this should involve PROTACs, molecular glue degraders, deubiquitinase inhibitors, and proteasome inhibitors. As this will require a maximum of sensitivity and the ability to process multiple samples at a time, the optimization of the workflow should involve every step of the process, questioning the setup from the start and in the following process fine-tune the procedure towards versatile applicability.

Finally, the envisioned assay should be valid to study uncharacterized research compounds, enabling the discovery of novel substances either targeting deubiquitinases, the proteasome, or inducing proximity between a target protein and an E3 ligase.

With this, TUBE-MS will bridge the gap between broad and unbiased mass-spectrometric readouts and ubiquitin-sensitivity of tailored, but low throughput, ubiquitome analyses.

4. Results

4.1 Establishment of a mass-spectrometric analysis of ubiquitinated proteins using TUBE-reagents

When establishing a multistep method that combines different aspects of already existing workflows, it is important to consider their compatibility. In the specific case of combining ubiquitin enrichment with a sensitive LC-MS/MS readout, it was crucial not only to efficiently capture ubiquitinated proteins, but also to minimize the presence of unmodified proteins, as these could compromise the sensitivity of proteomic detection. This chapter is focusing on the optimization of different stages in the envisioned TUBE-MS workflow, primarily on the ubiquitin enrichment, in order to attain a specific and sensitive assay.

4.1.1 Recombinant expression and biotinylation of ubiquitin enrichment reagents

The enrichment of ubiquitinated proteins from cell lysate is the first step in the intended assay setup. In order to investigate the effect of small molecules on protein ubiquitination in the most native state as possible, it was particularly important to reduce cell stressors apart from the actual compound treatment to a minimum. Thus, the enrichment handles were recombinantly expressed and not part of the cell treatment itself or overexpressed in mammalian cells.

The enrichment handle of choice was firstly a tandem ubiquitin binding entity (TUBE) derived from Ubiquilin-1 without a selectivity for the Ub-linkage type, but one for longer Ub chains (see chapter 2.5.1)[110]. To also allow for the investigation of mono-Ub or ubiquitinated proteins with shorter chains, the UBD derived from a deubiquitinase in *Orientia tsutsugamushi* OtUBD was chosen (see chapter 2.5.1)[108]. Both tools needed a tag system to allow for immobilization onto a solid particle for separation from liquid. From the broad repertoire of covalent and non-covalent tags for immobilization, biotin offered the most promising properties for efficient and stable binding to avidin-like proteins, such as streptavidin, while not requiring coupling conditions for chemical ligation prior to ubiquitin capturing. Furthermore, streptavidin beads allowed for a tight control of the TUBE/ OtUBD stoichiometry, and thus promised to reduce batch-to-batch variations. For the conjugation of biotin onto the ubiquitin enrichment handles, two different approaches were

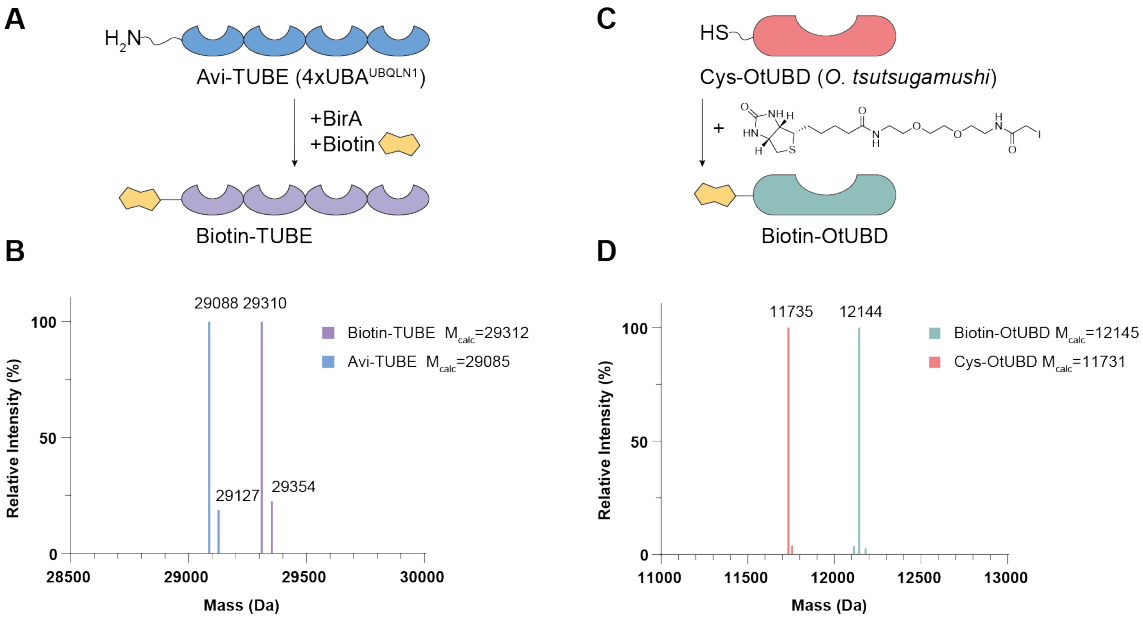

***Figure 13**: Biotinylation of recombinantly expressed ubiquitin enrichment handles. **A**. Schematic representation of the biotinylation reaction of the Avi-tagged TUBE using BirA. **B**. Deconvoluted LC-MS spectrum of the purified Avi-TUBE (blue) and the reaction product of the BirA biotinylation after purification (purple). **C**. Schematic representation of the biotinylation reaction of cysteine-containing OtUBD (Cys-OtUBD) using Biotin-(PEO)$_3$-iodoacetamide. **D**. Deconvoluted LC-MS spectrum of the purified Cys-OtUBD (orange) and the biotinylated OtUBD (green) after purification. The panels A. and B. were modified from Führer, S. et al. Small Molecule-Induced Alterations of Protein Polyubiquitination Revealed by Mass-Spectrometric Ubiquitome Analysis. Angew. Chem. Int. Ed. 64, e202508916 (2025) under a CC-BY 4.0 license.*

successful. The TUBE reagent was a fusion protein of the four-times repeat of the UBA of Ubiquilin1 with an AviTag. This tag consists of 15 amino acids, including a lysine onto which biotin can be ligated via an amide bond using the conjugating enzyme BirA (see Figure 13A)[128]. The expression and purification of the Avi-tagged fusion protein and its subsequent biotinylation was successful, yielding Biotin-TUBE after size-exclusion chromatography (SEC) with the desired mass (see Figure 13B).

The second ubiquitin enrichment handle, OtUBD contained a cysteine before the UBD's N-terminus. This allowed for the covalent coupling of biotin to OtUBD by the reaction with Biotin-(PEO)3-iodoacetamide at pH 8.0 (see Figure 13C). Not having a conjugating enzyme in the reaction mixture in this case came with the advantage of a facilitated purification by a five-step sequential dialysis (see section 7.2.4). Finally, Biotin-OtUBD was obtained with the desired molecular weight, confirmed by LC-MS (see Figure 13D).

In an initial *in vitro* pulldown Biotin-TUBE confirmed its ability to actually bind and enrich differently linked tetraUb chains without a preference for specific linkage types (see Figure 14). While Streptavidin magnetic beads carrying Biotin-TUBE were able to isolate M1-, K63-, and K48-linked tetraUb from solution, the same beads carrying Biocytin as a control were not able to do so, which becomes evident from the absence of a Ub signal in the pulldown (PD) fractions. This indicates that the enrichment capability of Biotin-TUBE is actually derived from the protein and not from unspecific aggregation of Ub chains onto the solid support.

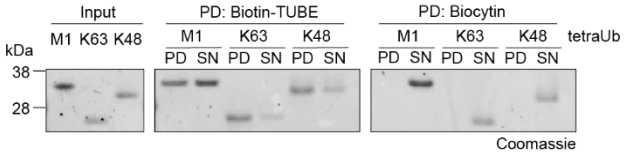

Figure 14: *Coomassie-stained SDS-PAGE of In vitro pulldown (PD) of differently linked tetra-ubiquitin chains using Biotin-TUBE and supernatants (SN) after enrichment compared to beads with only biocytin bound. Recombinant Ub chains were kindly provided by Dr. Kim Wendrich. This figure was taken from: Führer, S. et al. Small Molecule-Induced Alterations of Protein Polyubiquitination Revealed by Mass-Spectrometric Ubiquitome Analysis. Angew. Chem. Int. Ed. 64, e202508916 (2025) under a CC-BY 4.0 license.*

Having the expressed and purified enrichment handles with confirmed functionality in hand, the basis for the isolation of ubiquitinated proteins from cell lysates was laid. However, since conjugated ubiquitin chains in cell lysates introduce much more complexity to the isolation problem, it was crucial to first establish assay conditions that will be compatible with complex biological mixtures and at the same time enable for a mass-spectrometric analysis of the enriched fractions. For this, the ubiquitin pulldown using Biotin-TUBE needed further optimization in view of its application in a cell-based assay.

4.1.2 Identification of optimal assay conditions

Lysates from mammalian cells contain all components of the ubiquitin system, including Ub conjugates, Ub-conjugating enzymes, deubiquitinases (DUBs), and the proteasome (see section 2.2), besides the plethora of non-Ub-related proteins. Since the fine-tuned signaling of Ub is destroyed during cell lysis, it is of utmost importance to preserve the ubiquitination state of the cell as closely as possible to the point immediately before lysis. In this regard, the prevention of Ub chain degradation, whether by the proteasome or DUBs, must be inhibited. Concurrently, an efficient readout of the ubiquitome should not be impeded by the unspecific enrichment of non-ubiquitinated proteins. The present chapter thus focuses on the identification of optimal assay conditions in terms of the preservation of ubiquitin chains in cell lysates. Furthermore, it considers

the washing conditions of TUBE-carrying beads after Ub enrichment, and the separate elution of Ub proteins off the solid support to reduce background effects in MS analyses.

4.1.2.1 Preservation of poly-Ubiquitin chains in cell lysates

Since deubiquitinases in cell lysates can cause the degradation of ubiquitin chains and conjugates, which would cause a signal loss in the TUBE pulldown, it is important to inhibit these proteases during and after cell lysis. To achieve this, it is possible to add different substances to the lysis buffer. These can be broadly divided into alkylating and chelating agents that inhibit cysteine- and metallo-DUBs, respectively (see Figure 15A). The potency of these additives in

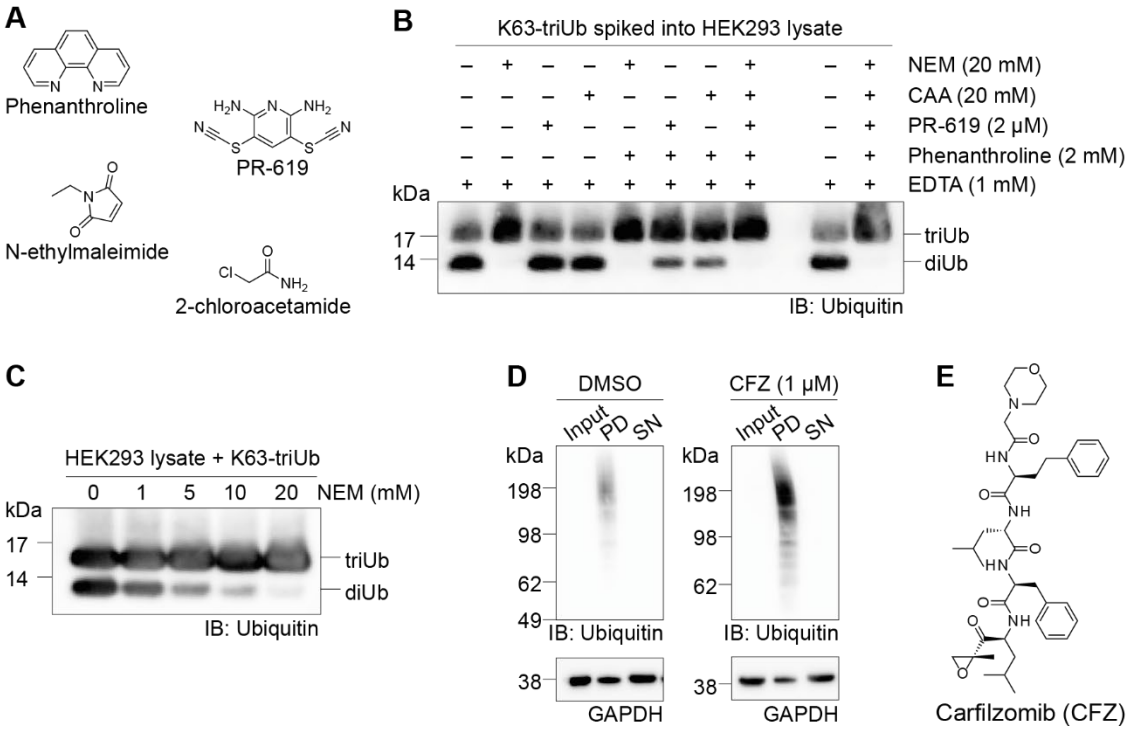

Figure 15: *Investigation of different buffer additives to achieve preservation of ubiquitin chains in cell lysate from decay by deubiquitinases.* ***A****. Structures of potentially DUB-inhibiting buffer additives tested in panel B.* ***B****. Western blot analysis of triUb chains which were spiked into HEK293 lysate with supplements as indicated after incubation for 1h at 4 °C.* ***C****. Western blot analysis of triUb chains which were spiked into HEK293 lysate containing different concentrations of N-ethylmaleimide (NEM) after incubation for 1h at 4 °C.* ***D****. Western blot against Ub of Pulldown (PD) and supernatant (SN) fractions after enrichment of endogenous polyubiquitin chains from MM1.S cell lysate using Biotin-TUBE under native conditions. The pulldown was performed with and without proteasomal inhibition of the cells.* ***E****. Structural formular of the proteasome inhibitor Carfilzomib (CFZ). Recombinant Ub chains were kindly provided by Dr. Kim Wendrich. Parts of this figure (panel B&C) were taken from Führer, S. et al. Small Molecule-Induced Alterations of Protein Polyubiquitination Revealed by Mass-Spectrometric Ubiquitome Analysis. Angew. Chem. Int. Ed. 64, e202508916 (2025) under a CC-BY 4.0 license.*

combination with the chelator EDTA as a constant lysis buffer ingredient strongly varies, as an experiment of the decay of K63-linked triUb chains in cell lysate showed (see Figure 15B). The

addition of the panDUB inhibitor PR-619 (see section 2.4.3) is not able to preserve ubiquitin chains in the lysate alone, but synergizes with the chelator phenanthroline, even though no complete inhibition of DUB activity was reached. The alkylating agent 2-chloroacetamide (CAA) showed the same behavior. Interestingly, the addition of *N*-ethylmaleimide (NEM) alone was sufficient to fully prevent the decay of K63 triUb in this experiment, so no additional phenanthroline was required to see the desired effect. To keep the concentration of NEM in the lysis buffer as low as possible, a titration experiment revealed the critical NEM concentration to achieve full DUB inhibition (see Figure 15C). Under the same conditions as in the previous experiment, a 20 mM concentration of NEM was crucial to obtain the protection of Ub chains in the lysate.

It is evident that, with this knowledge in hand, the conservation of the Ub signal, starting from the cell lysis time point, was secured. However, the process of turnover of ubiquitin chains within the cell remained unaltered. In the context of native ubiquitin signaling characterization or investigation of deubiquitinase inhibitors, this is the desired outcome. However, when it comes to the characterization of degrader molecules such as PROTACs, the detected polyubiquitin signal could become subject to proteasomal degradation of the target protein, depending on the degradation kinetics. To also cover this circumstance, we further investigated the effect of cell treatment with a proteasomal inhibitor, in this case carfilzomib (CFZ) on the polyubiquitin pool in MM1.S cells by performing a TUBE pulldown under native conditions (see Figure 15D&E). The pretreatment using carfilzomib showed to be a suitable procedure to enhance the polyubiquitin signal in the TUBE pulldown fractions. In this case, the chosen 1 µM concentration might in such high doses, impair cell viability after longer treatment times and should be reevaluated before being used in actual experimental setting for the characterization of small molecules. Concurrently, this experiment demonstrated that the Biotin-TUBE reagent is indeed capable of efficiently enriching endogenous polyubiquitin from more complex mixtures, such as MM1.S lysate.

The pulldown experiment conducted under native conditions revealed an augmented polyubiquitin signal following TUBE enrichment. However, a prominent signal from unmodified GAPDH was also observed within the pulldown fractions. This signal almost reached the intensity of the input and supernatant signals, suggesting that a significant number of unmodified proteins are co-enriched with the polyubiquitin pool. This could potentially hamper the analysis of less abundant polyUb signals in mass spectrometry and Western blot analyses by overshadowing them, thereby stressing the necessity to optimize the washing conditions of the TUBE enrichment further and move away from the native enrichment used until this stage.

4.1.2.2 Pulldown lysis and washing conditions and stoichiometry

To reduce the fraction of unmodified proteins being co-enriched with the TUBE pulldown, it was necessary to investigate other lysis and washing conditions. Inspired by a protocol of M. Zhang and colleagues[108], Biotin-TUBE bore the potential to also be functional under more harsh lysis conditions using urea to reduce unspecific binding of proteins to the TUBE beads or co-purification of interacting proteins. A TUBE pulldown experiment from Jurkat cell lysate using seven different urea concentrations in the lysis buffer, ranging from 0-12 M urea, revealed that Biotin-TUBE

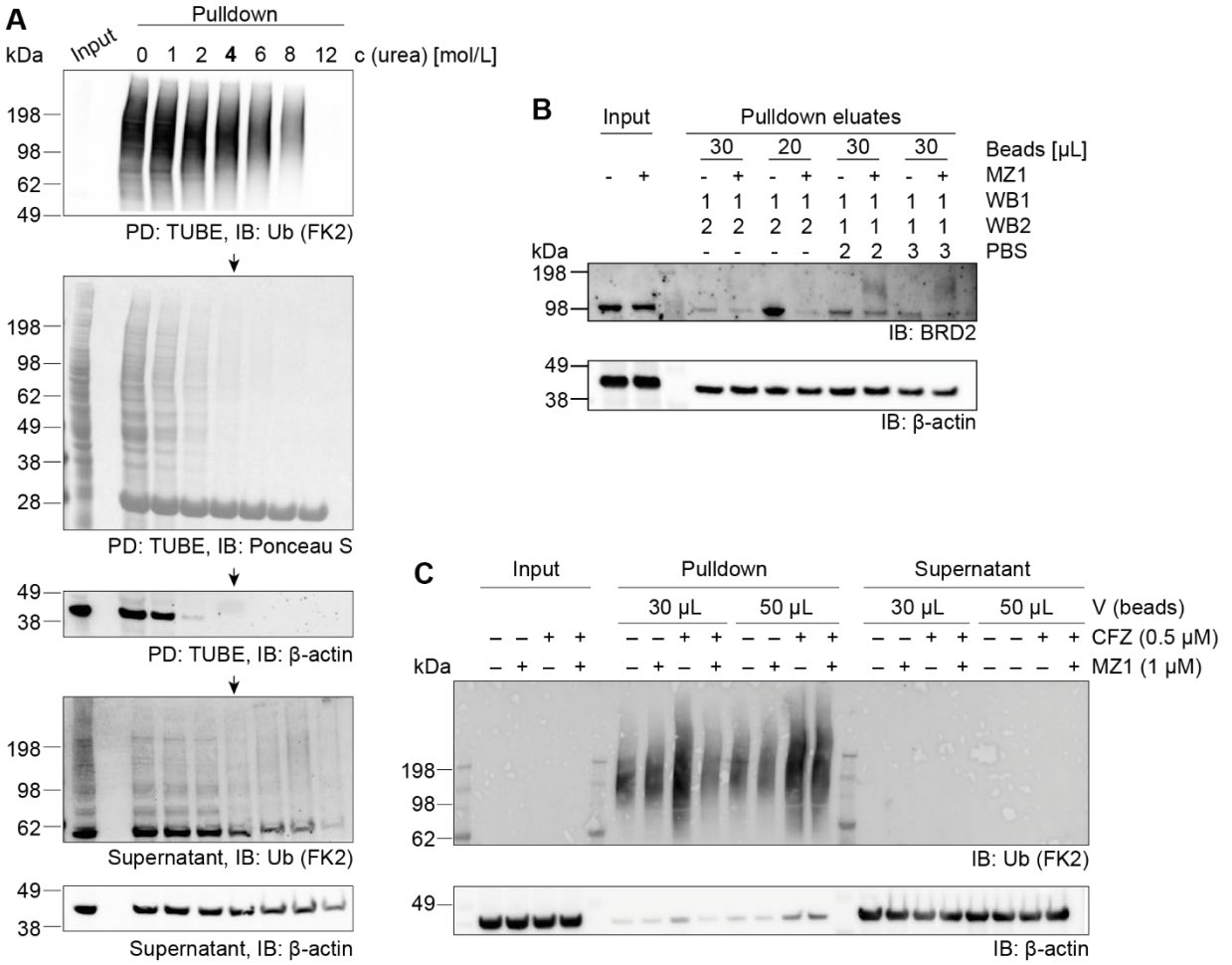

Figure 16: *Establishment of optimized lysis and washing conditions as well as bead stoichiometry for the TUBE pulldown to enhance its specificity and signal intensity.* ***A****. Western blot analysis of the investigation of TUBE stability and consequently Ub enrichment efficiency when using different concentrations of urea in the lysis buffer. The image of the immunoblot (IB) against β-actin in the pulldown (PD) fractions was overexposed to visualize also traces of the antigen.* ***B****. Western blot of input and PD fractions from Jurkat cells treated with CFZ and MZ1 vs. DMSO and washed differently with three different washing buffers (WB1/2 or PBS) as indicated.* ***C****. Western blot of input, pulldown and supernatant fractions of Jurkat cells treated with CFZ and MZ1 as indicated. The pulldown was performed either with 30 µL or 50 µL of streptavidin magnetic beads to determine the optimal bead volume for signal maximization. This figure was partially taken and modified from Führer, S. et al. Small Molecule-Induced Alterations of Protein Polyubiquitination Revealed by Mass-Spectrometric Ubiquitome Analysis. Angew. Chem. Int. Ed. 64, e202508916 (2025) under a CC-BY 4.0 license.*

indeed could perform well at urea concentrations up to 4 M before the enrichment efficiency decreases at higher concentrations (see Figure 16A). At the same time, the signal from unmodified and co-purified proteins steadily decreased, as shown by the Ponceau S and β-actin signals in Figure 16A, which indicates a significant improvement of the signal-to-noise-ratio in the TUBE pulldown. In view of these results, I then continued to perform the enrichment of ubiquitinated proteins in lysis buffer containing 4 M urea (results are indicated with an arrow in Figure 16A).

Another important aspect when identifying the optimal conditions for polyubiquitin enrichment by Biotin-TUBE was the washing of the beads after protein isolation. In another pulldown experiment, Jurkat cells were treated with Carfilzomib and the PROTAC MZ1 to polyubiquitinate BRD2 (see section 2.4.2) and thus create high molecular weight (MW) species above the MW of unmodified BRD2 in the immunoblot of pulldown eluates. This should allow for the identification of the optimal signal-to-noise ratio, depending on the washing conditions, with a higher resolution than the detection of the overall polyubiquitin signal. The in-depth characterization of MZ1 in the TUBE assay by immunoblot and mass spectrometry is shown and discussed in chapter 4.2.1. The testing of three different washing buffers (WB1, containing 4 M urea, WB2, containing no urea and PBS, see section 7.1.1) in different combinations and repetitions showed the best signal-to-noise ratio to appear after washing the beads once with each WB1 and WB2 and twice with PBS (see Figure 16B). In the same experiment, the variation of the bead volume between 20 µL and 30 µL was not conclusive under the given washing conditions, thus necessitating a further attempt with increased bead volumes, using the optimized washing conditions. In this approach, the pulldown eluates following the use of either 30 µL or 50 µL for polyubiquitin isolation from Jurkat lysate treated with MZ1, CFZ or DMSO, as indicated, did not show a visible difference in polyubiquitin enrichment (see Figure 16C). This finding indicates that 30 µL of streptavidin magnetic beads with Biotin-TUBE immobilized are sufficient to enrich the majority of the polyubiquitome. Interestingly, the signal of unmodified β-actin that gets co-purified increases upon proteasomal inhibition with CFZ in almost all PD eluate fractions. This could be attributed to the changed bead surface that is created by the greater number of enriched polyubiquitinated proteins, allowing for more unspecific interactions with non-ubiquitin proteins. This would create a different protein background, a so-called “beadome”, which has to be considered when comparing protein levels mass-spectrometric readouts[129]. One potential solution to this problem could be the separate elution of the polyubiquitome from the TUBE reagent, thereby allowing the beads with their beadome proteins adsorbed onto them to be separated.

4.1.2.3 Elution conditions for background reduction in mass spectrometry

As it is well established that the interaction between biotin and streptavidin is strong, and as the previous results had shown that it can withstand high concentrations of urea (see section 4.1.2.2, Figure 16A), it appeared possible to separate the enriched polyubiquitome from the Biotin-TUBE

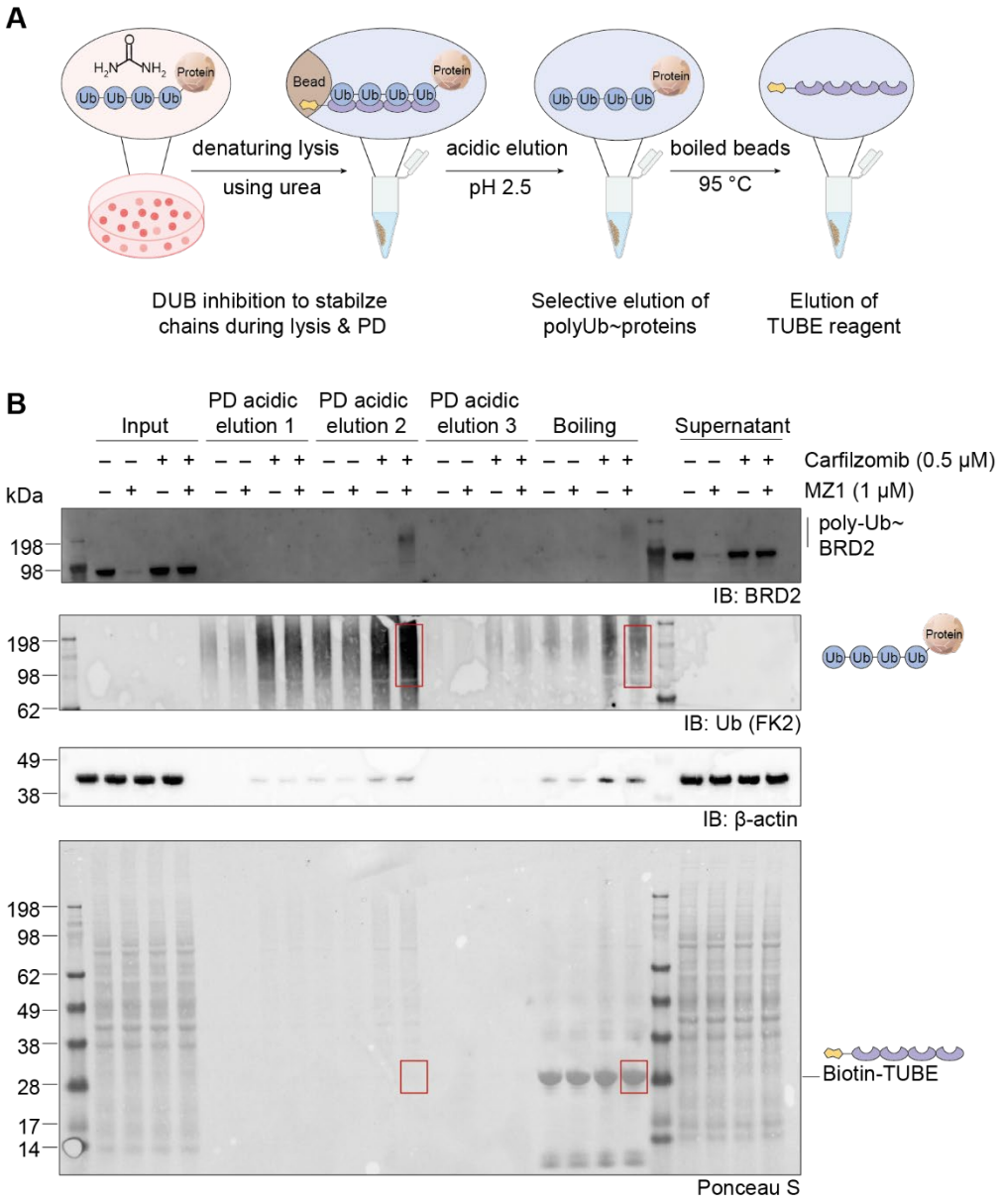

Figure 17: *Separate elution of enriched polyubiquitinated proteins from TUBE beads by incubation at pH 2.5.* ***A****. Schematic illustration of the workflow for elution of polyubiquitinated proteins corresponding to the results shown in panel B.* ***B****. Western blot of Input, pulldown (PD) eluates and supernatant fractions of TUBE-PD from Jurkat cells treated with MZ1 for 4 h and carfilzomib for 5 h, as indicated. After enrichment, beads were subjected to three subsequent acidic elutions and finally one boiling step to elute bound proteins. Red boxes highlight the comparisons of the same pulldown sample after the second acidic and the boiling elution, each in a ubiquitin blot and a Ponceau S stain of the same membrane. This figure was modified from Führer, S. et al. Small Molecule-Induced Alterations of Protein Polyubiquitination Revealed by Mass-Spectrometric Ubiquitome Analysis. Angew. Chem. Int. Ed. 64, e202508916 (2025) under a CC-BY 4.0 license.*

immobilized onto the beads by an intermediate-strength elution. To confirm this hypothesis, I treated Jurkat cells with carfilzomib and MZ1 in different combinations, followed by a semi-denaturing lysis using 4 M urea and enrichment by Biotin-TUBE. Following the enrichment, beads were incubated three subsequent times at pH 2.5 and once heated to 95 °C (see Figure 17A). The western blot comparison of the eluate fractions with signals against ubiquitin, β-actin and Ponceau S total protein stain revealed that two acidic elution steps are sufficient so recover a majority of the polyubiquitome from the beads and only a weak polyUb signal is gained after the final boiling step C (see Figure 17B, upper red boxes). The third acidic elution did not release many more Ub proteins, which becomes evident from the comparably low Ub signal in the immunoblot. In line with these results, the second acidic elution step showed the highest signal intensity of polyubiquitinated BRD2 for lysate from Jurkat cells treated with MZ1 and CFZ. At the same time, the Ponceau S stain showed that the TUBE reagent (MW ≈ 29 kDa) remained bound to the beads until the final elution at 95 °C (see Figure 17B, lower red boxes). The Ponceau S and β-actin immunoblot also gave insights into the number of unmodified proteins being co-eluted with the polyubiquitinated proteins: While the Ponceau S signal for the acidic eluates mainly became visible at higher molecular weights, potentially representing polyUb proteins, it was far more intense and spread over the whole MW range of the blot for the boiled eluates, indicating that many co-purified proteins were released in this step. The signals of β-actin followed the same trend and were more intense in the boiling fractions than in the acidic eluates.

Taken together, this experiment on the one hand demonstrated that polyUb proteins can be separately released from the beads, leaving TUBE reagent bound with only minor loss in Ub signal compared to the boiling fractions. This yielded a significant background reduction by the removal of the TUBE protein, which would otherwise be detected in the mass-spectrometric analyses. On the other hand, the acidic elution brought the advantage of reducing the signal of unmodified proteins in the PD fractions, as a substantial portion of these proteins was only liberated from the beads after boiling. Conclusively, as the third acidic elution did not seem to contribute markedly to the Ub signal, the protocol of choice for the release of polyUb proteins after TUBE-Pd for mass-spectrometric readouts would be to perform two subsequent acidic elutions at pH 2.5 and to combine the eluates before digestion. This procedure should allow for a high-sensitivity and low-background detection of polyubiquitinated proteins using proteomics.

Considering the multitude of optimized parameters in terms of lysis, enrichment, stoichiometry, washing, and elution, the TUBE pulldown procedure was ready to be used for the characterization of small molecules supposed to alter protein ubiquitination.

4.2 Mass spectrometric analysis of the polyubiquitome by small molecules

The main purpose of the previously established TUBE enrichment protocol was its application in the mass-spectrometric analysis of small molecules. When characterizing the alterations of the polyubiquitome caused by treatment of cells with small molecules, one has to consider the different points of action in the ubiquitin system at which the substances can interfere, namely the enhanced ubiquitination by E3 ligases, the deubiquitination by DUBs and the inhibition of degradation by the proteasome (see section 2.4). Consequently, an assay which can cover as many MoAs as possible has to be tested with multiple classes of drug-like compounds. To address this necessity, this chapter is showing the results of the first applications of TUBE-MS on small molecules: First on well-characterized examples from the families of PROTACs and DUB inhibitors, followed by a small screening of derivatives of a destabilizing molecule against IDO1 and finally, three uncharacterized members of a newly established proteasome cluster from cell painting analyses.

Before the TUBE assay could give reliable results for substances of unknown MoA, it was important to choose a first case of a small molecule whose point of interference with the UPS is well-known. As a proof of principle, we thus chose the PROTAC MZ1.

4.2.1 Characterization of the PROTAC MZ1 by TUBE-pulldowns

In mass spectrometric assays using enrichment of a specific post-translational modification, it is necessary not only to define the dose of the small molecule, as is the case for many cell-based assays, but also to define the additional prerequisites for conserving the readout signal, in this case the polyubiquitinated proteins. This on the other hand has to be considered in view of the point of interference that should be covered in the screening, or, as in the example covered here, the known MoA. MZ1 is a potent PROTAC, targeting the bromodomain proteins BRD2, BRD3 and BRD4 for degradation using the E3 ligase VHL (see section 2.4.2)[71]. Since the substance has shown to degrade its target BRD2 efficiently within 4 h in the optimization experiments for the TUBE pulldown conditions (see 4.1.2.3, Figure 17), we first sought to identify the suitable prerequisites to gain optimal compatibility of the TUBE pulldown with a proteomics analysis.

4.2.1.1 Identifying suitable assay conditions for mass spectrometry-compatibility

Based on the results that MZ1 showed during the pulldown fine-tuning, it was clear that the detection of enhanced ubiquitination caused from MZ1 treatment by mass spectrometry required the inhibition of the proteasome. This assumption was confirmed by an initial experiment in which pulldown fractions from Jurkat cells with intact proteasome did only show ubiquitination signals

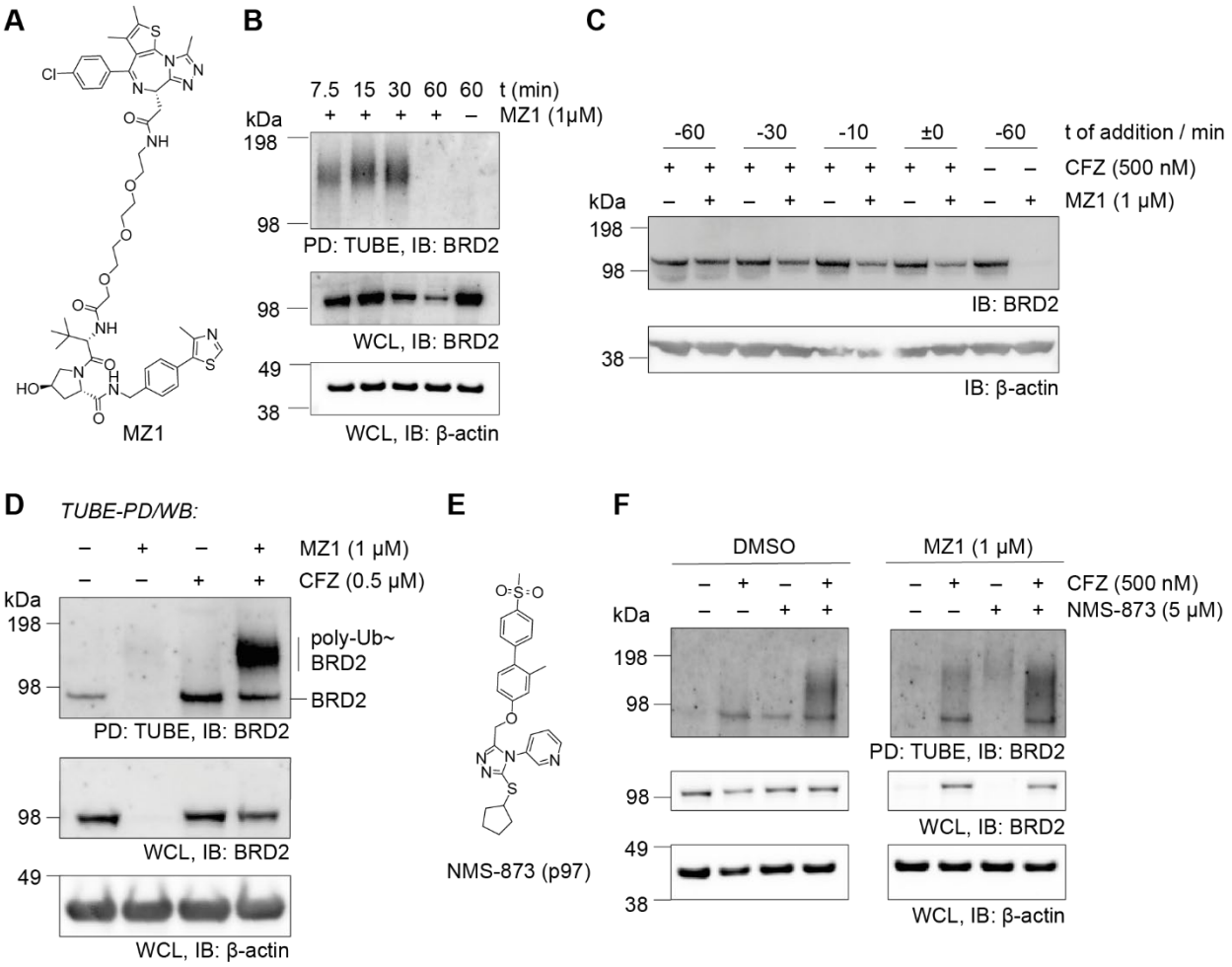

Figure 18: *Defining the prerequisites that are needed for an efficient detection of ubiquitinated BRD proteins by mass spectrometry after TUBE pulldown.* ***A****. molecular structure of the PROTAC MZ1.* ***B****. TUBE pulldown time course experiment of Jurkat cells being treated with MZ1 for up to 1 h without proteasome inhibition. Cells were treated with MZ1 or DMSO as indicated for the given durations.* ***C****. Identification of the optimal addition time point of the proteasome inhibitor carfilzomib (CFZ) for complete inhibition of BRD2 degradation through MZ1 treatment. Jurkat cells were treated with MZ1 or DMSO for 4h and CFZ for the additional duration prior to MZ1 addition as indicated. The western blot analysis shows the BRD2 abundance form whole cell lysate.* ***D****. Immunoblot against BRD2 of TUBE pulldown eluates and input factions from Jurkat cells being either treated with CFZ or DMSO for 5 h and MZ1 for 4 h.* ***E****. Structural formula of the p97 inhibitor NMS-873.* ***F****. Immunoblot of TUBE PD eluates and input fractions of Jurkat cells being treated with CFZ, NMS-873 and MZ1 in different combinations as indicated. CFZ and NMS-873 were added onto the cells 1 h prior to the addition of MZ1 or DMSO for incubation for 4 h. This figure was modified from Führer, S. et al. Small Molecule-Induced Alterations of Protein Polyubiquitination Revealed by Mass-Spectrometric Ubiquitome Analysis. Angew. Chem. Int. Ed. 64, e202508916 (2025) under a CC-BY 4.0 license. The results shown in panel B, D and F are representative for at least 3 biological replicates.*

until 30 min post treatment (see Figure 18A&B). Since these short treatment times were not compatible with potential further applications for less-well characterized substances, whose effects might only become detectable after longer treatment times, proteasomal inhibition was the alternative of choice to conserve the ubiquitination signal of BRD proteins for at least 4 h of cellular treatment. The necessary duration of cell pretreatment with the proteasome inhibitor carfilzomib (CFZ) to reach full rescue of BRD2 degradation became evident from a titration experiment using different addition time points of CFZ relative to the treatment of Jurkat cells with MZ1 for 4 h (see Figure 18C). Only a pretreatment of 60 min with CFZ could achieve a full conservation of BRD2 signal in the analysis of whole proteome abundance, indicating that the inhibition of the proteasome with CFZ in Jurkat cells takes around 1 h. Thus, for degraders with fast cell penetration and degradation kinetics such as MZ1, this duration of pretreatment is crucial. With this knowledge in hand, we conducted a TUBE PD from Jurkat cells treated with MZ1 and CFZ for the optimal durations and compared them to cells with intact proteasome (see Figure 18D). Indeed, in the immunoblot of the PD eluates against BRD2 the desired ubiquitination signal appeared above the MW of unmodified BRD2 if cells are treated with MZ1 and CFZ. This result confirmed CFZ as a suitable prerequisite for the characterization of fast degrader molecules using TUBE-MS.

Apart from inhibiting the proteasome, blocking other factors that are essential for degrading polyubiquitinated proteins was an attractive approach for investigating their effects on the polyUb signal of POIs. One of them was the unfolding and shuttling factor p97, also called VCP[130]. Its central role in many proteolytic pathways promised to further enhance the signal of ubiquitinated degrader target proteins when combined with CFZ[130]. The p97 inhibitor NMS-873 served as an suitable compound to elucidate this hypothesis (see Figure 18E)[131]. In a TUBE-PD experiment comparing all possible combinations of CFZ and NMS-873 pretreatment and MZ1 incubation, the inhibition of p97 indeed showed a signal-enhancing effect on the ubiquitination of BRD2 (see Figure 18F). Interestingly, p97 inhibition not only boosted the polyubiquitination of BRD2 in cells with MZ1, but also increased the target's background ubiquitination in the DMSO control, indicating a substantial influence of both inhibitors on the ubiquitome inside the cell. In view of these results, the dual background inhibition of the proteasome and p97 was beneficial for gaining overall BRD2 signal intensity. However, it remained unclear if the background ubiquitination would hamper the assay window in a proteomics analysis and how this inhibition would impair the sensitive detection of all MZ1 targets. This is why the next consecutive step was the investigation of both pulldown conditions in an unbiased mass spectrometric setup.

4.2.1.2 Multiplexing by TMT-labeling for enhancement of proteome depth and identification rates

The first application of the TUBE enrichment in combination with mass spectrometry happened on the basis of the previously tightly optimized assay conditions for MZ1 as a proof of principle. In a proteomics experiment combining the 4 M urea lysis TUBE enrichment from CFZ and MZ1 or DMSO treated Jurkat cells with an acidic elution, and an SP3 on-bead digestion[132], the MZ1 target BRD4 was significantly enriched compared to the DMSO control (see Figure 19A). Previous attempts using a label-free quantification (LFQ) for this setup failed due to the polyubiquitin-enrichment resulting in insufficient detection of the MZ1 target proteins in the untreated condition. We therefore implemented tandem mass tag (TMT) labelling of the digested peptide samples to increase proteome depth and reduce missing values, even in an enriched proteome. However, even though BRD4 was identified with 8 razor and unique peptides and thus significantly changed in the MZ1 condition over four replicates (see Figure 19C), BRD2 did not reach a significant enrichment in the treated fractions (see Figure 19B). This most likely occurred due to only two razor and unique peptides being identified, causing higher deviations in the overall LFQ intensity of BRD2, thus affecting its fold change and p-value. This result was surprising in view of the clear results in the immunoblot-based readout of these conditions (see section 4.2.1.1, Figure 18D), but could be explained with the different elution procedures. While for the western blot-based analysis, the protein-coated beads were boiled with biotin solution and LDS, for the mass-spectrometric readout streptavidin magnetic beads were subjected to the background-reducing acidic elution shown in Figure 17 (see section 7.2.6.1), which might have caused the fraction of unmodified BRD2, which was unspecifically enriched, to decrease. This could have lowered the identified unique and razor peptides for BRD2.

Motivated by the signal-boosting effect achieved by the dual pretreatment of Jurkat cells with CFZ and NMS-873 (see Figure 18F), I therefore conducted another TUBE-MS experiment investigating these conditions with SP3 on-bead digestion and TMT multiplexing (see Figure 19D). In this approach, both MZ1 target proteins were significantly changed in their abundance upon MZ1 treatment, suggesting that p97 inhibition did not affect the assay window. Contrary, BRD2 and BRD4 were both identified with 8 and 7 razor and unique peptides respectively (see Figure 19E&F), which confirmed the expected identification-boosting effect caused by a certain degree of BRD2 background ubiquitination upon p97 inhibition. This was also reflected in a decent log2-fold change (FC) of both proteins in the analysis (see Figure 19H). Moreover, the TMT multiplexing yielded substantially more identified proteins (6185), among which ubiquitin was the most abundant (see Figure 19G).

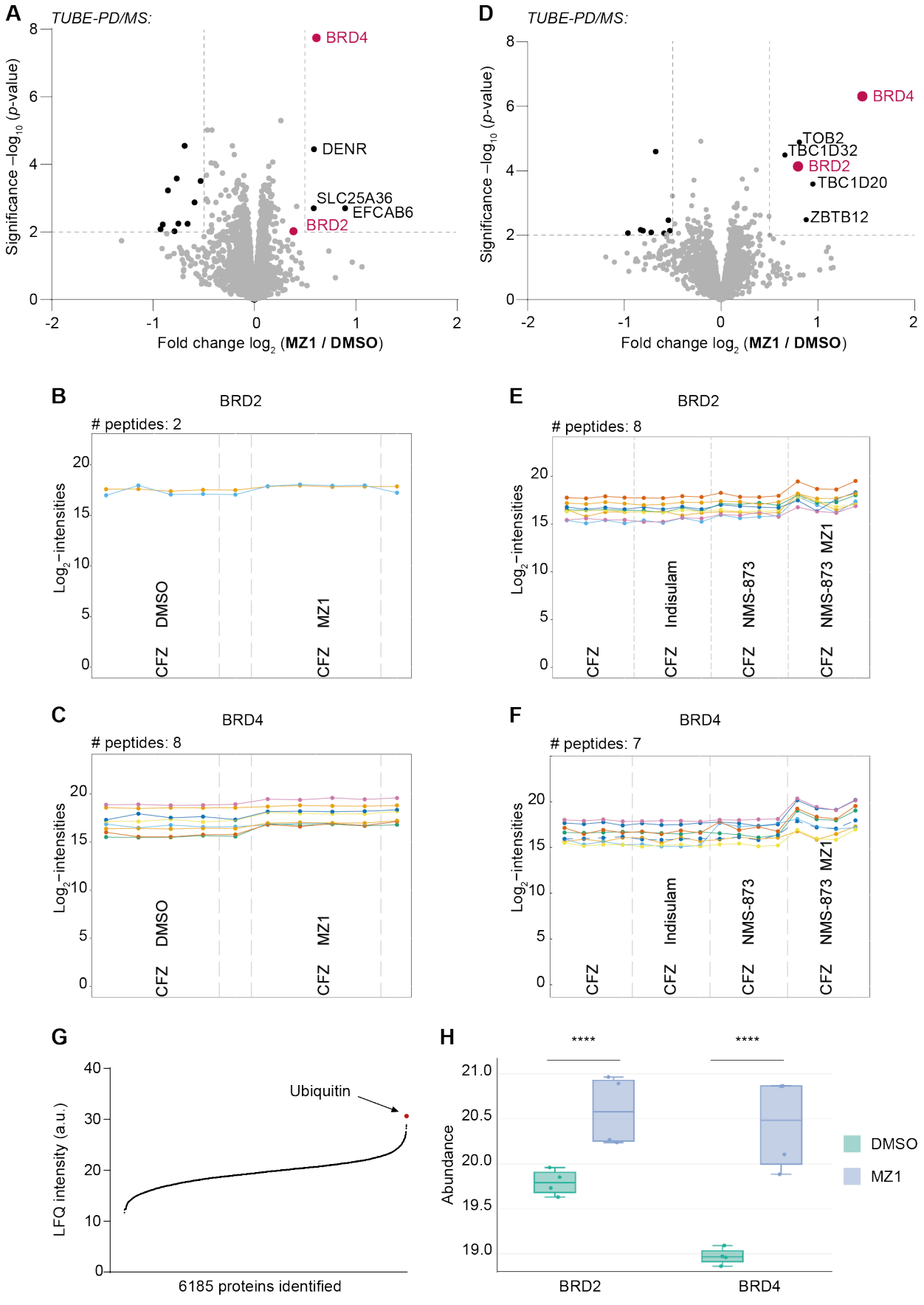
A
TUBE-PD/MS:
BRD4
DENR
SLC25A36
EFCAB6
BRD2
Significance −log10 (p-value)
Fold change log2 (MZ1 / DMSO)
D
TUBE-PD/MS:
BRD4
TOB2
TBC1D32
BRD2
TBC1D20
ZBTB12
Significance −log10 (p-value)
Fold change log2 (MZ1 / DMSO)
B
BRD2
peptides: 2
Log2−intensities
CFZ
DMSO
CFZ
MZ1
E
BRD2
peptides: 8
Log2−intensities
CFZ
Indisulam
CFZ
NMS-873
CFZ
NMS-873 MZ1
C
BRD4
peptides: 8
Log2−intensities
CFZ
DMSO
CFZ
MZ1
F
BRD4
peptides: 7
Log2−intensities
CFZ
Indisulam
CFZ
NMS-873
CFZ
NMS-873 MZ1
G
LFQ intensity (a.u.)
Ubiquitin
6185 proteins identified
H
****
****
Abundance
BRD2
BRD4
DMSO
MZ1

***Figure 19**: Proteomic analysis of TUBE PD eluates after enrichment from lysate of Jurkat cells being treated with MZ1 with either only CFZ or CFZ and NMS-873 for proteasome and p97 inhibition. **A**. Volcano plot of proteomics results comparing the TUBE eluates from Jurkat cells treated with either with MZ1 for 4 h and CFZ for 1 h pretreatment or DMSO for 4 h and CFZ for 1 h pretreatment. All conditions were analyzed in 4 biological replicates using FragPipe and FragPipe Analyst. **B**. Peptide level intensities of BRD2 over conditions from the experiment shown in A. The analysis was performed using MSstatsShiny. **C**. Peptide level intensities of BRD4 over conditions from the experiment shown in A. The analysis was performed using MSstatsShiny. **D**. Volcano plot of proteomics results comparing the TUBE eluates from Jurkat cells treated with either with MZ1 for 4 h and NMS-873 and CFZ for 1 h pretreatment or DMSO for 4 h and NMS-873 and CFZ for 1 h pretreatment. All conditions were analyzed in 4 biological replicates using FragPipe and FragPipe Analyst. **E**. Peptide level intensities of BRD2 over conditions from the experiment shown in D. The analysis was performed using MSstatsShiny. **F**. Peptide level intensities of BRD4 over conditions from the experiment shown in D. The analysis was performed using MSstatsShiny. **G**. LFQ intensities of all proteins identified in the experiment shown in D. with the most abundant protein (Ubiquitin) being highlighted. **H**. Boxplot comparing the individual abundances of MZ1 targets BRD2 and BRD4 across replicates in the respective conditions (DMSO or MZ1) from the experiment shown in D.*

This figure was taken and modified from Führer, S. et al. Small Molecule-Induced Alterations of Protein Polyubiquitination Revealed by Mass-Spectrometric Ubiquitome Analysis. Angew. Chem. Int. Ed. 64, e202508916 (2025) under a CC-BY 4.0 license.

This could be primarily attributed to the separate elution of ubiquitinated proteins from the TUBE reagent under acidic conditions, while previous attempts in the group often identified the TUBE protein as the most abundant protein after digestion, whether after boiling the beads or performing on-bead digestion. Overall, these results were promising indicators for a functional TUBE-MS assay in this first proof of principle using MZ1. However, the drastic alterations on the UPS that CFZ and p97 dual inhibition most likely caused are not suitable for an ubiquitome analysis as close as possible to the native cell physiology, which is why TUBE-MS was benchmarked under less biased conditions, namely without CFZ and in the case of deubiquitinase inhibition.

4.2.2 Mass-spectrometric characterization of deubiquitinase inhibitors by TUBE-MS

Deubiquitinase inhibitors bear a great therapeutic potential (see section 2.4.3). In this regard, their testing in the TUBE-MS assay was a suitable next step to further characterize both, the method and the small molecules themselves. The PROTAC test case using MZ1 pointed towards some limitations concerning the bias of the readout when using proteasomal inhibition in combination with the p97 inhibitor NMS-873. We thus sought to explore the sensitivity and capability of TUBE-MS to characterize small molecules altering ubiquitination without the signal-enhancing effects derived from other inhibitors. As well-characterized inhibitors of a panel of different USP DUBs, FT671 (USP7), IU1-47 (USP14) and Spautin-1 (USP10/13) promised to show some known and some new target proteins to be changed in their ubiquitination state upon DUB inhibition (see Figure 20A). Indeed, all DUB inhibitors caused significant changes in the polyubiquitome (see Figure 20B-D). In general, the inhibition of the respective DUB yielded in the enrichment or of literature-reported substrates (annotated in blue) of USP7 in the case of FT671 (Figure 20B) and USP14 in the case of IU1-47 (see Figure 20C). This is in line with the expectation that DUB inhibition leads to the conservation of the polyubiquitinated substrate proteins and thus enrichment in TUBE-MS. However, since in this setup no proteasomal inhibition was present, depending on the kinetics of the signal, the enhanced polyubiquitination of a DUB substrate could cause a faster turnover of the ubiquitin signaling, meaning that degradative ubiquitination could happen quicker and the proportionally decreased overall protein abundance yields less polyubiquitinated protein to be enriched. This effect had to be considered for the interpretation of the TUBE-MS results of Jurkat cells being treated with the USP10/13 inhibitor Spautin-1 (see Figure 20D). While the inhibition of USP10 and USP13 led to the enrichment and thus enhanced ubiquitination of several mitochondrial proteins (annotated in purple), it also caused a signal decrease on 29 ribosome-associated proteins (annotated in orange). The enrichment of mitochondrial proteins is in line with a recent report on Spautin-1-dependent mitophagy, even though its exact influence on the polyubiquitination of mitochondrial proteins remains unclear[133]. The decreased presence of ubiquitinated ribosomal proteins in the compound-treated cells can be connected with the reported role of USP10 in the rescue of 40S ribosomal subunits from lysosomal degradation[134]. Consequently, the inhibition of USP10 could lead to the enhanced lysosomal degradation of ribosomes, proportionally decreasing also the polyubiquitination of

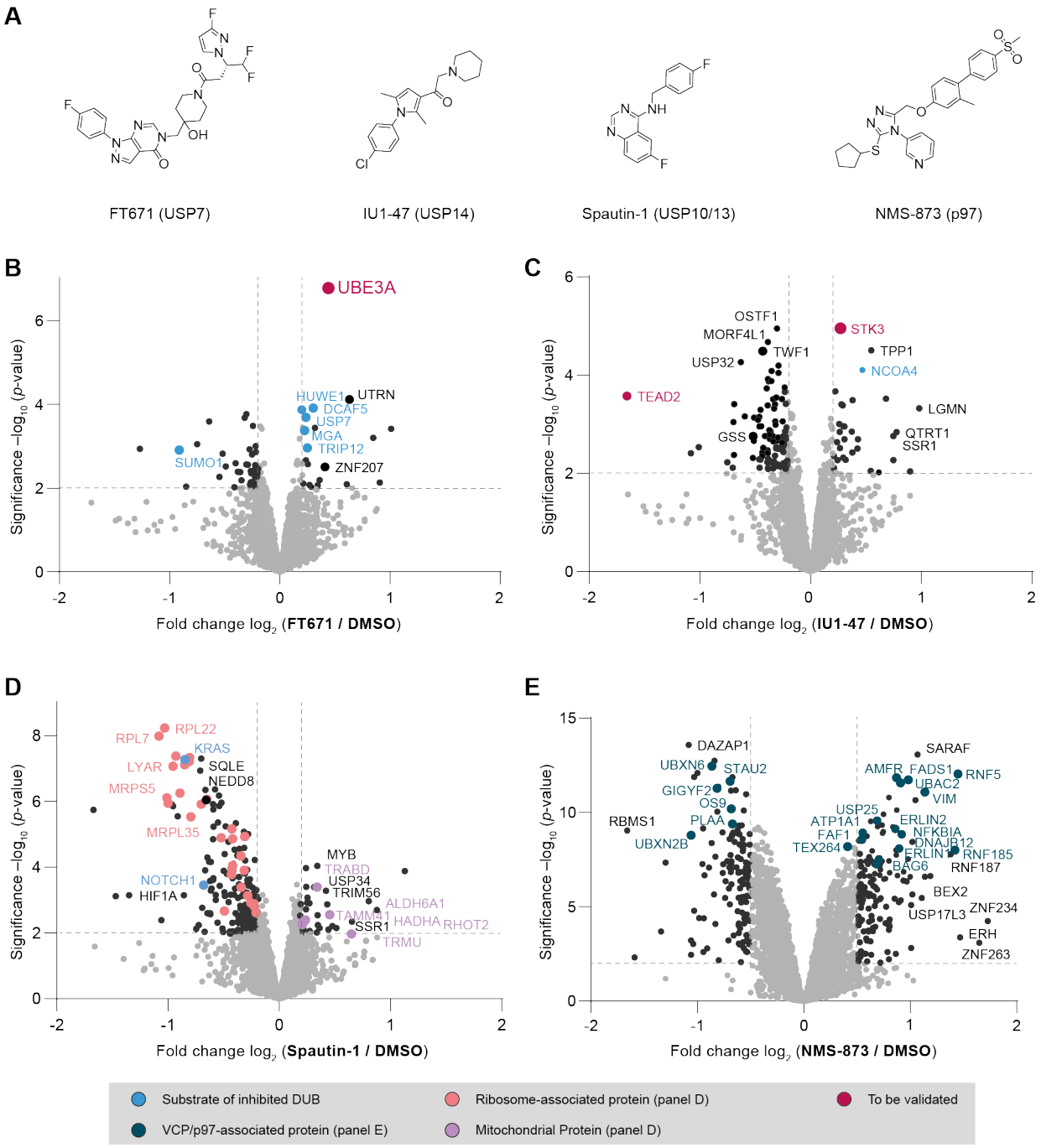

Figure 20: *Characterization of three different DUB inhibitors and the p97 inhibitor NMS-873 as comparison using TUBE-MS.* ***A****. Structural formulas of the inhibitors tested in the panels B-E.* ***B****. Volcano plot of TUBE-MS results of Jurkat cells being treated with the USP7 inhibitor FT671 (1 µM) for 4 h without proteasomal inhibition.* ***C****. Volcano plot of TUBE-MS results of Jurkat cells being treated with the USP14 inhibitor IU1-47 (25 µM) for 4 h without proteasomal inhibition.* ***D****. Volcano plot of TUBE-MS results of Jurkat cells being treated with the USP10/13 inhibitor Spautin-1 (10 µM) for 4 h without proteasomal inhibition.* ***E****. Volcano plot of TUBE-MS results of Jurkat cells being treated with the p97 inhibitor NMS-873 (5 µM) for 5 h with proteasomal inhibition (500 nM CFZ). All proteomics measurements shown in this figure were measured in four biological replicates and analyzed using FragPipe and Fragpipe Analyst. The legend annotates selected hit proteins. This figure was modified from Führer, S. et al. Small Molecule-Induced Alterations of Protein Polyubiquitination Revealed by Mass-Spectrometric Ubiquitome Analysis. Angew. Chem. Int. Ed. 64, e202508916 (2025) under a CC-BY 4.0 license.*

these proteins. This phenomenon had to be further investigated and to be kept in mind when using TUBE-MS without proteasomal inhibition. To further characterize the alterations in the polyubiquitome that NMS-873 dual treatment with CFZ causes, we also compared the TUBE-MS fractions of Jurkat cells treated with both inhibitors to the ones treated only with CFZ (see Figure 20E). In contrast to the DUB inhibitor panel, we saw a drastic influence on the polyubiquitome, with several p97 associated proteins being changed in their ubiquitination state, which confirms the assay's sensitivity towards changes in protein ubiquitination. However, if one considers that this dataset already contained all CFZ-induced changes on the polyubiquitome as a background signal, the additional alterations caused by NMS-873 are so severe that it might overshadow subtle changes in protein polyubiquitination caused by non-characterized small molecules, which disqualifies this inhibitor combination to become a default for TUBE-MS discovery screenings. For a more unbiased screening, the compromise of looking at both sides of the volcano plot rather than to only focus on the enriched fractions, as it was the case cells with inhibited proteasome, and meanwhile lower the FC cut-offs from 0.5 to 0.2, as it was for the DUB inhibitor screening, was the more appealing setup to proceed with.

Overall, all three DUB inhibitors caused significant changes on the polyubiquitome, even though a signal-enhancing effect from carfilzomib or NMS-873 was missing, which proved the assay to be a versatile tool also for other application cases than PROTACs. As this dataset however was not capable to differentiate between degradative and non-degradative ubiquitination nor to discriminate the observed effects from the global protein abundance that caused proportionally enhanced ubiquitination, further validation experiments were necessary for some selected hit proteins (see Figure 20, marked in red).

4.2.2.1 Validation of selected Hit proteins

Recent reports linked the deubiquitinase USP14 to the Hippo pathway, which is regulating cancer progression in pancreatic ductal adenocarcinoma among others[135]. As the inhibition of USP14 not only caused the enhanced ubiquitination of its reported substrate the nuclear receptor coactivator 4 (NCOA4)[136], but also altered two members of the Hippo pathway, further validation of the latter proteins appeared promising. Orthogonally to the analysis of the protein's ubiquitination status, an immunoblotting experiment of the whole cell lysates used for proteomics gave insights into the protein regulation upon USP14 inhibition. At first, the western blot probing against the STK3 kinase showed a significant upregulation of the protein, which confirms the hypothesis, that the enrichment of the protein in TUBE-MS could also be derived from an enhanced expression and thus an equivalently higher degree of ubiquitination of STK3 (see Figure 21A&B). Contrary to this

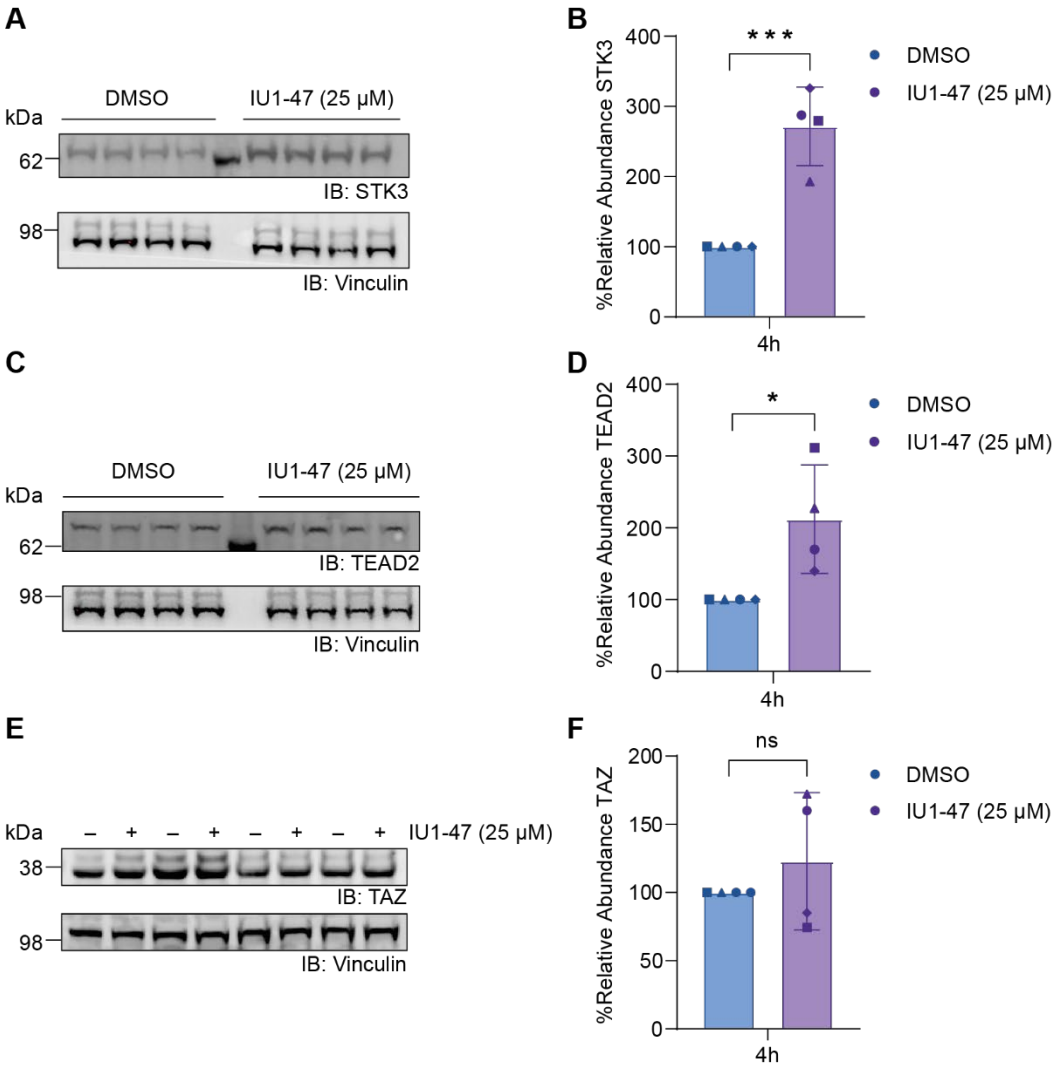

Figure 21: *Western blot analysis of selected members of the Hippo pathway in whole cell lysate from Jurkat cells treated with IU1-47 (25 µM) for 4 h.* ***A****. Immunoblot of whole cell lysate from Jurkat cells treated with IU1-47 or DMSO against STK3 and Vinculin as normalization signal. The immunoblot shows all four replicates of the experiment.* ***B****. Densiometric quantification of results shown in A normalized to Vinculin. STK3 is significantly upregulated in the treated condition.* ***C****. Immunoblot of whole cell lysate from Jurkat cells treated with IU1-47 or DMSO against TEAD2 and Vinculin as normalization signal. The immunoblot shows all four replicates of the experiment.* ***D****. Densiometric quantification of results shown in C normalized to Vinculin. TEAD2 is significantly upregulated in the treated condition.* ***E****. Immunoblot of whole cell lysate from Jurkat cells treated with IU1-47 or DMSO against TAZ and Vinculin as normalization signal. The immunoblot shows all four replicates of the experiment.* ***F****. Densiometric quantification of results shown in E normalized to Vinculin. TAZ is not significantly regulated in the treated condition. This figure was partially taken and modified from Führer, S. et al. Small Molecule-Induced Alterations of Protein Polyubiquitination Revealed by Mass-Spectrometric Ubiquitome Analysis. Angew. Chem. Int. Ed. 64, e202508916 (2025) under a CC-BY 4.0 license.*

finding, the second identified Hippo pathway member TEAD2 was less abundant in the treated conditions in TUBE-MS but at the same time showed increased levels in the whole cell lysate (see Figure 21C&D). This conflict pointed towards an uncoupling of global, unmodified protein abundance and TEAD2 ubiquitination, but the exact mechanism remained unclear. Notably, the

detection of TEAD2 in the immunoblot remained challenging and thus was prone to errors in the readout. In the attempt to further elucidate the connection between USP14 inhibition and the Hippo pathway, another essential member of it was analyzed by western blot. TAZ was not identified in the TUBE-MS analysis, so it was lacking a comparison in proteomics, but still was promising to elucidate the hypothesis of a Hippo pathway regulation by USP14 inhibition. The immunoblot of all lysates used for TUBE-MS did not show a regulation of TAZ by USP14 inhibition (see Figure 21E&F). Conclusively, these validation experiments could confirm the effect of expression regulation of certain proteins on the TUBE-MS analysis, even though the exact impact of IU1-47 on the hippo pathways remained unclear. Potentially, longer treatment time points are necessary to visualize the full impact of USP14 on the Hippo pathway, so future studies could include a proteome profiling of Jurkat cells after longer treatment using IU1-47.

In the TUBE-MS analysis of deubiquitinase inhibitors, the manyfold influences that the inhibition of the USPs 10 and 13 by Spautin-1 had on the polyubiquitome sparked an interest in further validating some of the significantly changed proteins. In this regard, KRAS as a reported upstream effector of USP10 activity was a promising validation candidate[137]. In the lack of a KRAS-specific antibody, an initial monitoring of panRas abundance in Jurkat cells using Spautin-1 over a duration of 48 h did not show an enhanced degradation of the protein class that would immediately confirm the observed reduction of polyubiquitination of KRAS in the TUBE-MS analysis (see Figure 22A&B). The challenging detection of KRAS by the usage of a panRas antibody continued in a following TUBE enrichment with a western blot-based readout, as the small molecular weight and the simultaneous detection of KRAS, NRAS and HRAS did not allow to draw any conclusions concerning the potential reduction of KRAS in the TUBE pulldown (see Figure 22C). Conclusively, no direct regulation of KRAS levels or its ubiquitination was confirmed by the validation experiments, so further attempts to elucidate the connection between USP10/13 inhibition and KRAS with orthogonal methods are necessary.

As the treatment of Jurkat cells with Spautin-1 furthermore caused the reduced ubiquitination of many ribosomal proteins, one protein from this group was selected for the monitoring of its global abundance in Spautin-1-treated cells. In a direct comparison with its levels in DMSO-treated cells, the levels of RPL23A did not significantly change (Figure 22D&E). Notably, also for this antigen the detection by immunoblot remained challenging. Nevertheless, a drastic regulation of RPL23A was unlikely. The reduced ubiquitination in TUBE-MS could have been an actual effect of Spautin-

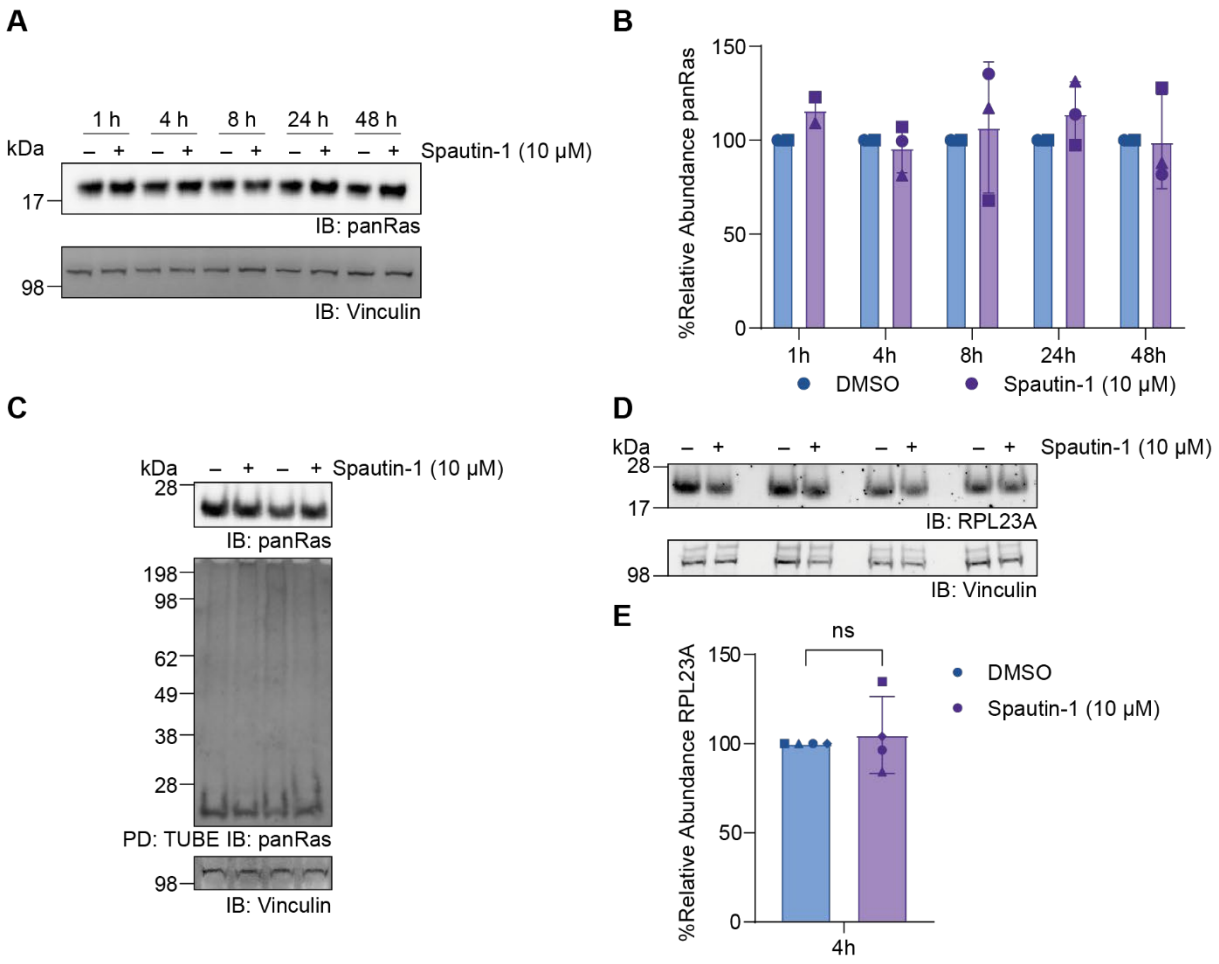

***Figure 22**: Validation of the Spautin-1 hit proteins KRAS and RPL23A by immunoblot-based experiments. **A**. Western blot analysis of the protein abundance of Ras proteins in whole cell lysate over a time course of 48 h, comparing cells treated with Spautin-1 and DMSO. **B**. Quantification of the results shown in A indicates no regulation of panRas protein levels upon Spautin-1 treatment. **C**. Immunoblot of TUBE pulldown eluates and input samples from Jurkat cells being treated with Spautin-1 for 4 h. **D**. Immunoblot against the ribosomal protein RPL23A from whole cell lysate from Jurkat cells being either treated with Spautin-1 or DMSO for 4 h. **E**. Quantification of the results shown in D shows no significant regulation of global RPL23A abundance. All results depicted in this figure are representative for at least three biological replicates if not indicated otherwise.*

1 treatment. Similar to KRAS, the actual role of USP10 and USP13 on the ubiquitination of ribosomal proteins remained unclear, making further validation experiments necessary in the future.

Finally, the inhibition of USP7 by the well-established small molecule FT671 resulted in the enrichment of several literature-reported substrate of the DUB in the TUBE-MS analysis (see Figure 20B, highlighted in blue). Besides the annotated USP7 substrates MGA, TRIP12, HUWE1 and DCAF5, of which the last three are E3 ligase proteins, USP7 itself was enriched[138,139]. This is consistent with reports assigning USP7 to auto-deubiquitinate itself, which in turn would mean

enhanced ubiquitination upon its inhibition by small molecules[140]. Indeed, the monitoring of USP7 levels over 48 h in lysates from Jurkat cells treated with FT671 showed decreased USP7 abundances over all replicates (see Figure 23). Notably, the change became already visible after

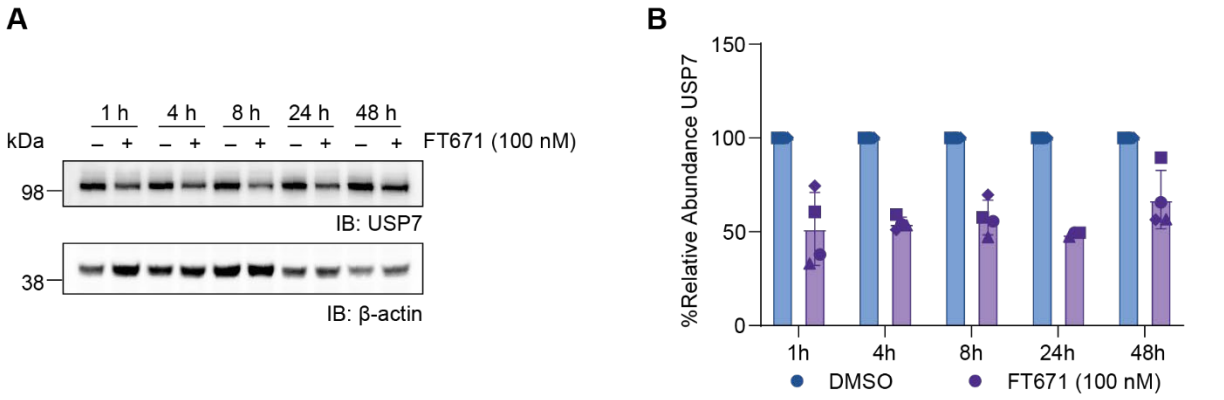

Figure 23: *Validation of USP7 as a hit protein in the TUBE-MS analysis of FT671.* ***A****. Immunoblotting analysis of the protein abundance of USP7 in whole cell lysate over a time course of 48 h, comparing cells treated with FT671 and DMSO. The shown result is representative for four biological replicates.* ***B****. Quantification of the results shown in A indicate downregulation of USP7 protein levels upon FT671 treatment.*

1 h of compound treatment and persisted up to 24 h in this extent. The reason for this reduction could either be the degradation of USP7, as a consequence of its inability to stabilize itself by deubiquitination when it is inhibited with FT671, or a relocalization or internalization of USP7 to cell compartments, which do not become accessible by the chosen cell lysis conditions. Either way, it was likely that this reduction was an immediate consequence of the cell treatment with FT671, as it already occurred after the first hour of incubation. Even though the exact mechanism of this phenomenon remains to be elucidated, the gained results were a good starting point for further experiments.

Nevertheless, when inspecting the TUBE-MS results of FT671, the most prominent and significant protein remained to be validated, which was the E3 ligase UBE3A.

4.2.2.2 Further characterization of UBE3A ubiquitination upon USP7 inhibition

UBE3A was reported to play an important role in human papilloma virus (HPV) infections due to its ability to ubiquitinate the tumor suppressor p53, thus making it an attractive target for drug discovery[141]. Still, until today, there was no immediate connection known between the E3 ligase and USP7, stressing the necessity to explore this hit protein more closely. At first, the enhanced polyubiquitination of UBE3A should become visible in an orthogonal readout, using TUBE-enrichments coupled to a western blot-based readout and varying concentrations of the FT671 inhibitor. This experiment confirmed the results of the proteomics analysis and showed a dose-dependent polyubiquitination of UBE3A upon treatment with FT671 (see Figure 24A). Another

ubiquitin enrichment comparing the signal from the polyUb preferring TUBE with the non-selective OtUBD (see section 4.1.1) indicated that the observed ubiquitination of UBE3A is mainly derived from longer chains rather than from a homologous mixture of also shorter chains, since no strong additional bands from mono- or diUb UBE3A appeared in the OtUBD eluates (see Figure 24B). Furthermore, the question arose if the observed ubiquitination of UBE3A is a consequence of the

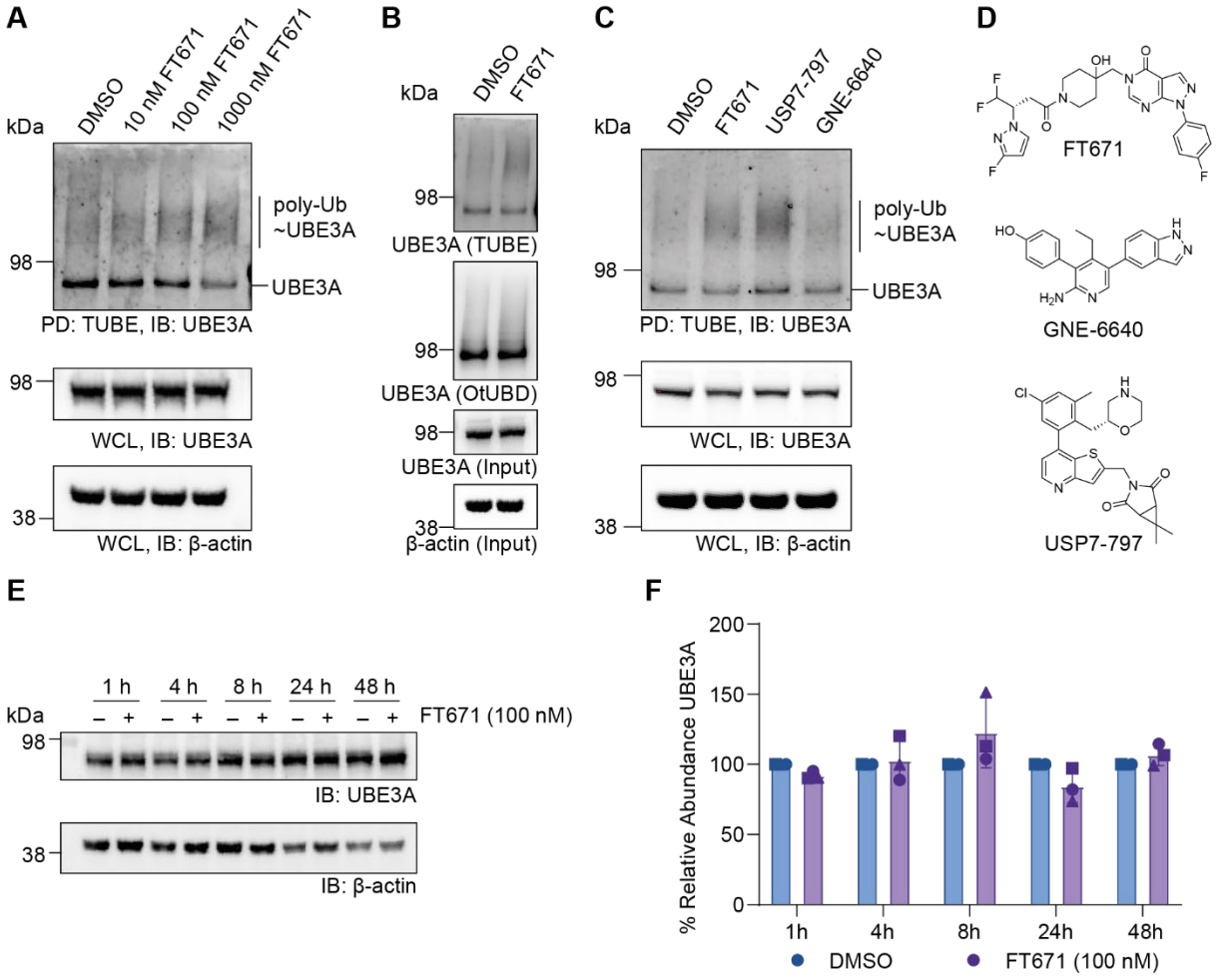

Figure 24: *Validation of the TUBE-MS hit protein UBE3A in the context of USP7 inhibition.* ***A****. Western blot analysis of TUBE PD and input fractions from Jurkat cell lysate after different treatment doses of FT671 or DMSO for 4 h as indicated. Immunoblotting against UBE3A and β-actin revealed a dose-dependent ubiquitination of UBE3A upon FT671 treatment.* ***B****. Western blot analysis of input fractions and eluates from ubiquitin enrichment from Jurkat cells being treated with FT671 (1 µM) or DMSO for 4 h against UBE3A and β-actin. Enrichment was either performed using Biotin-TUBE or Biotin-OtUBD as indicated.* ***C****. Immunoblot of TUBE PD eluates and input fractions from Jurkat cell lysate after treatment with three different USP7 inhibitors FT671 (1 µM), USP7-797 (0.5 µM), or GNE-6640 (5 µM) for 4 h against UBE3A and β-actin.* ***D****. Structural formulas of the inhibitors used in C.* ***E****. Immunoblot against UBE3A and β-actin from Jurkat cell lysate after treatment with either FT671 or DMSO for the indicated durations as a time course experiment.* ***F****. Quantification of the results shown in E suggest no regulation of global UBE3A abundance upon inhibition of USP7 using FT67. All experiments shown in this figure are representative for at least three biological replicates. This figure was partially taken and modified from Führer, S. et al. Small Molecule-Induced Alterations of Protein Polyubiquitination Revealed by Mass-Spectrometric Ubiquitome Analysis. Angew. Chem. Int. Ed. 64, e202508916 (2025) under a CC-BY 4.0 license.*

inhibition of USP7 as it would have been the case for a (novel) target of USP7 or if UBE3A is an off-target of FT671. Since preliminary attempts to answer this question by CoIP and cellular thermal shift assay (CETSA) experiments were not successful (see Supplementary Figure 1), variations of the TUBE PD using different USP7 inhibitors were more promising. Next to FT671, the structurally unrelated inhibitors USP7-797 and GNE-6640 had the same influence on the polyubiquitination of UBE3A, even though to different extents, which can be explained by different inhibitor potencies and MoAs (see Figure 24C&D). This proved the polyubiquitination of UBE3A to be related to USP7 inhibition, whether as an immediate USP7 substrate or through downstream effects and not derived from off-target effects of FT671.

Finally, the monitoring of the global target protein levels under treatment conditions, using FT671 or DMSO as a control, allowed for conclusions concerning the nature of the polyubiquitination that UBE3A carried. In a time course experiment comparing FT671-treated conditions with the untreated conditions in Jurkat cells, followed by immunoblotting, UBE3A did not show any major changes in its global levels up to 48 h of treatment (see Figure 24E&F). This indicated that the polyubiquitination of UBE3A was of a non-degradative nature.

Even though the exact mechanisms that connect UBE3A to USP7 remain to be elucidated, the findings in this context allowed for several conclusions concerning the quality and potential of the TUBE-MS method: First, the established assay can work with but does not necessarily require proteasomal inhibition to give meaningful results. Second, the low fold changes (FC) in the TUBE enrichment compared to other proteomics methods do not disqualify it from being a sensitive assay. As the hit protein UBE3A showed, also hits with low $\log_2$ FC can represent actual alterations of protein polyubiquitination when confident p values are reached. Finally, TUBE-MS is indeed able to detect also non-degradative ubiquitination, which gives the method a major advantage over comparable methods such as proteome profiling.

As TUBE-MS proved to work reliably for small molecules with confirmed MoA in the ubiquitin system, the next step was to investigate the assay’s potential regarding uncharacterized small molecules in the setup of a discovery screening.

4.2.3 Mass-spectrometric characterization of IDO1 degrader derivatives

Besides the common degrader molecule classes PROTACs and molecular glue degraders (see section 2.4), some small molecules possess a unique MoA that differs from the rationally designed degraders. A recent example is a family of monovalent pseudo-natural products (pseudoNPs), which destabilize the enzyme indoleamine-2,3-dioxygenase 1 (IDO1)[142]. IDO1 plays a crucial role in the tumor microenvironment[142]. Even though at the first glance, one might compare the mechanism of degradation with a molecular glue degrader, crystallization of IDO1 with one of the IDO1 degraders (iDegs) revealed that these molecules bind competitively to the natural co-factor heme, deeply buried inside its binding pocket[142]. By that the K-helix of the protein becomes mobilized and ubiquitinated by the natural IDO1 responsible E3 ligase KHLDC3, leading to its degradation[142]. This mechanism distinguishes the iDeg compound class from traditional E3-ligase-binding MGDs, opening up a new MoA for the targeted degradation of therapeutically relevant proteins.The discovery of the iDegs happened through an activity-based assay in cells, which read out the catalysis product of IDO1 and the enzyme arylformamidase, Kynurenine, a metabolite of Tryptophane[142]. With the advantage of covering both, inhibited catalytic activity as well as reduced protein abundance as a consequence of small molecule treatment, a negative result in this assay disqualified the substances from being neither a degrader, nor an inhibitor of IDO1. In the characterization of this substance family, several iDeg derivatives without activity in the Kynurenine assay accumulated. However, since the parental compounds had shown to be potent degraders, it was promising to test some of the inactive iDegs in TUBE-MS, using a cell line that does not express IDO1. With this, potential new molecules inducing ubiquitination could be identified. We thus chose a panel of 12 iDeg derivative compounds (Cmps), of which 10 were inactive in the Kynurenine (Kyn) assay, one was a potent degrader of IDO1 (Cmp 11, 38T2) and one was active in the Kyn assay, but contained a structurally distinct core scaffold (Cmp 12, iDeg7). I tested these substances in the TUBE-MS assay using 16 h of treatment time for each compound without proteasomal inhibition, 10 µM concentration in three biological replicates per Cmp or DMSO control and three TMTpro16-plex labels in Jurkat cells, which do not express IDO1 under normal conditions. A general inspection revealed that, compared to previous TUBE-MS analyses, less proteins were identified, ranging from around 3300 to 3900 identified proteins per plex. The reason for this could have been the increased treatment times from 4-5 to 16 h or technical limitations in the mass spectrometric readout. Nevertheless, every tested Cmp gave multiple hit proteins in the volcano plot evaluation of the TUBE-MS results (see Figure 25 and Figure 26).

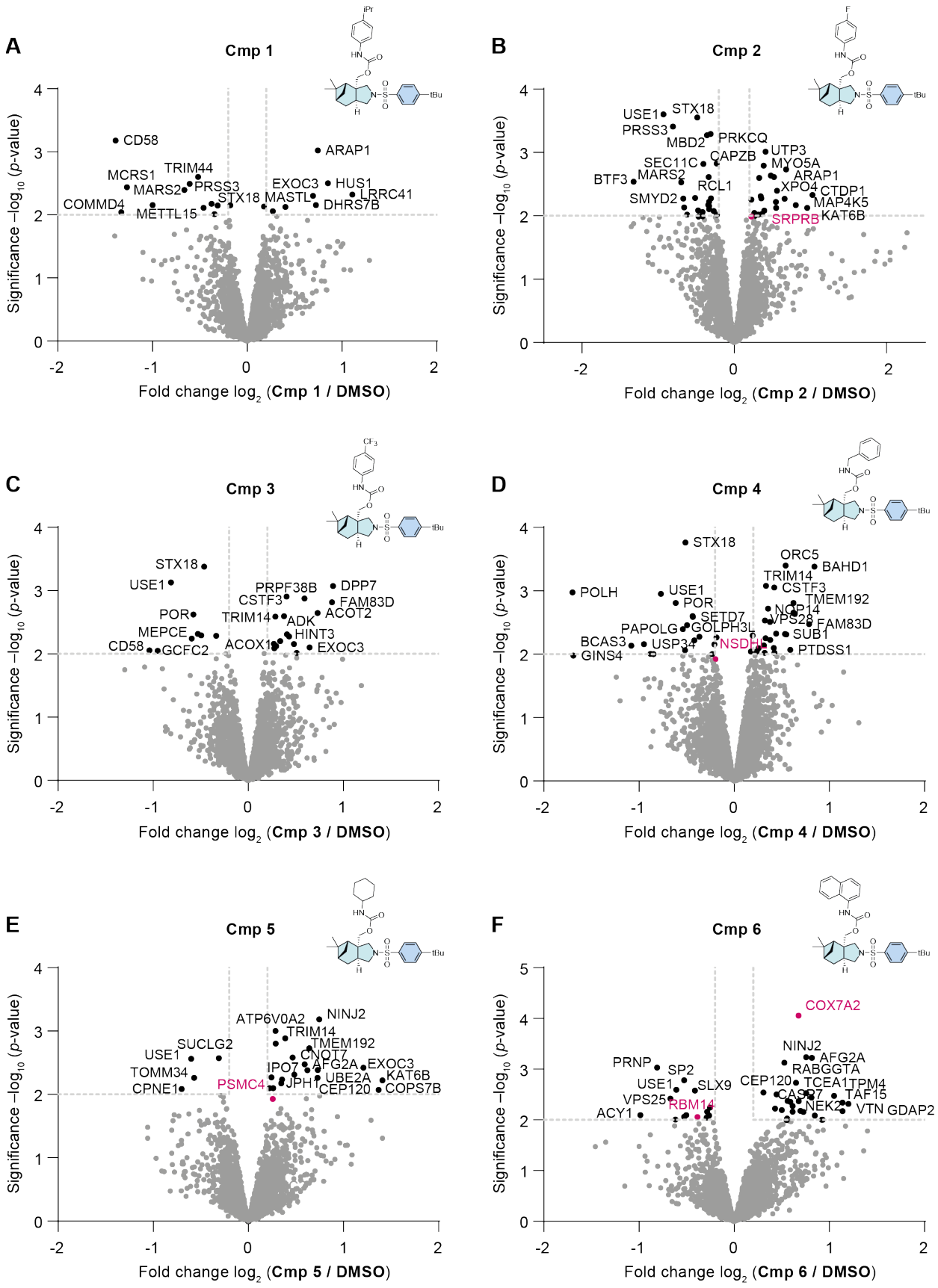
A
Cmp 1
Significance –log10 (p-value)
Fold change log2 (Cmp 1 / DMSO)
CD58
ARAP1
TRIM44
MCRS1
MARS2
PRSS3
EXOC3
HUS1
STX18
MASTL
LRRC41
COMMD4
METTL15
DHRS7B
B
Cmp 2
Fold change log2 (Cmp 2 / DMSO)
USE1
STX18
PRSS3
MBD2
PRKCQ
UTP3
CAPZB
SEC11C
MYO5A
BTF3
MARS2
ARAP1
RCL1
XPO4
CTDP1
SMYD2
MAP4K5
KAT6B
SRPRB
C
Cmp 3
Fold change log2 (Cmp 3 / DMSO)
STX18
USE1
PRPF38B
DPP7
CSTF3
FAM83D
ACOT2
POR
TRIM14
ADK
MEPCE
HINT3
CD58
GCFC2
ACOX1
EXOC3
D
Cmp 4
Fold change log2 (Cmp 4 / DMSO)
STX18
ORC5
BAHD1
TRIM14
CSTF3
POLH
USE1
TMEM192
POR
NCAPH2
SETD7
VPS28
FAM83D
PAPOLG
GOLPH3L
SUB1
BCAS3
USP34
NSDHL
PTDSS1
GINS4
E
Cmp 5
Fold change log2 (Cmp 5 / DMSO)
ATP6V0A2
NINJ2
TRIM14
SUCLG2
TMEM192
USE1
CNOT7
IPO7
AFG2A
EXOC3
TOMM34
UBE2A
KAT6B
PSMC4
JPH1
CEP120
COPS7B
CPNE1
F
Cmp 6
Fold change log2 (Cmp 6 / DMSO)
COX7A2
NINJ2
AFG2A
PRNP
SP2
RABGGTA
USE1
SLX9
CEP120
TCEA1TPM4
VPS25
CASP7
TAF15
RBM14
NEK2
ACY1
VTN GDAP2

Figure 25: A.-F. *Volcano plots of TUBE-MS results of iDeg derivative compounds (Cmps) 1-6 with their respective structural formula. Common motifs of the substances are highlighted. Jurkat cells were treated in three biological replicates per condition for 16 h with each substance in 10 µM concentration or DMSO as control. MS results were analyzed using FragPipe and FragPipe Analyst. Proteins were considered when they reached a p-value of -log10 ≤ 2 and -0.2 ≥ log2 FC ≥ 0.2. Proteins which were previously annotated to be heme-binding according to Homan et al., J Am Chem Soc (2022) 144(33)[143] are highlighted in red.*

As the parental compounds had a heme-competitive binding mode, the first filtering step in order to identify suitable hit proteins for further validations was to highlight previously annotated heme-binding proteins[142,143]. Though a variety of heme binders were significant hits (see Figure 25 and Figure 26, marked in red), the majority of hit proteins with confident p-values and FCs were not related to heme binding[143]. Another criterion for the selection of validation candidates involved the hit rate a protein had among the different Cmps. If the respective protein was significant in multiple analyses across the different TMTpro16-plex labels, it was more likely to be a positive hit. In combination with the annotation of being a heme-binding protein[143], the following hit proteins were promising candidates for further validation experiments (see Table 1).

Table 1: *Hit proteins form the TUBE-MS analysis of iDeg derivatives that were selected for further validation. The compounds that were used for the validation of the respective protein are underlined.*

Gene name	Significant in compound(s)	Hit score total	Significant over plexes	Potentially heme-binding
STX18	1,2,3,4,11,**12**	6	yes	no
USE1	2,3,4,5,**6**	5	yes	no
NINJ2	4,5,**6**,8	4	yes	no
POR	2,**3**,4,7	4	yes	yes
TRIM14	**3**,4,5	3	yes	no
DIABLO	(1),9,**12**	3	yes	no
MYO5A	2,**9**,10	3	yes	no
EMC7	**9**, 10	2	no	yes
RBM14	**6**	1	no	yes
COX7A2	**6**	1	no	yes

The further validation of these hit proteins involved the monitoring of their global abundance in whole cell lysate and the orthogonal detection of their polyubiquitination state using TUBE pulldowns couples to immunoblotting analyses.

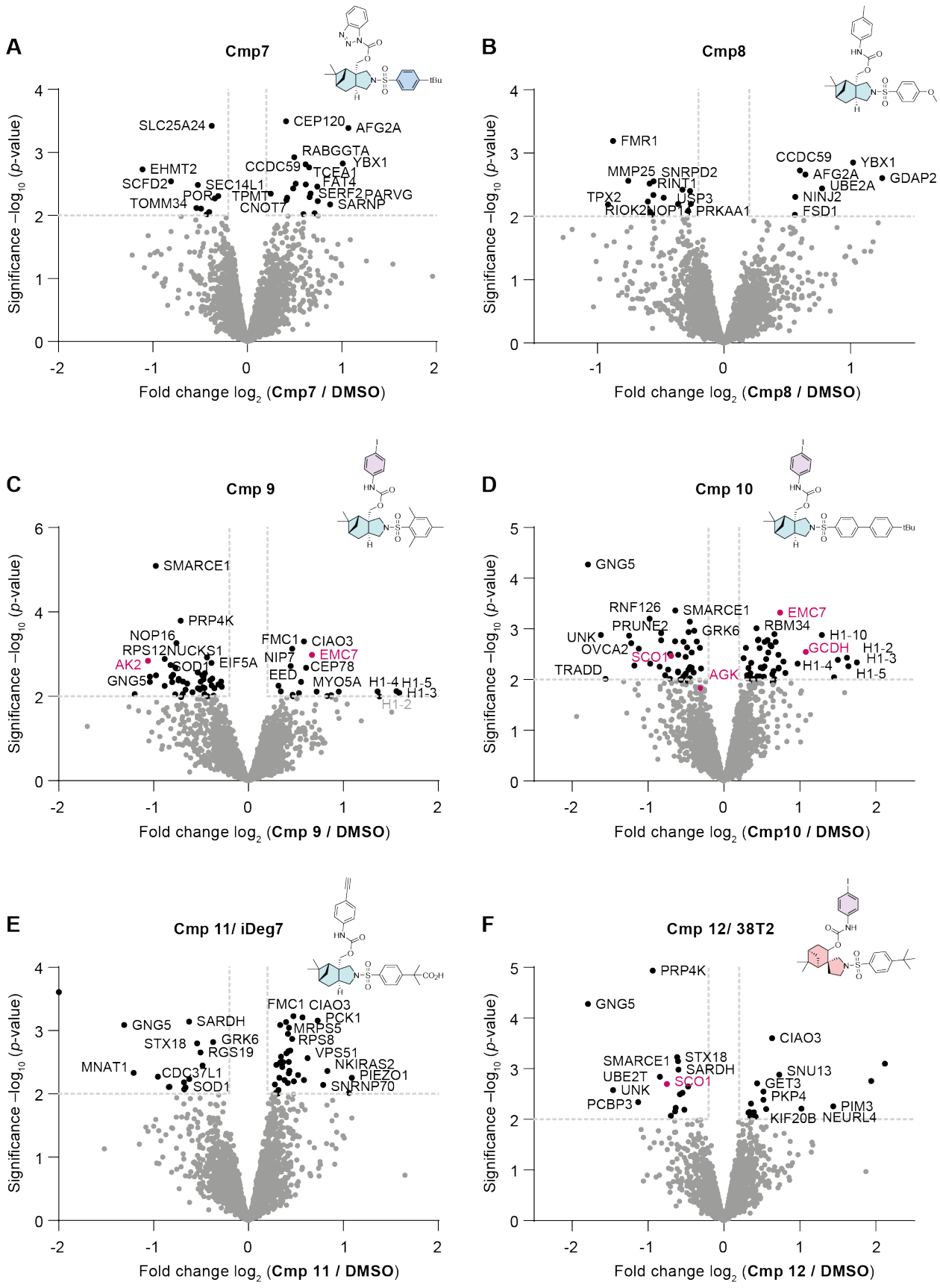
A
Cmp7
SLC25A24
CEP120
AFG2A
RABGGTA
YBX1
EHMT2
CCDC59
TCEA1
SCFD2
SEC14L1
FAT4
POR
TPMT
SERF2PARVG
TOMM34
CNOT7
SARNP
Significance –log10 (p-value)
Fold change log2 (Cmp7 / DMSO)
B
Cmp8
FMR1
CCDC59
YBX1
MMP25
SNRPD2
AFG2A
GDAP2
RINT1
UBE2A
TPX2
USP3
NINJ2
RIOK2
NOP14
PRKAA1
FSD1
Fold change log2 (Cmp8 / DMSO)
C
Cmp 9
SMARCE1
PRP4K
NOP16
FMC1
CIAO3
RPS12
NUCKS1
NIP7
EMC7
AK2
SOD1
EIF5A
CEP78
GNG5
EED
MYO5A
H1-4
H1-5
H1-3
H1-2
Fold change log2 (Cmp 9 / DMSO)
D
Cmp 10
GNG5
RNF126
SMARCE1
EMC7
PRUNE2
GRK6
RBM34
UNK
H1-10
OVCA2
GCDH
H1-2
SCO1
H1-3
TRADD
AGK
H1-4
H1-5
Fold change log2 (Cmp10 / DMSO)
E
Cmp 11/ iDeg7
FMC1
CIAO3
GNG5
SARDH
PCK1
MRPS5
STX18
GRK6
RPS8
RGS19
VPS51
MNAT1
NKIRAS2
CDC37L1
PIEZO1
SOD1
SNRNP70
Fold change log2 (Cmp 11 / DMSO)
F
Cmp 12/ 38T2
PRP4K
GNG5
CIAO3
SMARCE1
STX18
SARDH
SNU13
UBE2T
SCO1
GET3
UNK
PKP4
PCBP3
PIM3
KIF20B
NEURL4
Fold change log2 (Cmp 12 / DMSO)

Figure 26: A.-F. *Volcano plots of TUBE-MS results of iDeg derivative compounds 7-12 with their respective structural formula. Common motifs of the substances are highlighted. Jurkat cells were treated in three biological replicates per condition for 16 h with each substance in 10 µM concentration or DMSO as control. MS results were analyzed using FragPipe and FragPipe Analyst. Proteins were considered when they reached a p-value of -log10 ≤ 2 and -0.2 ≥ log2 FC ≥ 0.2. Proteins which were previously annotated to be heme-binding according to Homan et al., J Am Chem Soc (2022) 144(33)[143] are highlighted in red.*

4.2.3.1 Validation of selected hit proteins

For the confirmation of the observed effects in the TUBE-MS analysis, the proteins from Table 1 were each assigned to a compound from their respective significance group and validated in terms of its global abundance in a time course experiment comparing treated with untreated conditions up to 48 h. Secondly, TUBE enrichments with a western blot readout gave insights into the polyubiquitination signals of the POIs. The validation campaign involved compounds 3,6,9, and 12.

Compound 3

The treatment of Jurkat cells with the iDeg derivative 3 yielded in the significant enrichment of the E3 ligase TRIM14 and the reduction of abundance of the polyubiquitination of the NADPH-

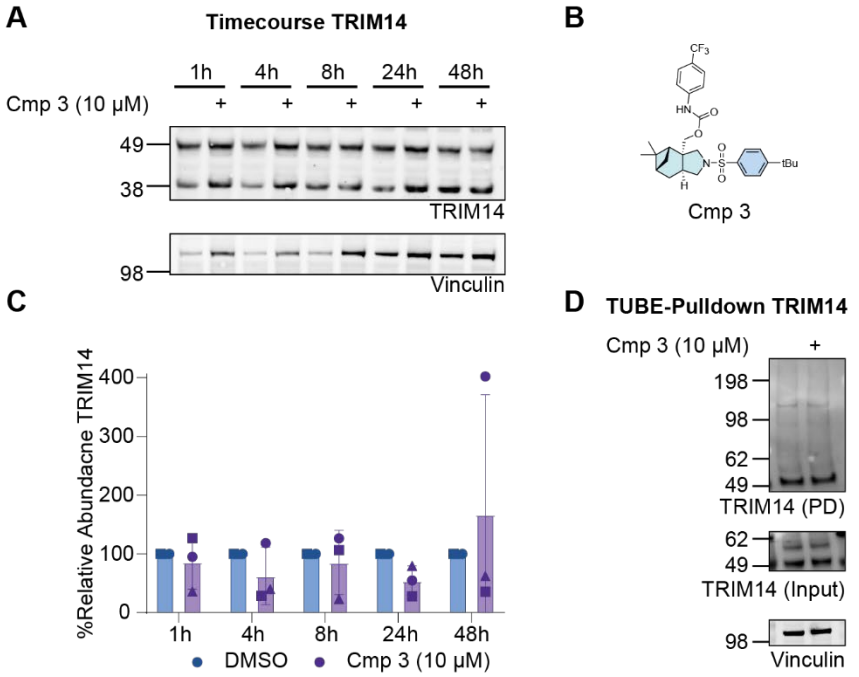

Figure 27: *Validation of the iDeg derivative screening hit protein TRIM14 using Cmp 3.* ***A****. Immunoblot of the time course experiment of global TRIM14 abundance in Cmp 3-treated Jurkat cells compared to DMSO for the incubation durations as indicated.* ***B****. Structural formula of the iDeg derivative Cmp 3.* ***C****. Quantification of the results shown in A.* ***D****. Immunoblot against TRIM14 and Vinculin of TUBE PD eluates and input fractions from Jurkat cells treated with Cmp 3 or DMSO for 16 h. All results shown in this figure are representative for at least three biological replicates. These experiments were performed together with Sarah Ballmann in the course of her Bachelor thesis.*

cytochrome P450 reductase POR in the TUBE-MS analysis[144,145]. In a first time course experiment examining the overall abundance of TRIM14 under Cmp 3-treated conditions compared to the DMSO conditions, the E3 ligase did not show a change in global abundance in the Jurkat cell lysate (see Figure 27A-C). Notably, the detection of the target protein turned out to be challenging, as the used polyclonal antibody gave several unspecific bands in the immunoblot detection. Furthermore, a western blot-based TUBE pulldown from Jurkat cells treated with Cmp 3 showed a slight increase of the polyubiquitination smear in the treated conditions, which was consistent with the findings in the TUBE-MS screen (see Figure 27D). However, the extent of this signal difference was small and could not be solidified in the other replicates of this experiment. Collectively, the increased signal derived from TRIM14 in the TUBE-MS was most likely not derived from a compound-induced ubiquitination that led to the degradation of the target protein. For a definite devalidation of TRIM14 as a hit protein, further experiments with more solid detection methods are needed.

The second Cmp 3-responsive hit protein was POR. Similar to the previous experiments concerning TRIM14, POR did not show a substantial decrease in overall protein abundance in the time course experiments (see Figure 28A-C). As the quality of the POR detection with the

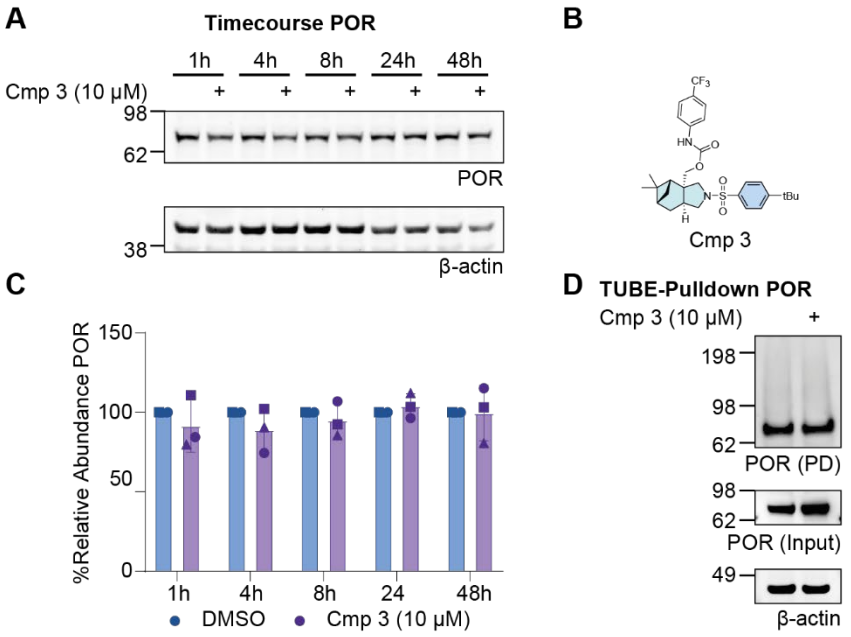

Figure 28: *Validation of the iDeg derivative screening hit protein POR using Cmp 3.* ***A****. Immunoblot of the time course experiment of global POR abundance in Cmp 3-treated Jurkat cells compared to DMSO for the incubation durations as indicated.* ***B****. Structural formula of the iDeg derivative Cmp 3.* ***C****. Quantification of the results shown in A.* ***D****. Immunoblot against POR and β-actin of TUBE PD eluates and input fractions from Jurkat cells treated with Cmp 3 or DMSO for 16 h. All results shown in this figure are representative for at least three biological replicates. These experiments were performed together with Sarah Ballmann in the course of her Bachelor thesis.*

respective antibody was of good quality, the observed steadiness of the global POR level upon Cmp3 treatment was reliable. However, the western blot-based TUBE-PD from Jurkat cells in this case could not confirm the observed TUBE-MS trend of less polyubiquitination of POR upon Cmp3 treatment, mainly due to a low degree of polyubiquitin smear detection in the immunoblot (see Figure 28D). This indicates that POR naturally only possesses a small fraction of its overall pool to be ubiquitinated, whether due to a slow turnover by degradative ubiquitination or other signaling mechanisms. Conclusively, the exact connection between Cmp 3 and POR ubiquitination remains unclear, though the underlying mechanism most likely is not based on compound-induced degradation.

Compound 6

Among other proteins, the treatment of Jurkat cells with Cmp 6 in the TUBE-MS screening caused the changed ubiquitination of SNARE protein USE1, the membrane protein NINJ2, the RNA-binding protein RBM14 and the mitochondrial cytochrome C oxidase COX7A2[146-149]. As a potentially heme-binding protein, COX7A2 was of particular interest for the hit validation. However, neither a time course experiment, nor a WB-based TUBE pulldown allowed for any

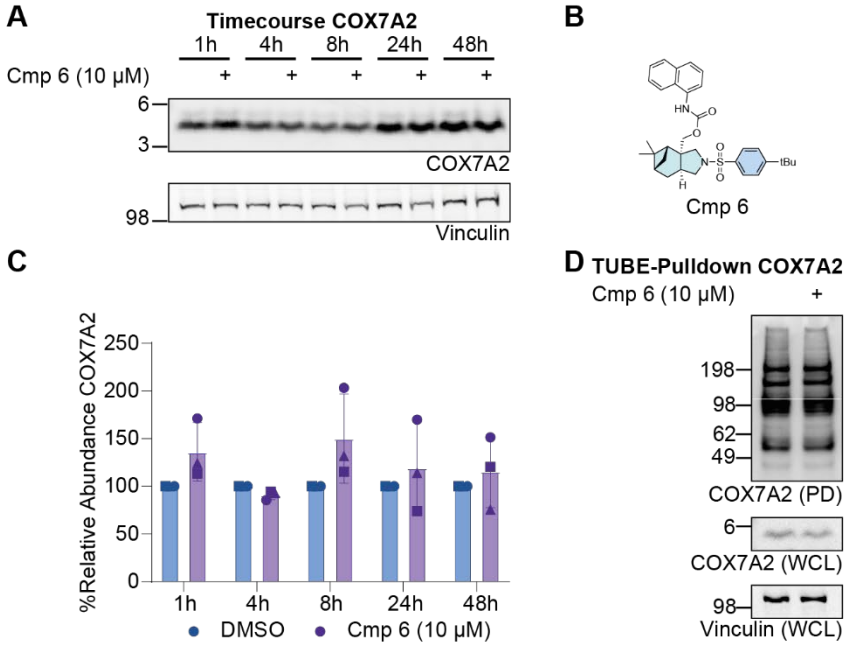

Figure 29: *Validation of the iDeg derivative screening hit protein COX7A2 using Cmp 6.* ***A****. Immunoblot of the time course experiment of global COX7A2 abundance in Cmp 6-treated Jurkat cells compared to DMSO for the incubation durations as indicated.* ***B****. Structural formula of the iDeg derivative Cmp 6.* ***C****. Quantification of the results shown in A.* ***D****. Immunoblot against COX7A2 and Vinculin of TUBE PD eluates and input fractions from Jurkat cells treated with Cmp 6 or DMSO for 16 h. The results shown in panel A are representative for three biological replicates, the experiment shown in panel D was performed only once, due to the challenging detection of the antigen. These experiments were performed together with Sarah Ballmann in the course of her Bachelor thesis.*

conclusion concerning its regulation upon Jurkat treatment with Cmp 6 (see Figure 29). As the overall constant abundance of COX7A2 pointed towards a non-degradative regulation of COX7A2, the detection of the ubiquitinated protein in the TUBE-WB experiment was hampered by the appearance of many unspecific bands, thus not allowing for a conclusive confirmation of the TUBE-MS experiments. Overall, the validation experiments of COX7A2 allowed for the exclusion of an immediate, degradative effect of Cmp 6 on the target protein.

Next, we investigated the influence of Cmp 6 on the global levels of USE1 in a time course experiment (see Figure 30A-C). Even though constant in the average protein abundance, the

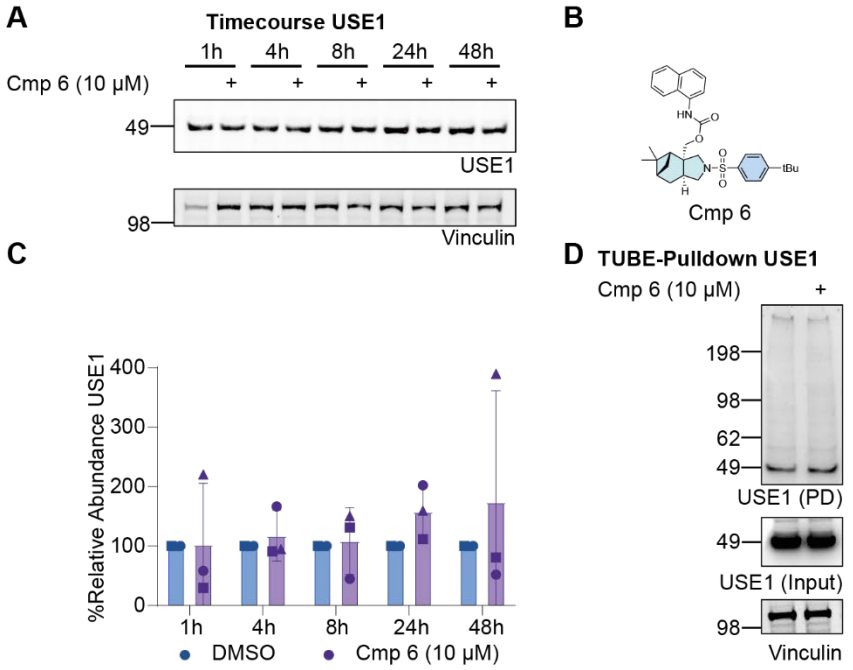

Figure 30: *Validation of the iDeg derivative screening hit protein USE1 using Cmp 6.* ***A****. Immunoblot of the time course experiment of global POR abundance in Cmp 6-treated Jurkat cells compared to DMSO for the incubation durations as indicated.* ***B****. Structural formula of the iDeg derivative Cmp 6.* ***C****. Quantification of the results shown in A.* ***D****. Immunoblot against USE1 and Vinculin of TUBE PD eluates and input fractions from Jurkat cells treated with Cmp 6 or DMSO for 16 h. All results shown in this figure are representative for at least three biological replicates. These experiments were performed together with Sarah Ballmann in the course of her Bachelor thesis.*

individual abundance values of USE1 showed severe variances. By visual inspection of the immunoblots, no regulation of the protein in its unmodified levels appeared, allowing for the exclusion of a degradative regulation by Cmp 6. In the immunoblot-based TUBE enrichment, the TUBE-MS results of decreased ubiquitination of USE1 by Cmp 6 treatment were only confirmed by one replicate, but not reproducibly detected in the other replicates (see Figure 30D). The generally low intensity of USE1 ubiquitination in the western blot and its broad distribution over a wide range of MWs made the data interpretation challenging. These results gave a first hint that

the TUBE pulldown readout by immunoblotting may not be the optimal validation strategy for high-sensitivity mass spectrometry results of small proteins.

To further characterize the hit proteins which not only were significant in the results of Cmp 6, but also other iDeg derivatives, we tested whole cell lysate of Jurkat cells treated with Cmp 6 against NINJ2 in an immunoblotting experiment (see Figure 31 A-C).

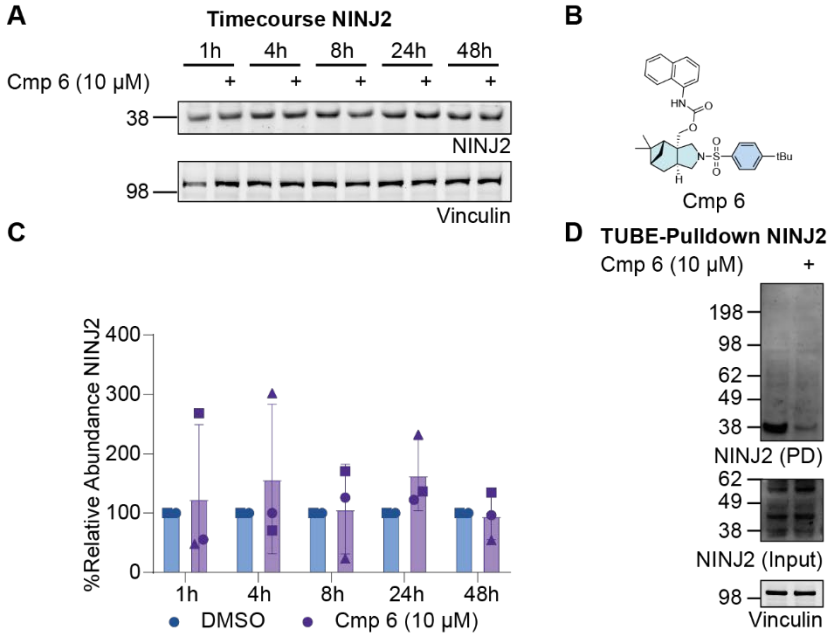

***Figure 31**:Validation of the iDeg derivative screening hit protein NINJ2 using Cmp 6. **A**. Immunoblot of the time course experiment of global NINJ2 abundance in Cmp 6-treated Jurkat cells compared to DMSO for the incubation durations as indicated. **B**. Structural formula of the iDeg derivative Cmp 6. **C**. Quantification of the results shown in A. **D**. Immunoblot against NINJ2 and Vinculin of TUBE PD eluates and input fractions from Jurkat cells treated with Cmp 6 or DMSO for 16 h. All results shown in this figure are representative for at least three biological replicates. These experiments were performed together with Sarah Ballmann in the course of her Bachelor thesis.*

Similar to the previous iDeg validation results, NINJ2 showed no change in the global expression levels in cells over a duration of up to 48 h. Contrary to the TUBE-MS results of this protein, the immunoblot-based TUBE enrichment showed no increase in the signal derived from the polyubiquitin smear, but a reduced amount of unmodified NINJ2 being pulled down (see Figure 31D). As evident from the input fractions of the TUBE-pulldown, the antibody used for the detection of NINJ2 gave signals also for many unspecific bands, complicating the data interpretation in this case. Lastly, the low MW of NINJ2 caused the polyubiquitin smear to be distributed over a longer distance, decreasing signal density and thus the characterization of polyubiquitination of the protein. Conclusively, we could not confirm the effect of Cmp 6 treatment on NINJ2 polyubiquitination, but were able to exclude that the observed effects in TUBE-MS are derived from a Cmp 6-induced degradation of the protein.

Finally, the transcription regulator RBM14 was left as a potentially heme-binding protein to respond to Cmp 6 treatment. In the time course experiment, the protein showed constant expression levels (see Figure 32A-C). However, the TUBE-PD from Jurkat lysate derived from

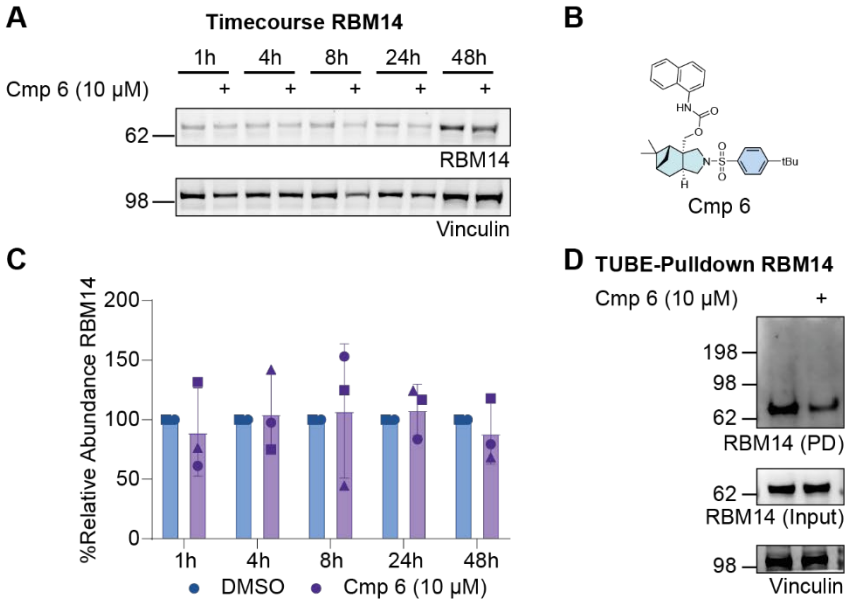

Figure 32: *Validation of the iDeg derivative screening hit protein RBM14 using Cmp 6.* ***A****. Immunoblot of the time course experiment of global RBM14 abundance in Cmp 6-treated Jurkat cells compared to DMSO for the incubation durations as indicated.* ***B****. Structural formula of the iDeg derivative Cmp 6.* ***C****. Quantification of the results shown in A.* ***D****. Immunoblot against RBM14 and Vinculin of TUBE PD eluates and input fractions from Jurkat cells treated with Cmp 6 or DMSO for 16 h. All results shown in this figure are representative for at least three biological replicates. These experiments were performed together with Sarah Ballmann in the course of her Bachelor thesis.*

Cmp 6- or DMSO- treated cells, could confirm the observation made in the TUBE-MS analysis (see Figure 32D). Even though the signal intensity of polyubiquitinated RBM14 was low compared to other reported cases, such as UBE3A (see section 4.2.2.2), the validation target showed repeatedly reduced polyUb-RBM14 signal in the treated condition, which reflected the TUBE-MS results. In view of the intended discovery of new degrader molecules however, the constant protein levels in the time course experiment argued against an immediate compound-derived effect, especially after a prolonged incubation of 16 h in the initial screening, which allows also expression-related effects to occur more likely than for shorter treatment times. Thus, the validation of Cmp 6 concluded without the identification of a novel degrader target.

Compound 9

Besides several other significant hits, the treatment of cells with Cmp 9 and its ubiquitome analysis using TUBE-MS caused the enrichment of the endoplasmic reticulum membrane protein complex protein EMC7 and the actin-based motor protein MYO5A[150,151]. Though, after 16 h of

treatment, the probability of these enriched proteins to be degrader targets was low, it was still possible to monitor potential non-degradative effects.

First, the time course experiment of MYO5A abundances in Jurkat cells showed no substantial change in intervals up to 48 h, despite a slight trend towards elevated levels within the first 4 h (see Figure 33A-C). Due to its high MW and comparably low signal intensity, the detection of

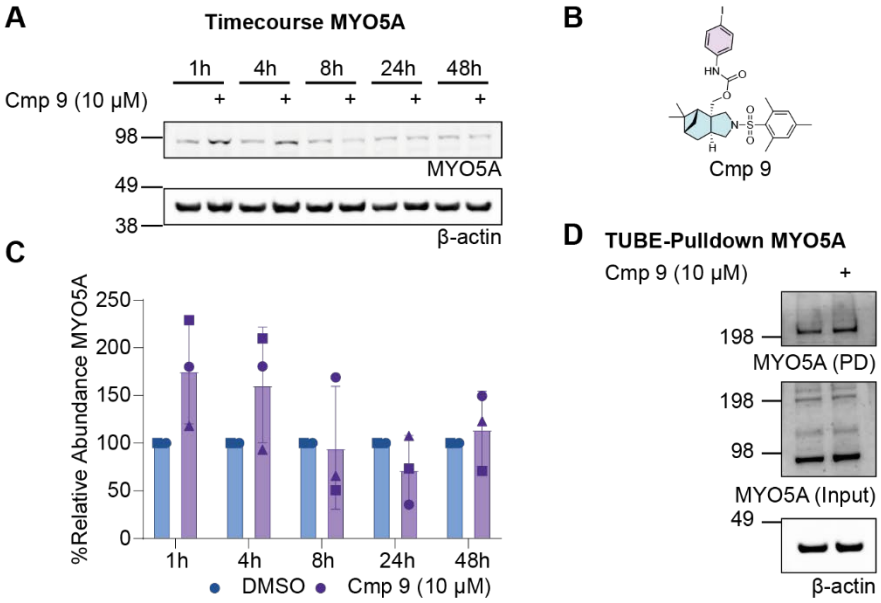

Figure 33: *Validation of the iDeg derivative screening hit protein MYO5A using Cmp 9.* ***A****. Immunoblot of the time course experiment of global MYO5A abundance in Cmp 9-treated Jurkat cells compared to DMSO for the incubation durations as indicated.* ***B****. Structural formula of the iDeg derivative Cmp 9.* ***C****. Quantification of the results shown in A.* ***D****. Immunoblot against MYO5A and β-actin of TUBE PD eluates and input fractions from Jurkat cells treated with Cmp 9 or DMSO for 16 h. All results shown in this figure are representative for at least three biological replicates. These experiments were performed together with Sarah Ballmann in the course of her Bachelor thesis.*

MYO5A in the immunoblot remained challenging, which most likely caused the drastic variance in the individual experimental replicates. The TUBE pulldown however, confirmed the effect of enhanced polyubiquitination in the treated conditions from the TUBE-MS analysis (see Figure 33D). An advantage over the previous validation proteins in this case was the high MW of MYO5A causing a stacking of the polyUb signal in a denser MW-area, facilitating the detection of the protein. We indeed observed elevated signals of polyUb-MYO5A in the Cmp 9-treated conditions, proving the reliability of the TUBE-MS results and indicating a non-degradative polyubiquitination of MYO5A as a consequence of Cmp 9 treatment. Nevertheless, the actual mechanism of this effect remains to be elucidated.

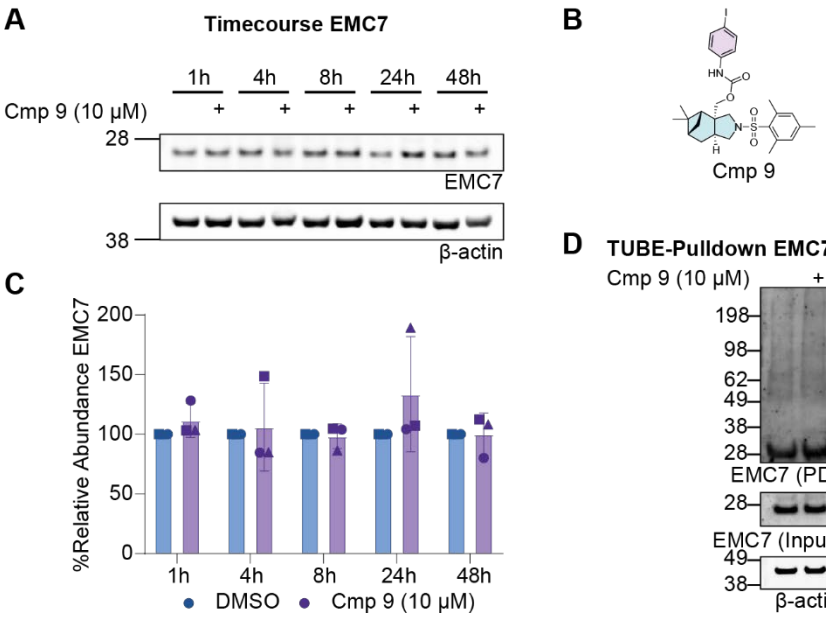

Figure 34: *Validation of the iDeg derivative screening hit protein EMC7 using Cmp 9.* ***A****. Immunoblot of the time course experiment of global EMC7 abundance in Cmp 9-treated Jurkat cells compared to DMSO for the incubation durations as indicated.* ***B****. Structural formula of the iDeg derivative Cmp 9.* ***C****. Quantification of the results shown in A.* ***D****. Immunoblot against EMC7 and β-actin of TUBE PD eluates and input fractions from Jurkat cells treated with Cmp 9 or DMSO for 16 h. All results shown in this figure are representative for at least three biological replicates. These experiments were performed together with Sarah Ballmann in the course of her Bachelor thesis.*

In line with the effects observed for the global MYO5A levels, EMC7 did not change its expression levels in the time course experiment (see Figure 34A-C). In the TUBE-WB experiments however, it confirmed its results from the TUBE-MS assay (see Figure 34D). Indeed, EMC7 showed elevated signals of polyubiquitination in the Cmp 9-treated conditions, which, together with the time course experiments, gave a first hint towards a non-degradative ubiquitination in response to the small molecule. If this effect is primarily related to Cmp 9 and the other iDeg derivatives, which caused EMC7 enrichment, remains unclear. Still, the annotation of EMC7 as a heme-binding protein[143] supports a connection to the iDeg derivative treatment.

Compound 12

Compound 12 (iDeg7) was the only further validated substance, which had a proven activity towards IDO1. Thus, the motivation behind its characterization in the TUBE-MS assay was, in the first place, a confirmation of its selectivity. However, the proteomics analysis after 16 h of treatment gave several hit proteins to be changed in their polyubiquitination state, so their validation was crucial to exclude off-targets of Cmp 12. In this regard, DIABLO, a mitochondria-derived activator of caspases, and Syntaxin 18 (STX18), an ER SNARE protein, were promising candidates, as they were also hit proteins in analyses of other iDeg derivatives[152,153].

DIABLO, as the first of the two validation candidates for Cmp 12, in a first time course experiment did not show any clear trends towards an altered abundance in treated Jurkat cells up to 48 h (see Figure 35A-C). A slight decrease in the levels after 4 h of treatment became visible, but

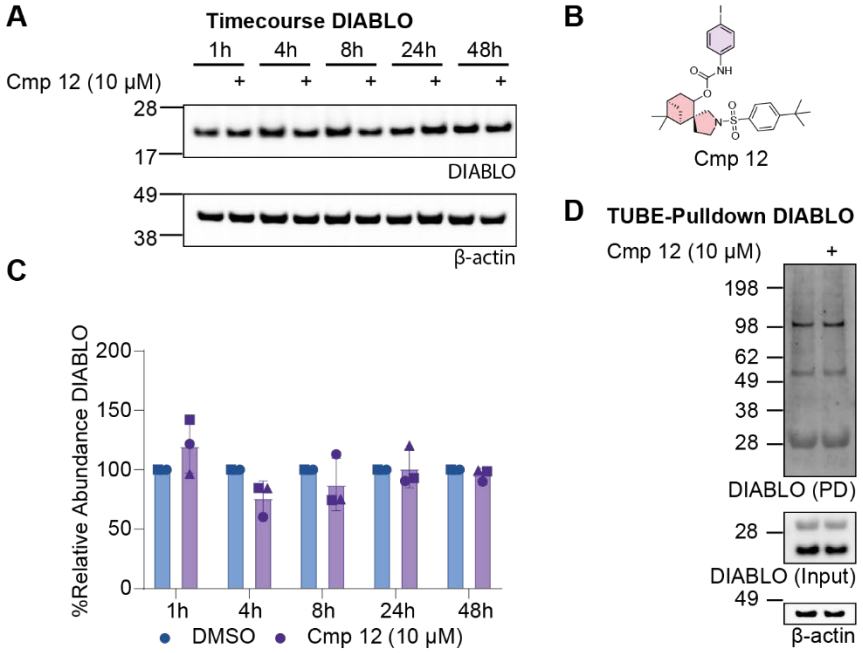

Figure 35: *Validation of the iDeg derivative screening hit protein DIABLO using Cmp 12.* ***A****. Immunoblot of the time course experiment of global DIABLO abundance in Cmp 12-treated Jurkat cells compared to DMSO for the incubation durations as indicated.* ***B****. Structural formula of the iDeg derivative Cmp 12.* ***C****. Quantification of the results shown in A.* ***D****. Immunoblot against DIABLO and β-actin of TUBE PD eluates and input fractions from Jurkat cells treated with Cmp 12 or DMSO for 16 h. All results shown in this figure are representative for at least three biological replicates. These experiments were performed together with Sarah Ballmann in the course of her Bachelor thesis.*

quickly went back to the DMSO levels, which disproved the hypothesis of DIABLO being a degrader target of Cmp 12. Similar to these results, the TUBE enrichment with an immunoblot-based readout could not confirm the results from the TUBE-MS analysis, which showed DIABLO to be less polyubiquitinated under treated conditions (see Figure 35D). Instead, the detection of polyubiquitination of the low MW protein in the immunoblot remained challenging and did not show a difference between the treated and the control conditions. Conclusively, DIABLO could be devalidated as an off-target of Cmp 12.

Finally, we validated Syntaxin 18 as a potential degrader off-target. Interestingly, the initial results of the global protein levels suggested a degradative effect of Cmp 12 on STX18 (see Figure 37A-C). After closer inspection, however, it was clear that the regulation by Cmp 12 rather happened

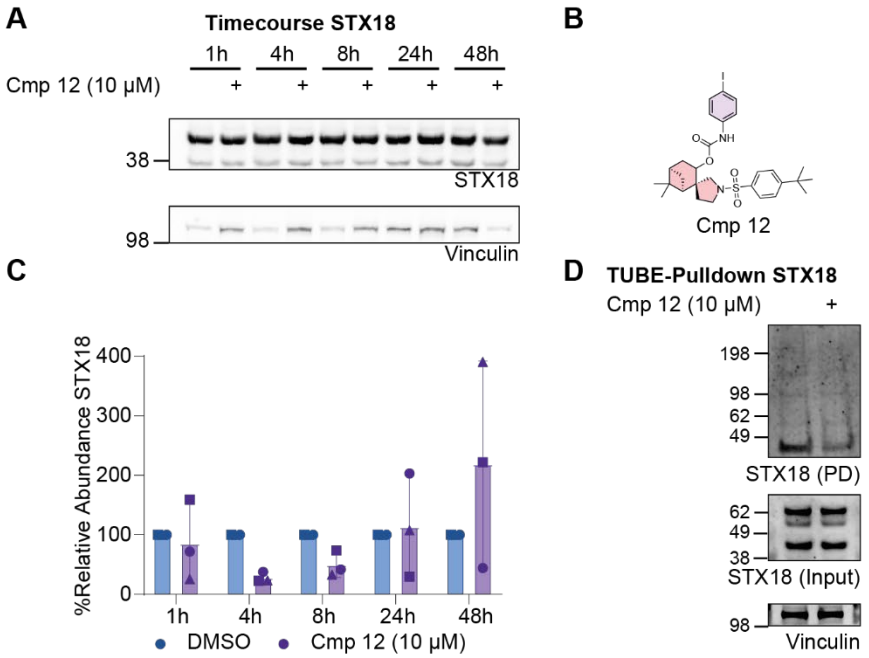

Figure 37: *Validation of the iDeg derivative screening hit protein STX18 using Cmp 12.* ***A****. Immunoblot of the time course experiment of global STX18 abundance in Cmp 12-treated Jurkat cells compared to DMSO for the incubation durations as indicated.* ***B****. Structural formula of the iDeg derivative Cmp 12.* ***C****. Quantification of the results shown in A.* ***D****. Immunoblot against STX18 and Vinculin of TUBE PD eluates and input fractions from Jurkat cells treated with Cmp 12 or DMSO for 16 h. All results shown in this figure are representative for at least three biological replicates. These experiments were performed together with Sarah Ballmann in the course of her Bachelor thesis.*

on the level of the housekeeping protein, in this case Vinculin, whose levels were steadily changing, irrespective of the replicate of this experiment. This hypothesis was confirmed by a

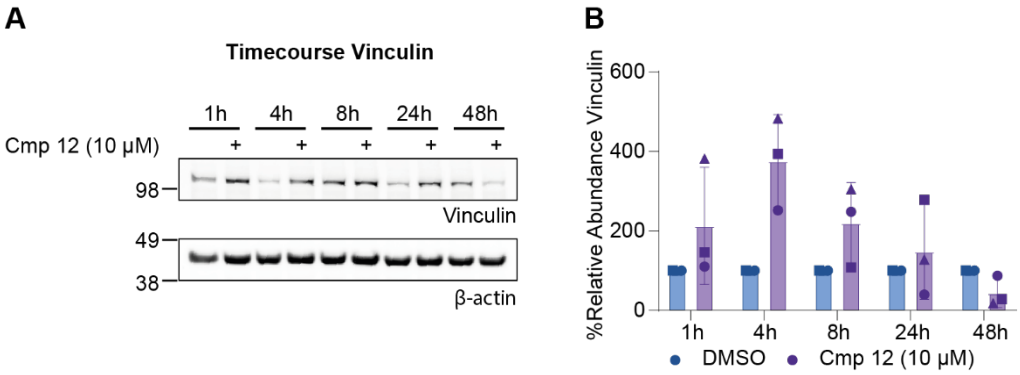

Figure 36*: Time course experiment showing the upregulation of Vinculin by Cmp 12.* ***A****. Immunoblot of the time course experiment of global Vinculin abundance in Cmp 12-treated Jurkat cells compared to DMSO for the incubation durations as indicated.* ***B****. Quantification of the results shown in A. The results shown in this figure are representative for three biological replicates. The experiments were performed together with Sarah Ballmann in the course of her Bachelor thesis.*

direct comparison between the two housekeeping genes used for the validation experiments of Cmp 12 (see Figure 36). The quantification of Vinculin against β-actin revealed a more than 3-fold increase of Vinculin levels within the first 4 h of incubation with Cmp 12. While the exact reason for this regulation remains unclear, it indicated that STX18 was not actually changed in its abundance by Cmp 12 treatment. Notably, the TUBE pulldown fractions from compound-treated vs. control cells in the immunoblot against STX18 confirmed the TUBE-MS results observed for STX18 (see Figure 37D). As in the proteomics results, the enrichment of polyubiquitnated proteins showed less modified STX18 in the treated condition. However, this effect was difficult to detect, as the signal intensity was low and broadly distributed over the blotting area. Additionally, also less unmodified STX18 was enriched, which could have impaired also the mass spectrometric results in the initial screening. Furthermore, the steady levels of STX18 in the timecourse experiment suggested a non degradative influence of Cmp 12 on the target protein, devalidating it as an off-target of iDeg7.

STX18 concluded the validation campaign of the ten selected hit proteins from the iDeg derivative screening by TUBE-MS. Even though no novel degrader targets were identified, the immunoblotting-based TUBE enrichments confirmed several effects seen in the proteomics analysis (e.g. STX18, RBM14, MYO5A, EMC7). However, the signal quality of the WB-based TUBE pulldowns was often low and barely distinguishable. This points out two major drawbacks of the TUBE-MS validation by immunoblotting. Firstly, the success of the orthogonal readout strongly depends on the availability and quality of the respective antibody. Secondly, POIs with low molecular weights cause a highly distributed polyUb signal in the western blot, reducing the intensities of often low abundant signals, as it is the case for a setup without proteasomal inhibition, to a minimum.

One way to circumvent the latter issue could be to increase the input amounts of lysate that are sufficient for proteomics, but in many cases not for an immunoblot-based readout. A second strategy to also avoid false-positive results in the overall abundance measurements by the regulation of the housekeeping gene, as it happened for the regulation of Vinculin by Cmp 12 could be to monitor the abundances of all unmodified proteins by mass spectrometry namely a proteome profiling of the input lysates used for TUBE-MS.

This was the procedure of choice for the next application cases of TUBE-MS, the characterization of hit compounds from a phenotypic screen to validate their proposed MoA in the UPS.

4.2.4 Characterization of proteasome cluster compound candidates by mass spectrometry

The cell painting assay is a morphological profiling approach that enables the characterization of small molecules, genetic perturbations, or entire disease states by quantifying phenotypic changes in, in this case, 579 features of treated cells after staining and fluorescence microscopy[154]. The combination of the results of all features for each compound allows to generate a so-called fingerprint profile consisting of a heat map barcode for the substance's phenotypic features[154].

Similar profiles are often caused by the same MoA, which can be used to predict the MoA of other substances[154]. As this prediction is not always straightforward, defining bioactivity clusters for reference substances based on profile similarity facilitates MoA prediction[154]. This approach is further supported by extracting cluster sub-profiles containing only the features that are similarly altered by substances with similar profiles[154].

If a well-characterized small molecule is part of a certain cluster, its profile in many cases leads to the assignment of a bioactivity to the respective cluster based on multiple reference compounds[154]. Once a cluster is established, it can facilitate the discovery of novel bioactive small molecules via profiling by the cell painting assay and the identification of biosimilar substances[154,155]. However, to be a reliable tool in drug discovery, the cluster's actual bioactivity has to be validated[155]. In the past, this need was successfully met with proteomic analyses of global protein level changes induced by potential cluster members[155]. Among further downstream validation experiments, proteome profiling can give a first hint towards the regulation of protein families, signaling pathways or whole cell states[155]. As such, proteomics is a powerful tool as a follow-up method on phenotypic screens.

Small molecules that act on the UPS have great therapeutic potential (see section 2.4). The general alterations in protein ubiquitination that are caused by proteasome inhibitors, leading to cell death in many tumors, are already used in the clinics, for example in the treatment of myeloma (see section 2.4)[49]. Therefore, it would be invaluable to facilitate the discovery of substances acting either on the proteasome itself or connected pathways and proteins by a cluster allowing for biosimilar assignment in phenotypic screens, such as the cell painting assay.

For this purpose, the group of Dr. Slava Ziegler, together with the compound management and screening center (COMAS) of the Max Planck Society, run a cell painting analysis (CPA) to

identify if well-characterized and structurally different proteasome inhibitors are active in the assay and if the individual reference substances show similar CPA profiles. This approach was successful and furthermore identified several research compounds, which showed biosimilarity to the proteasome inhibitors. For the validation of the cluster-related activity, proteomics was the method of choice and since TUBE-MS provided the basis for a targeted investigation of compound-induced ubiquitination and deubiquitination, I tested three initial cluster substances in comparison to the proteasome inhibitor carfilzomib using the assay.

As the previous validation campaign for the iDeg derivatives displayed the disadvantages of immunoblot-based validations of overall protein abundances (see section 4.2.3.1) and since untargeted proteomics is able to quantify thousands of protein abundances in one analysis, we additionally ran a follow-up proteome profiling of the TUBE-MS input lysates. This allowed for a direct comparison of common TUBE-MS- and proteome profiling-increased proteins for each compound (see Figure 38). The TUBE-MS analysis contained a TMTpro16-plex labeling for multiplexing, while the proteome profiling included two TMT10-plexes with each two test compounds in three biological replicates. Consequently, we identified 5297 proteins in the TUBE-MS analysis, while the proteome profiling detected 5853 proteins for CFZ and Cmp 13 and 5858 proteins for Cmp 14 and 15. The increased identification rate for the proteome profiling was in line with the expectation that the TUBE-MS analysis is dealing with a reduced proteome after the enrichment of polyUb proteins. In view of this, the number of identified proteins for this TUBE analysis was particularly high, especially when comparing it to the around 3000 proteins identified in the iDeg derivative screening (see section 4.2.3).

Carfilzomib

As the reference compound for this potential cluster, carfilzomib (CFZ) showed the most significant changes in the polyubiquitome analysis with 792 enriched proteins (see Figure 38A). Contrary to the expected tilt of the volcano plot towards the enriched side, caused by the accumulation of polyubiquitinated proteins inside the cell upon proteasomal inhibition, 485 proteins also showed less ubiquitination. Notably, some of these changes might be a result of the necessary median-centered normalization of the dataset, in order to obtain reliable quantification results also for the three research compounds 13, 14, 15. However, one example from this protein group was mortality factor 4-like 1 (MORF4L1, highlighted in red), which has previously been shown to be less ubiquitinated upon proteasomal inhibition and was also altered in a TUBE-MS analysis of CFZ after only 1 h of treatment (see Supplementary Figure 2C)[156]. Interestingly, this protein did not show significantly changed overall abundance in the proteome profiling (see Figure

38B), indicating that it is actual ubiquitination which causes the decrease in the TUBE-MS analysis. This is in line with a report stating that MORF4L1 levels globally increase upon proteasomal inhibition, while its ubiquitination decreases[156]. Interestingly, compared to the fraction of proteins with altered polyubiquitination in the TUBE-MS analysis, only for a few proteins altered protein levels were observed in the proteome profiling upon CFZ treatment; stressing the potential of TUBE-MS to monitor actual polyubiquitination (see Figure 38B). In both analyses of the CFZ datasets, one protein was among the most significantly enriched respectively upregulated proteins: the activating transcription factor 4 (ATF4). ATF4 is associated with the integrated stress response and plays a crucial role in Alzheimer's disease, and it was found to be upregulated upon proteasomal inhibition.[157] In this case, the increased expression levels most likely led to a proportionally increased polyubiquitination. Conclusively, the TUBE-MS and proteome profiling data for CFZ reflected the expected accumulation of polyubiquitinated proteins, while having a comparably low impact on the overall protein levels inside the cell during the comparably short incubation time of 5 h.

Compound 13

The first uncharacterized test substance in this dataset was Cmp 13. Although the TUBE-MS results for this compound were not as extensive as for CFZ, we observed the enrichment of 36 polyubiquitinated proteins, including the deubiquitinase MINDY1, the serin incorporator SERINC5, the RNA polymerase mediator MED25 and the scaffold attachment factor and estrogen receptor corepressor SAFB2 (see Figure 38C)[158]. At the same time, six proteins were differentially abundant in the proteome profiling of Cmp 13. Unlike CFZ, none of the proteins with altered polyubiquitination in the TUBE-MS analysis of Cmp 13 were significantly altered in their global levels. This indicates that the hit proteins from TUBE-MS indeed represented transformed polyubiquitination events as a consequence of Cmp 13 treatment and were not related to a different expression of the proteins (see Figure 38D). Furthermore, Cmp 13 shared SQLE as a significantly less ubiquitinated protein with CFZ. The squalene monooxygenase (SQLE) is known to require the proteasome to reach its active form by truncation, making it a proteasome substrate and thus affected by the inhibition of the latter[159]. Taken together, the number of enriched proteins and the common hit protein with CFZ hinted towards a MoA of Cmp 13 in the ubiquitin system. However, its exact mechanism remained unclear.

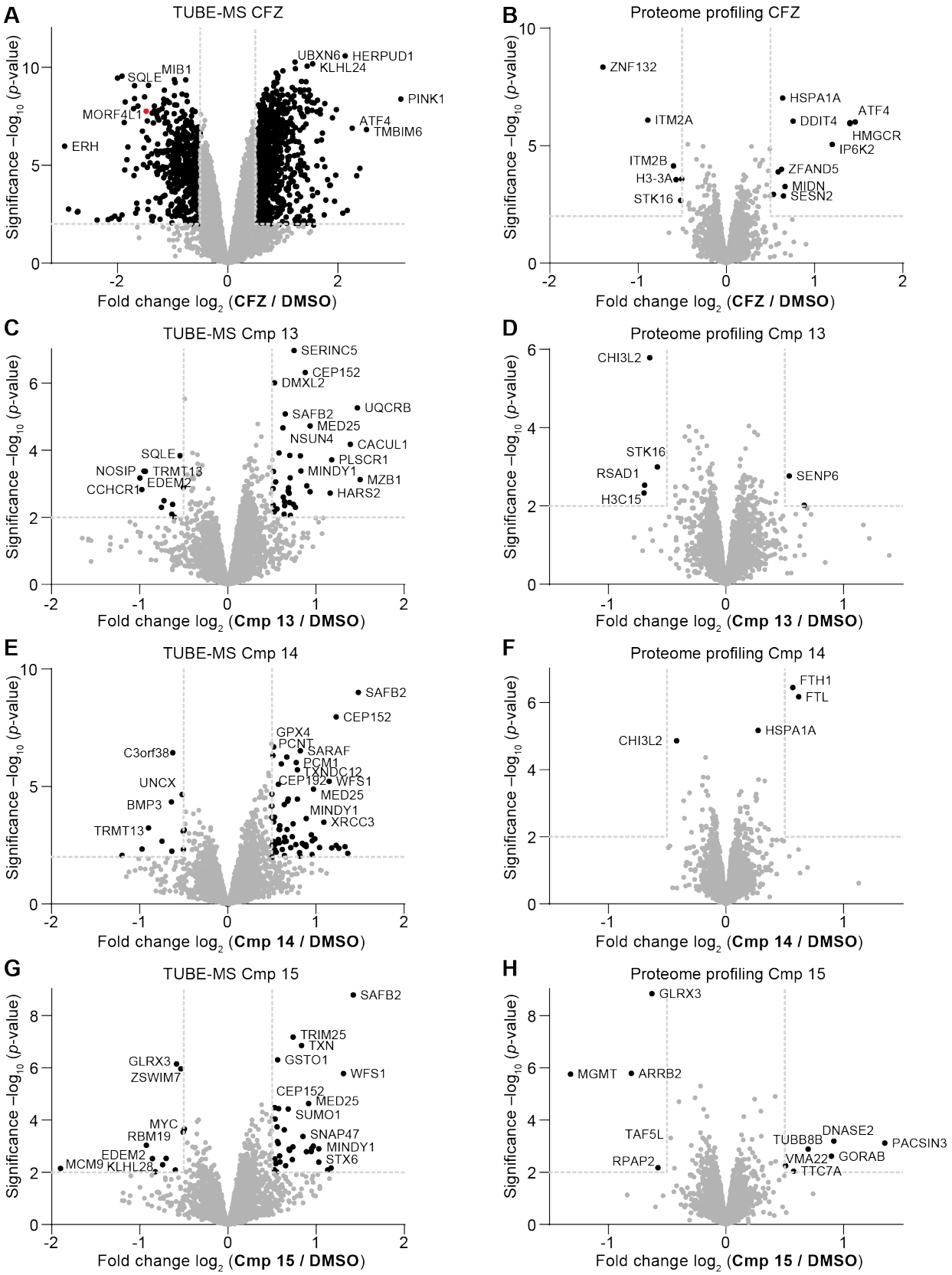
A
TUBE-MS CFZ
Significance –log10 (p-value)
Fold change log2 (CFZ / DMSO)
UBXN6
HERPUD1
KLHL24
PINK1
ATF4
TMBIM6
SQLE
MIB1
MORF4L1
ERH
B
Proteome profiling CFZ
Significance –log10 (p-value)
Fold change log2 (CFZ / DMSO)
ZNF132
HSPA1A
ATF4
DDIT4
HMGCR
IP6K2
ITM2A
ITM2B
H3-3A
ZFAND5
MIDN
SESN2
STK16
C
TUBE-MS Cmp 13
Significance –log10 (p-value)
Fold change log2 (Cmp 13 / DMSO)
SERINC5
CEP152
DMXL2
UQCRB
SAFB2
MED25
NSUN4
CACUL1
PLSCR1
MINDY1
MZB1
HARS2
SQLE
NOSIP
TRMT13
EDEM2
CCHCR1
D
Proteome profiling Cmp 13
Significance –log10 (p-value)
Fold change log2 (Cmp 13 / DMSO)
CHI3L2
STK16
RSAD1
H3C15
SENP6
E
TUBE-MS Cmp 14
Significance –log10 (p-value)
Fold change log2 (Cmp 14 / DMSO)
SAFB2
CEP152
GPX4
PCNT
SARAF
PCM1
TXNDC12
CEP192
WFS1
MED25
MINDY1
XRCC3
C3orf38
UNCX
BMP3
TRMT13
F
Proteome profiling Cmp 14
Significance –log10 (p-value)
Fold change log2 (Cmp 14 / DMSO)
FTH1
FTL
HSPA1A
CHI3L2
G
TUBE-MS Cmp 15
Significance –log10 (p-value)
Fold change log2 (Cmp 15 / DMSO)
SAFB2
TRIM25
TXN
GSTO1
WFS1
CEP152
MED25
SUMO1
SNAP47
MINDY1
STX6
GLRX3
ZSWIM7
MYC
RBM19
EDEM2
MCM9
KLHL28
H
Proteome profiling Cmp 15
Significance –log10 (p-value)
Fold change log2 (Cmp 15 / DMSO)
GLRX3
MGMT
ARRB2
TAF5L
RPAP2
DNASE2
TUBB8B
PACSIN3
VMA22
GORAB
TTC7A

Figure 38: *Mass spectrometric characterization of Compounds 13, 14 and 15 compared to the proteasome inhibitor carfilzomib.* ***A.-B****. Volcano plots of the TUBE-MS (panel* ***A****) or proteome profiling results (panel* ***B****) of Jurkat cells treated with carfilzomib (0.25 µM) compared to DMSO.* ***C.-D****. Volcano plots of the TUBE-MS (panel* ***C****) or proteome profiling results (panel* ***D****) of Jurkat cells treated with Cmp 13 (10 µM) compared to DMSO.* ***E.-F****. Volcano plots of the TUBE-MS (panel* ***E****) or proteome profiling results (panel* ***F****) of Jurkat cells treated with Cmp 14 (30 µM) compared to DMSO.* ***G.-H.*** *Volcano plots of the TUBE-MS (panel* ***G****) or proteome profiling results (panel* ***H****) of Jurkat cells treated with Cmp 15 (30 µM) compared to DMSO. All results shown in this figure are based on the treatment of Jurkat cells with the respective compound for 5 h. All conditions were analyzed in three biological replicates. MS results were analyzed using FragPipe and FragPipe Analyst. Proteins were considered significant when they reached a p-value of -log10 ≤ 2 and -0.5 ≥ log2 FC ≥ 0.5. The digestion, TMT-labeling and fractionation of the lysates for the proteome profiling analysis (panels B, D, F and H) were performed by Celine Da Cruz Lopes Guita.*

Compound 14

Similar to Cmp 13, Cmp 14 showed a higher number of enriched proteins in the TUBE-MS analysis compared to the DMSO control (see Figure 38E). Notably, SAFB2, MINDY1, and MED25 were also significantly more polyubiquitinated upon addition of Cmp 14, compared to treatment with Cmp 13. In the proteome profiling however, the only differentially abundant proteins were the ferritin proteins FTH1 and FTL, which did not show altered ubiquitination in the TUBE-MS analysis (see Figure 38F). This discrepancy in both analysis methods could either mean, that the enhanced polyubiquitination of proteins in the treated condition were of a non-degradative nature, the degradation of the polyubiquitinated proteins was inhibited, or the kinetics of the degradation was not progressing in the relatively short timeframe of the treatment. The latter case was unlikely, due to the high number of enriched proteins. Instead, an inhibited degradation pathway would argue in favor of a proteasome inhibitor-like MoA of Cmp 14 or for another target in the UPS. However, for the final elucidation of the target of Cmp 14, further experiments are necessary.

Compound 15

The TUBE-MS analysis of Cmp 15 revealed that it caused the enrichment of SAFB2, MINDY1, and MED25, similar to Cmp 13 and Cmp 14 (see Figure 38G). Additionally, upon treatment with Cmp 15, the E3 ligase TRIM25 became increasingly polyubiquitinated, which could either be caused by TRIM25 auto-ubiquitination, ubiquitination by other E3s or a decreased deubiquitination of TRIM25[160]. Interestingly, the UbL SUMO1 was also enriched in the TUBE-MS, but not upregulated in the proteome profiling, pointing towards the enrichment of SUMOylated proteins together with the polyubiquitin pool. As for the other two research compounds, the global levels of hit proteins from the TUBE-MS analysis were not altered (see Figure 38H). The only exception was Glutaredoxin-3 (GLRX3), which was not only less polyubiquitinated in the TUBE-MS results, but also less abundant in the proteome profiling upon treatment with Cmp 15. Interestingly, in both TUBE-MS and proteome profiling, the treatment with Cmp 15 caused the regulation of multiple RNA- (TAF5L, RPAP2, RBM19) and DNA-related proteins (MCM9, MGMT,

ZSWIM7), directing towards a target protein involved in these processes. Notably, the polyubiquitination of MCM9 and ZSWIM7 was reduced in the Cmp 15, as well as in the CFZ-treated conditions. However, for a definite assignment of a target, further validation experiments are needed.

From a general perspective, all three research compounds enhanced the polyubiquitination of several proteins, of which 12 proteins, including MINDY1, MED25 and SAFB2 were common for all tested substances, with MINDY1 and MED25 also being enriched in the CFZ control condition (see Figure 39A). Interestingly, all three uncharacterized compounds also caused the reduction of polyubiquitination of one common protein (see Figure 39B). EDEM2 is a glycosidase involved in the degradation of glycoproteins via the ERAD pathway[161]. Since this process is closely linked to proteasomal degradation[162], it could indicate a potential target for Cmps 13, 14, and 15 within the UPS. However, the extent of altered polyubiquitination by far did not reach the level caused by the reference compound CFZ. In the case of the shared target of the substances being the proteasome, polyubiquitin should have accumulated in the treated conditions of the TUBE-MS analysis. The comparison of the individual polyubiquitin LFQ-values of the respective substances in the pulldown fractions showed a clear enrichment of ubiquitin in the case of CFZ, in line with previous analyses of CFZ in TUBE-MS (see Supplementary Figure 2A-B), but only slightly

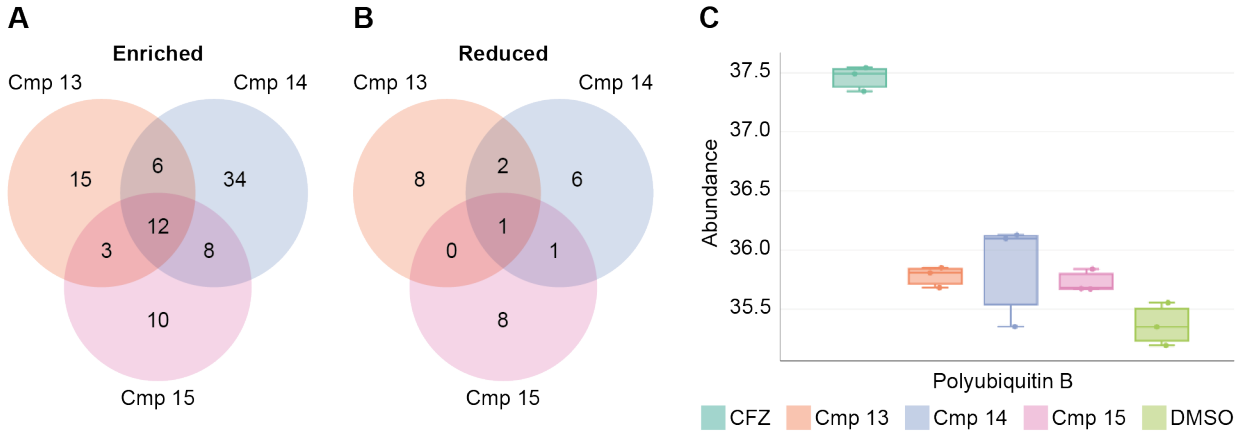

***Figure 39**: Comparison of significant proteins **A**. Venn diagram showing commonly enriched proteins form the TUBE-MS-analysis of compounds 13, 14 and 15 shown in Figure 38 C, E,G. **B**. Venn diagram showing commonly reduced proteins form the TUBE-MS-analysis of compounds 13, 14 and 15 shown in Figure 38 C, E,G **C**. Boxplot comparing the individual abundances of polyubiquitin across replicates in the respective conditions (CFZ, Cmp 13, Cmp 14 or Cmp 15) from the experiment shown in Figure 38 A, C, E and G. Data analysis for diagrams in panel A and B were performed using https://bioinformatics.psb.ugent.be/webtools/Venn/ . The boxplot shown in Panel C was generated using FragPipe Analyst.*

elevated levels for the research compounds (see Figure 39C). This is natural when considering that the reference compound was highly optimized, while the research compounds were initial hit substances. It thus could still be possible that the Cmps 13, 14 and 15 inhibited the proteasome,

but this is not certain at this stage. Another potential target of the compounds, which could have caused the assignment to the newly established proteasome cluster, is the shared hit protein MINDY1. As a member of the ubiquitin system, the distinct family of MINDY DUBs could also lead to the accumulation of polyubiquitination, especially as MINDY1 shows a preference for longer, K48-linked Ub chains[163,164]. These chains are also mainly associated with proteasomal degradation, which supports a connection between MINDY1 and the proteasome cluster (see section 2.2). In this case, the enrichment of MINDY1 could have been caused by a similar mechanism as the one postulated for USP7, the auto-deubiquitination (see section 4.2.2), which may have been inhibited by the substances. However, this remains to be validated, as MINDY1 contains a self-regulating Cys-loop, which becomes removed from the catalytic domain upon substrate interaction, making it less likely to possess activity on itself[164]. Another reason for the enrichment of MINDY1 may have been an indirect one, in which the preference and binding of MINDY1 to longer K48-Ub chains, caused the copurification of the DUB together with the polyUb proteins[163]. On the other hand, this cause should have mostly been prevented by the use of the semi-denaturing conditions during the pulldown enrichment. If the substance's target actually was MINDY1, this could come with a great therapeutic potential, as MINDY1 was found to be involved in cancer progression, involving the stabilization of estrogen receptor α (ERα)[165].

Conclusively, the TUBE-MS and proteome profiling data for the reference CFZ, as well as the research compounds 13, 14, and 15 did not allow for the direct confirmation of Cmp13-15 as proteasome inhibitors, but gave a first and broad insight towards a potential MoA in the proteasome cluster. Furthermore, the TUBE-MS analysis showed hit proteins, which were not significantly changed in the proteome profiling, adding more information to the compound's characterization. In order to see the outcome of the changed polyubiquitination of the hit proteins in the TUBE-MS, it might be a promising next step to perform another proteome profiling for the substances after a longer treatment time period, e.g. 12 or 24 h. This could give further insights into degraded or accumulated target proteins of the research compounds and allow for a definite assignment of their MoA.

Finally, the TUBE-MS results from this project demonstrate that the assay is able to detect polyUb accumulation (see Figure 39), even after short treatment time points and can give valuable information about the polyubiquitome of a cell in timeframes, where the proteome profiling is not able to recognize the downstream effects of polyUb-alterations yet.

5. Discussion

This thesis focused on the establishment and validation of a mass spectrometric method to detect altered protein polyubiquitination in response to cell treatment with small molecules. The obtained results from the application of TUBE-MS to various small molecules with different MoAs allow for insightful conclusions not only on the method itself, but also the ubiquitin system in general. This chapter is focusing on the discussion of the solidity and application scopes of TUBE-MS, but also its limitations in application and potential validation methods to support the results of the assay. Finally, it will bring TUBE-MS as a tool for drug discovery and small molecule characterization into context with existing methods, in order to identify its role of application in the study of protein ubiquitination.

5.1 TUBE-MS as a powerful method for the characterization of small molecules targeting the ubiquitin system

In the course of this thesis, I was able to establish and optimize a mass-spectrometric method to detect polyubiquitination on proteins, utilizing the **T**andem **U**biquitin **B**inding **E**ntity enrichment handle TUBE, which is based on the ubiquitin binder Ubiquilin1, coupled to the affinity tag Biotin (see section 4.1.1). The systematic identification of the optimal assay conditions for an efficient enrichment of polyUb and compatibility with a proteomics readout involved the adaption of the workflow at almost every stage. It started with the choice of biotin as an immobilization tag, which withstands also harsh buffer conditions, and laid the basis for the essential alteration in order to reduce unspecific enrichment of unmodified proteins and interactors of polyUb. Changing the standard lysis conditions, often used for affinity enrichments, towards a semi-denaturing approach using urea significantly lowered the fraction of non-Ub proteins in the pulldown eluates. Together with a washing conditions screening, the polyubiquitin enrichment obtained the optimal balance between the stability of the TUBE-target-interaction and the specific polyUb enrichment (see section 4.1.2.2). Additionally, the TUBE pulldown had to become compatible with a mass spectrometric readout, which should be as sensitive as possible. Sensitivity in proteomics often is endangered by contaminations of overly abundant proteins, overshadowing the peptide signals of interest[129]. In the case of TUBE-MS, the enrichment handle itself was one of these potentially

sensitivity-reducing factors, as compared of the enriched proteins, the TUBE reagent would have been the most abundant peptide source in the mass spectrometer. The implication of an acidic elution step resolved this challenge, as it allowed for the separation of the TUBE and its cargo proteins after enrichment, thus reducing the MS background (see section 4.1.2.3). The additional TMT-labeling of digested peptides, followed by fractionation could further increase the proteome depth. With this, TUBE-MS obtained its final setup and was ready for the application to different families of small molecules altering the ubiquitination of proteins. Collectively, the analyses of a PROTAC, three different DUB inhibitors, one proteasome inhibitor and 15 research compounds were successful, demonstrating the broad application range of the assay in almost every stage of the UPS. However, depending on the prerequisites taken in the cellular treatment and the MoA in the ubiquitin system, the outcome of the TUBE-MS analysis differed (see Figure 40). As the first

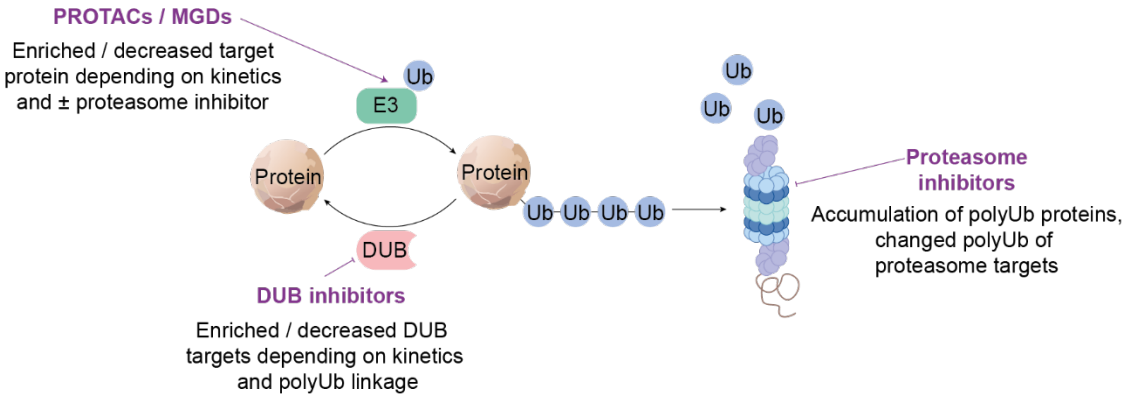

Figure 40: *Points of actions of different kinds of small molecules in the ubiquitin system and their respective signal outcome in the TUBE-MS assay.*

application case of TUBE-MS for small molecules in the optimized setup, the PROTAC MZ1 showed its target proteins BRD2 and BRD4 to be enriched in the treated conditions (see section 4.2.1). This confirmed the enhanced ubiquitination of the target proteins in previous immunoblot-based readouts. However, the detection of this effect required proteasomal inhibition. Depending on the PROTAC or molecular glue degrader tested, it might thus be beneficial to consider both significance sides of the volcano plot for the identification of degrader targets, if proteasomal inhibition is not used as a signal-conserving pretreatment. The impact of the latter on the polyubiquitome could also be proven by TUBE-MS (see section 4.2.4). Carfilzomib, as one of the most potent proteasome inhibitors, caused the accumulation of a significant fraction of the proteome in the polyubiquitome. However, some literature-reported proteasome targets were also less polyubiquitinated upon CFZ-treatment, indicating the capability of the method to also display individual protein polyubiquitination changes in complex environments containing drastic alterations of the polyubiquitome. Finally, the application of TUBE-MS to deubiquitinase inhibitors

confirmed that the assay is also able to recognize subtle changes on protein polyubiquitination in more native cell states without CFZ (see section 4.2.2). In this context, TUBE-MS was able to show the influence of the different inhibited DUBs on several of their respective reported substrates. Depending on the kinetics of the polyUb signal turnover in the given, relatively short treatment time of 4 h and the kind of polyUb linkage, DUB substrates could become either enriched or less ubiquitinated in the treated conditions. Even though one might consider this consideration of both volcano plot sides as a drawback, it comes with the advantage of sensitively detecting the altered polyubiquitination and also recognizing non-degradative ubiquitination, as the discovery of UBE3A polyubiquitination upon USP7 inhibition demonstrated (see section 4.2.2.2).

Collectively, one strength of TUBE-MS was its universal applicability to several kinds of small molecule-induced ubiquitination and deubiquitination. Furthermore, it proved to give an unbiased detection of the polyubiquitome, with a broader coverage of several thousand proteins at once, which was at the same time more sensitive than the immunoblot-based TUBE pulldown, having a lower throughput.

Compared to previous attempts to combine polyubiquitin pulldowns with a mass-spectrometric readout, we were able to identify and quantify several thousand proteins, utilizing an SP3 on-bead digest coupled to TMT multiplexing for the first time in this context[125]. The number of identified proteins is particularly noteworthy, as previous approaches, in many cases, were not able to detect more than 1000 polyubiquitinated proteins[122,124,126]. This could be primarily attributed to their necessity to use in-gel digestion in order to reduce the sensitivity-compromising effect of the TUBE reagent, which this TUBE-MS successfully circumvented by the acidic elution procedure[122,124,126]. Even though polyubiquitination had already been detected by LC-MS/MS in plants, yeasts, and parasite-infected erythrocytes, and the application of coupling to PROTACs had been suggested, we were the first to demonstrate its practical use in degraders, such as MZ1[121-124,127]. Furthermore, TUBE-MS showed alterations in the polyubiquitome already after short incubation times, starting from 4 h, which could be beneficial for the investigation of compounds exhibiting cytotoxicity after longer incubation times, such as the p97 inhibitor NMS-873[131].

Given its broad applicability and sensitive detection, as well as its major advantages over previous applications that combine polyubiquitin enrichment and proteomics, TUBE-MS is a versatile tool for characterizing small molecules with a known or unknown mode of action in the ubiquitin system. However, like every other method, TUBE-MS showed limitations throughout its validation,

which have to be considered and compromised by suitable follow-up methods validating its hit proteins.

5.2 Limitations of TUBE-MS and its potential follow-up methods

Despite its advances and strengths, the application of TUBE-MS on a multitude of compounds with different MoAs revealed certain limitations of the method. In the course of its validation, TUBE-MS was able to circumvent some of these by quick adaptions in the workflow. However, depending on the question supposed to be answered by TUBE-MS, it is important to consider these restrictions on the applicability.

The first limiting factor observed arose from the testing of the PROTAC MZ1 using the method (see section 4.2.1). As MZ1 is a highly potent degrader and its target proteins are quickly turned over by the proteasome, it was crucial to inhibit the proteasome in order to observe enriched PROTAC targets. Although, in a discovery setting, one most likely would not observe these drastic effects for initial hit compounds, it remains important to adapt the setup of TUBE-MS to the research question. As an example to prove that a reduced polyubiquitination observed in TUBE-MS without proteasome inhibitor is actually a compound-derived polyubiquitin effect, one could compare the data to a TUBE-MS analysis using carfilzomib in order to observe the same target protein for its enrichment under these conditions.

As the setup using carfilzomib (and the p97 inhibitor NMS-873) worked for the fast degrader MZ1 with its bromodomain target proteins, BRD2 and BRD4, it might be challenging for proteins with a higher native turnover in the cell. This is due to a high degree of endogenous polyubiquitination, which causes the polyUb protein to accumulate inside the cell within one hour of proteasome inhibition. If a degrader targeting this high-turnover protein is then added to the cell, a significant proportion of the protein will already be polyubiquitinated, which will drastically reduce the assay window in which the target can be detected. Additionally, inhibiting the proteasome could prevent the recycling of ubiquitin by proteasomal deubiquitinases, resulting in a depletion of the cellular free ubiquitin pool (see Figure 41)[166]. For less potent substances causing polyubiquitin alterations at later time points, this would disguise their biological activity, as no free ubiquitin would be available for further protein conjugations. For these cases, TUBE-MS has shown to work also reliably without proteasomal inhibition. However, this versatility comes at the price of some proteins being less abundant in the compound-treated fractions in the assay. Importantly, this

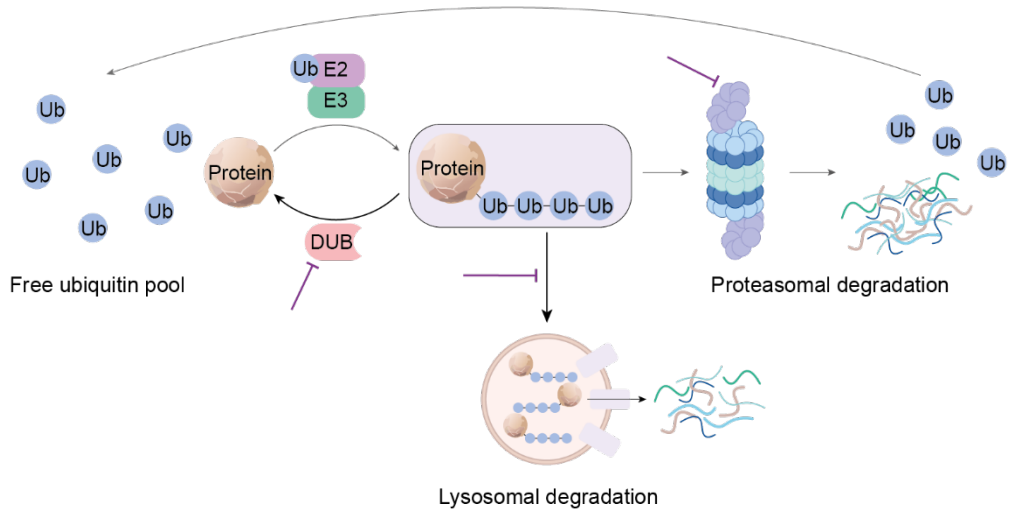

***Figure 41**: The balance between free and conjugated ubiquitin and the influence on it caused by different cellular processes, such as proteasomal degradation, lysosomal degradation, and deubiquitination. Potential points of interference using inhibitors are indicated with inhibition arrows in magenta.*

could again affect proteins with a short half-life and thus a higher rate of native polyubiquitination leading to a faster turnover of these polyubiquitin signals. Besides the inhibition of the proteasome conserving degradative ubiquitin signaling, other mechanisms in the cell are able to convert polyubiquitination. Among these, deubiquitination and lysosomal degradation play a role (see Figure 41)[167]. Even though the addition of NEM to the lysis buffer achieved the conservation of polyubiquitin chains from deubiquitination after cell lysis (see section 4.1.2.1), deubiquitination and lysosomal degradation could still occur in a native state, as well as in a proteasome-inhibited state inside the cell, causing a loss of signal of the compound-induced effect. When investigating potential deubiquitinase inhibitors, this is the desired effect (see section 4.2.2). In other contexts, such as targeted degradation however, the compensatory turnover of a polyubiquitin signal could lead to false negative results. It thus could be appealing to add also inhibitors of lysosomal degradation, e.g. Bafilomycin A[168] or pan DUB inhibitors such as PR619 (see section 2.4.3). As the inhibition of p97 with NMS-873 showed, however, the general inhibition of essential elements of the ubiquitin system leads to a substantial bias in the readout, which in the extreme could lead to the falsification of a compound characterization (see Figure 20E). In view of this risk, it remains the best option to choose as few additives for the cell treatment as possible and rather add further downstream validation methods to unravel the underlying mechanisms of changed protein polyubiquitination.

Conclusively, the compromise between keeping the additives to TUBE-MS at a minimum nevertheless has shown to be worth the trade with hit proteins potentially appearing on the other side of the volcano plot, since it comes with higher sensitivity and more conclusive results, as

shown by the analysis of the three DUB inhibitors FT671, IU1-47 and Spautin-1 (see section 4.2.2).

Another limitation of TUBE-MS became particularly visible in the detection of the ubiquitin-enriched fractions by immunoblotting. While the application of semi-denaturing lysis and washing conditions significantly improved the signal-to-noise-ratio between the polyubiquitination signal of the protein of interest, unmodified protein, however, was copurified. Firstly, ubiquitin binding proteins with a similar affinity to polyubiquitin chains as the TUBE reagent itself could still withstand the urea pulldown and washing conditions and thus be copurified irrespective of the optimized washing conditions. One example of these proteins could be MINDY1, which was enriched in the TUBE-MS analyses of the proteasome cluster compounds, as it possesses high affinity for longer, K48-linked Ub chains (see chapter 4.2.4)[163,164]. It could thus become necessary to consider UBD-containing proteins as potential false-positive hits in TUBE-MS in the future.

Secondly, the use of carfilzomib increased the proportion of unmodified proteins being enriched, regardless of whether the proteins contained a UBD (see section 4.2.1.1). This effect was probably caused by the beads having a larger surface area due to the presence of more enriched polyUb proteins. This phenomenon also became visible in the context of the validation of hit proteins from the iDeg derivative screen, where no proteasome inhibitor was used, but still a clear signal from unmodified protein was appearing in almost every TUBE pulldown analysis by western blot (see section 4.2.3.1). The most plausible explanation for this is the individual protein corona created by unspecific interactions of the bead surface and some proteins, which can vary based on the bead and immobilized handles[129]. This so-called “beadome” is a common phenomenon in the field of affinity-enrichment MS and generally acknowledged as a side-effect of the respective workflows[129]. With the consciousness about this effect, the inclusion of an acidic elution step prior to the mass spectrometric analysis not only showed the separation of the TUBE-protein staying on the beads and the polyUb proteins getting into solution, but also indicated a further reduction of the beadome background. This was suggested by a substantial fraction of the unmodified proteins remaining on the beads together with the TUBE reagent in this step (see section 4.1.2.3). As TUBE pulldowns intended for immunoblot analysis did not use acidic elutions, the fraction of unmodified proteins in the MS analysis was most likely smaller than that visible in western blot-based TUBE-PDs. Furthermore, unlike immunoprecipitation (IP)-based setups enriching the unmodified protein or highly abundant post-translational modifications such as phosphorylation, the overall site-occupancy for ubiquitination in the proteome is comparably low[102]. While around 28 % of proteins are phosphorylated, only around 0.05% of the cellular proteins are ubiquitinated

at all[102]. Considering that only a fraction of this occupancy consists of polyubiquitination, the necessary fold enrichment of polyUb proteins in the TUBE pulldown has to be particularly high. In view of this, the signal derived from unmodified proteins in this assay is not surprising, but remains to be considered. Finally, the TUBE-MS datasets characterizing the iDeg derivatives contained many hit proteins, which could not be validated further (see section 4.2.3). This raises the question of the reproducibility of TUBE-MS if the variability of certain proteins is high after polyubiquitinated proteins are enriched. In this context, it is important to consider the levels of individual peptides of the hit proteins in detail, and potentially only proceed with proteins that are highly confidently identified. One way to reduce the variability of protein levels could be to automate the TUBE-MS protocol, which would at the same time increase its throughput.

Collectively, even in view of its strong benefits, as many other assays, TUBE-MS cannot be a stand-alone method in the investigation of small-molecule-induced ubiquitination and should always be followed by suitable downstream analyses, which can confirm the observed effects on the hit proteins in the LC-MS/MS analysis.

In the course of the validation of hit proteins from TUBE-MS analyses, we used three different methods, which, in this context, revealed their strengths and weaknesses. They thus allowed for a closer inspection and discussion of their appropriateness to use them as a follow-up on TUBE-MS (see Figure 42).

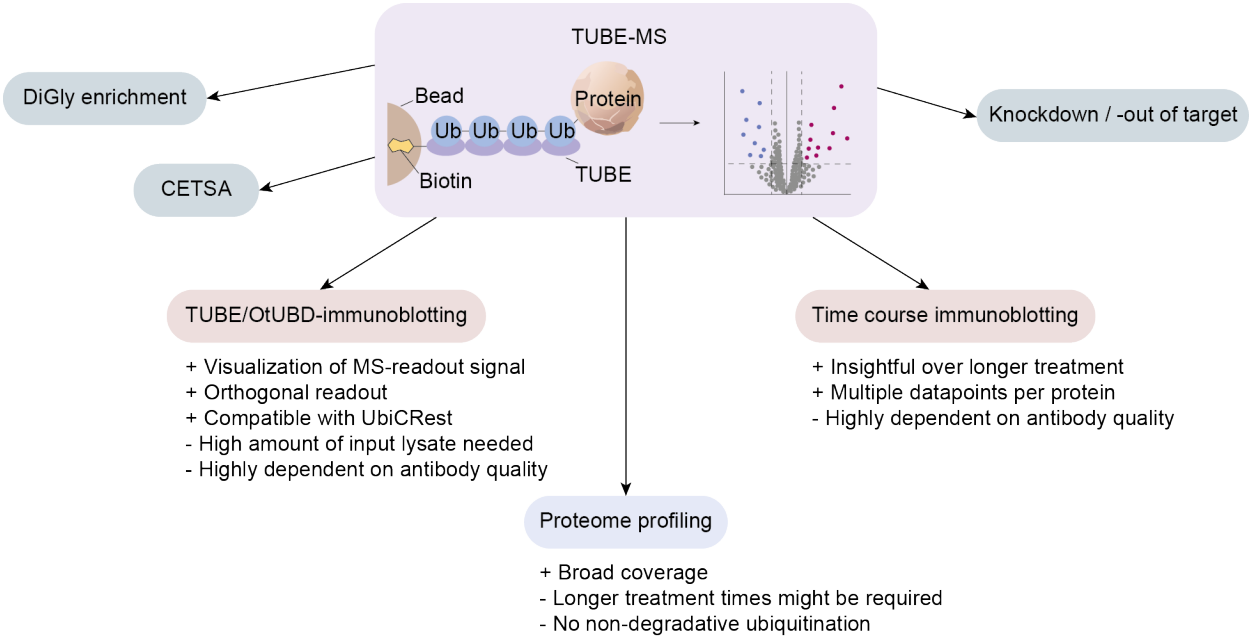

***Figure 42**: Potential follow-up methods for the validation of hit proteins from TUBE-MS analyses. When a method was used in this thesis, its observed advantages and disadvantages are indicated.*

As the most straightforward approach, the confirmation of the detected polyUb signal by an orthogonal readout of TUBE pulldown eluates was promising. For the initial setup of the mass-spectrometric assay, the immunoblot-based TUBE pulldown served as a reliable method for the visualization of the PROTAC-induced ubiquitination of BRD2 (see section 4.1.2 and 4.2.1.1). Furthermore, it enabled the validation of the non-degradative ubiquitination of UBE3A upon USP7 inhibition by FT671 not only in a dose-dependent, but also in a compound-independent manner (see section 4.2.2.2). However, as the validation of the hit proteins from the iDeg derivative screen revealed, the quality of the immunoblot-based TUBE pulldown is highly dependent on the availability and quality of an antibody specific against the respective antigen (see section 4.2.3.1). In addition, the degree of polyubiquitination of the target protein and its abundance itself can be limiting in the analysis, especially, if no signal-enhancing additives such as proteasome inhibitors are used. Given the low site occupancy of ubiquitination in the proteome[102], the polyUb signals of the hit proteins may be too low to ensure sufficient sensitivity for an immunoblot. Consequetly, this could compromise the ability to detect and validate the mass spectrometry results. One potential modification in this instance would be to further increase the scale of the TUBE enrichment for immunoblot-based readouts, with the objective of enhancing signal intensity in the membrane imaging. However, this would result in a more complex experimental setup, as higher amounts of cells and compound would be needed for each experiment. In view of the fact that the throughput for each protein in western blots is low, the utilization of TUBE enrichments with mass spectrometry as a more sensitive and unbiased readout was the original motivation of this project. Nevertheless, immunoblot-based TUBE or OtUBD pulldowns provide an easy-to-use and straightforward follow-up on mass spectrometric results. They show actual ubiquitination and can easily be adapted towards more specific compound-related questions such as doses, off-targets or linkage types, e.g., by its compatibility with the UbiCRest assay. This method characterizes the position of the lysine iso-peptide bond between individual ubiquitin molecules in chains by incubation with linkage-specific deubiquitinases[169].

The second method frequently used for the TUBE-MS hit validation was the monitoring of the global hit protein abundance over time. Using a relatively simple setup, the immunoblotting of the compound-treated lysates gave valuable insights into the substance-derived effects on the protein of interest, such as in the case of UBE3A, where the monitoring of the protein levels over a duration of 48 h allowed for first conclusions on the non-degradative manner of the FT671-induced UBE3A polyubiquitination (see section 4.2.2.2). However, it requires a housekeeping gene for the normalization of the protein levels, which in the case of iDeg derivate Cmp 12 was also regulated by the substance and thus falsified the conclusions concerning the actual hit

protein (see section 4.2.3.1). Additionally, in the same validation campaign, the immunoblot-based monitoring of protein levels revealed the same drawback as the TUBE-WB – the high dependency on antibody availability and quality. From a general perspective, the time-course treatment for the validation of hit proteins can provide valuable insights, as it covers multiple time points, thus generating several data points in a single experiment. This eliminates the need for a proteomics analysis at each time point, making it highly practical in this regard.

When time course treatments and immunoblot-based TUBE- or OtUBD pulldowns gave initial insights into the mechanism of a compound-induced ubiquitination or deubiquitination, such as UBE3A in the context of USP7, additional follow-up methods for the validation of TUBE-MS hit proteins can be beneficial. Two of these are well-established in the field of drug discovery and thus are promising also in the context of ubiquitination-alterations. Firstly, the cellular thermal shift assay (CETSA) allows for the proof of target engagement by the compound through a shift in the melting temperature of the protein[170]. In the context of small molecules altering polyubiquitination, this would consequently allow to either exclude off-target effects of the compounds or, as in the case of PROTACs and DUBTACs, show target engagement of both, the protein of interest and the corresponding DUB / E3 ligase. This approach is, however, limited by the size of the protein, as an attempt to show a FT671 compound binding to USP7 and / or UBE3A demonstrated (see Supplementary Figure 1). Another follow-up method for TUBE-MS validations and a potential next step for the investigation of the connection between UBE3A and USP7 could be to perform a genetic knockout (KO) or knockdown (KD) of either one of the proteins. The observed non-degradative ubiquitination of UBE3A upon USP7 inhibition could have the cellular function of relocalizing UBE3A within the cell or influencing its catalytic activity. If a direct connection between USP7 and UBE3A is existing, potentially through USP7 deubiquitinating UBE3A, the removal from USP7 in the cell through genetic methods should have the same result as its inhibition by FT671. This would allow the effects on UBE3A, such as localization, to be monitored, e.g. by fluorescence microscopy. At the same time, a USP7-independent UBE3A polyubiquitination validated by USP7-knockout would argue for an off-target effect of FT671 on UBE3A in a direct or indirect manner. This, however, is unlikely, as the TUBE-WB comparing the effect of three structurally different USP7 inhibitors showed the same effect observed for FT671 (see Figure 24C). Overall, both CETSA and KO/KD studies are promising as orthogonal validation methods for TUBE-MS. However, both of them would again require the detection of the target protein by western blot. To circumvent the challenges connected to this readout, another follow-up method is needed.

For the validation of hit proteins from the potential proteasome cluster compounds, we chose proteome profiling (PP) to monitor as many global protein levels as possible, to allow for the assignment of potential target proteins within the ubiquitin-proteasome system. With the identification of more than 5000 proteins, PP confirmed its strongest attributed advantage of a broad coverage over the whole proteome, monitoring more proteins than TUBE-MS did (see section 4.2.4). At the same time, since the proteome profiling used the input lysates for the TUBE-MS analysis, the comparatively short compound treatment time of 5 h was apparently insufficient to reveal significant changes in overall protein levels induced by the substance. It thus might be more insightful to perform PP as a follow-up method for substances tested in TUBE-MS after longer treatment times. Another major disadvantage of PP in this case was that it is not able to detect non-degradative ubiquitination, but only the reduced abundance of a protein. This drawback could be met with using diGly enrichments as a follow-up method for TUBE-MS (see section 2.5.1)[105,114]. However, this method does not allow conclusions on the overall abundance of proteins, making it rather an orthogonal validation approach to PP. These features of proteome profiling and diGly proteomics as follow-up methods are, at the same time, points to consider for their use as primary screens for the discovery of small molecules altering ubiquitination. This leads to the consideration of TUBE-MS in the context of other mass spectrometric methods to characterize compounds targeting the ubiquitin system.

5.3 TUBE-MS in the context of other proteomics-based methods

With the recent advances that the field of therapeutic targeting of the ubiquitin system experienced, a co-evolution of suitable discovery methods covering as many different MoAs is of utmost importance. To achieve a detection of small molecules altering the ubiquitin system that is as unbiased as possible, proteomics is one of the most promising approaches. Until today, the discovery of small molecules targeting the ubiquitin system by proteomics or their further characterization relied on three main families of methods, whose points of detection in the process of Ub conjugation differed (see Figure 43).

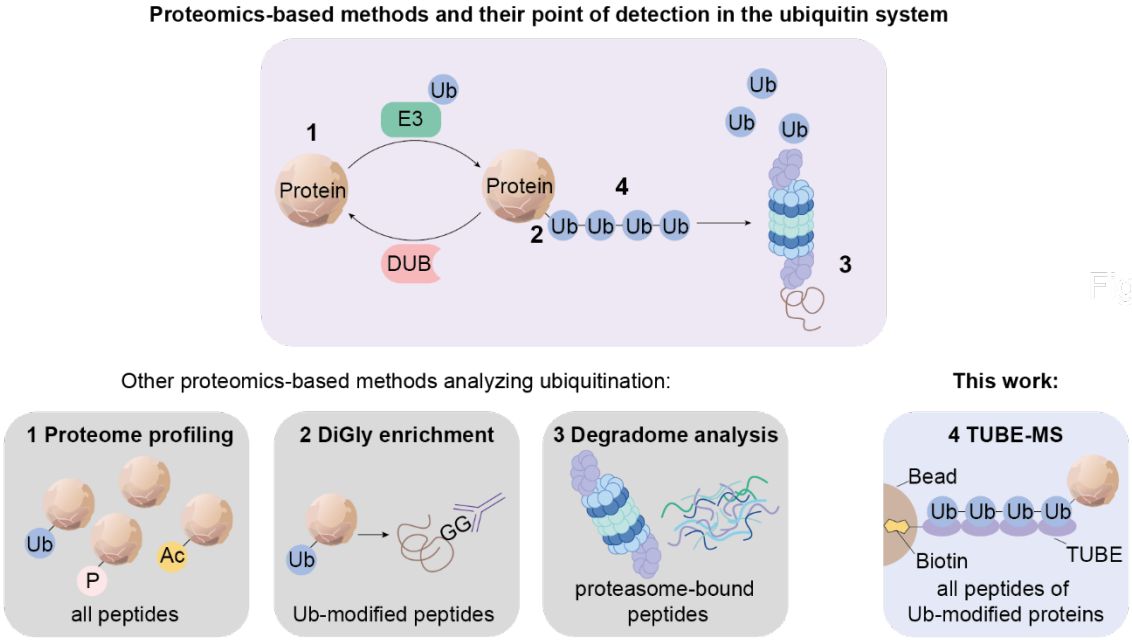

Figure 43: *Available proteomics-based methods for the detection of small molecule-induced ubiquitination and deubiquitination and their respective readout position in the UPS. Numbers assign the points of detection of the respective method. This figure was modified from Führer, S. et al. Small Molecule-Induced Alterations of Protein Polyubiquitination Revealed by Mass-Spectrometric Ubiquitome Analysis. Angew. Chem. Int. Ed. 64, e202508916 (2025) under a CC-BY 4.0 license.*

As a well-established and scalable assay, proteome profiling is a suitable approach for the detection of small-molecule induced changes in protein abundance, as it is the case for degraders such as MGDs or PROTACs (see section 2.5.2.1)[114,116,117]. As the validation of hit proteins from the iDeg screen however showed, PP might require longer treatment times than TUBE-MS, as the polyubiquitination of a protein in the case of degraders happens prior to their degradation. This, in turn, could lead to a greater emergence of secondary effects of the compound-treatment, which cannot be distinguished from the immediate compound-related effects in proteome

profiling. TUBE-MS, in contrast, is able to show the actual polyubiquitination of the protein and thus serves as a more direct proof of the substance's MoA in the UPS, which PP cannot give. As TUBE-MS shows compound-induced effects already at earlier time points than PP, it might also be suitable for bioactive molecules that become toxic after longer treatment times. These shorter timeframes required to detect compound effects also come with the benefit that TUBE-MS might show fewer secondary effects than PP. Lastly, proteome profiling covers all peptides and proteins, regardless of their post-translational modification. Thus, it cannot cover non-degradative ubiquitination, such as in the case of UBE3A, as TUBE-MS does. However, PP and TUBE-MS might work synergistically in the discovery of drug candidates, as they give insights concerning protein abundance vs. protein polyubiquitination, thus allowing for conclusions of the nature of the protein polyubiquitination.

When moving closer to the detection of actual ubiquitination by mass spectrometry, DiGly enrichments are effective tools for the analysis of peptides carrying a ubiquitin (see sections 2.5.1 and 2.5.2.1)[98,107]. As this method, however, is enriching for ubiquitination after the digestion of the protein, it is not able to distinguish between mono- or multiubiquitination, or between ubiquitin and the UBLs ISG15 and NEDD8, as they leave the same di-Glycine remnant on the formerly modified peptide lysine[102]. Moreover, the DiGly analysis can only identify proteins by the peptide that was ubiquitinated before, as other peptides become separated in the enrichment step. Ubiquitination thus has to happen on a razor and unique peptide in order to allow for a confident protein assignment. TUBE-MS, in contrast, enriches polyubiquitinated proteins instead of peptides, which leads to the diminishing of other UBL modifications and mono-ubiquitination in the enrichment. Still, it allows for the identification of the protein by all of its peptides, recognizing them also when ubiquitination did not happen on a razor and unique peptide. Consequently, the method enables the recognition of non-lysine ubiquitination, such as conjugation to serine and threonine[171]. However, this comes with the drawback that the exact location of the ubiquitin modification is not as easy to determine as in the DiGly analysis, since TUBE-MS has a more complex peptide mixture, from which GG-remnants have to be identified. Instead, TUBE-MS does not require the costly antibodies needed for the DiGly analysis, but uses the recombinantly expressed and stably biotinylated TUBE reagent, which withstands also harsh washing and high urea concentrations. Collectively, TUBE-MS has many advantages over DiGly analyses, but cannot fully replace the method. It is therefore imaginable to use DiGly enrichments as a follow-up on TUBE-MS to further characterize the location of the ubiquitin modification.

As many recently discovered small molecules targeting the UPS lead to the proteasomal degradation of their target proteins, the analysis of the cellular degradome is a suitable approach for the direct proof of enhanced POI-processing by the proteasome (see section 2.5.2.1)[120]. As this method captures proteasome-bound peptides, it can give valuable information about the fate of a protein after cellular compound treatment. However, the processing of a POI by the proteasome cannot give clear evidence about the direct connection to the substance treatment, as it detects its effect further downstream of the protein processing. Unlike TUBE-MS, the degradome analysis is neither capable of detecting non-degradative ubiquitination, nor of proving ubiquitination at all. Degradome analysis, however, could be a suitable orthogonal validation method after a potential degrader discovery in TUBE-MS.

Collectively, TUBE-MS has shown to indeed fill a gap in the need for the characterization of small molecule-induced ubiquitination and deubiquitination. It furthermore nicely adds to the repertoire of existing proteomics-based methods in this field, bridging the unbiased and broad detection range of a proteome profiling with the recognition of actual ubiquitination of a DiGly enrichment. Thereby, this method is unique in its ability to differentiate between mono- and polyubiquitination, while also identifying modified proteins from a completely digested peptide library.

It thus will be of great use for the discovery and characterization of bioactive molecules in the context of the ubiquitin system.

6. Summary and future perspective

The goal of this thesis was to establish and to validate a proteomics-based method for the discovery and characterization of small molecules targeting the ubiquitin system. This assay was based on a tandem ubiquitin binding entity (TUBE), which allows for the enrichment of polyubiquitinated proteins from complex mixtures without a preference for any ubiquitin chain linkage type. Conjugation of the TUBE protein to biotin using an AviTag system and BirA enabled for the controlled and tight immobilization of the reagent onto a solid support modified with streptavidin. This enrichment platform was stable under semi-denaturing conditions and capable of the isolation of the polyubiquitome from cell lysate with minimized background, while preserving high efficiency.

In a first validation approach, TUBE-MS was able to detect the enriched MZ1 PROTAC target proteins BRD2 and BRD4 in a mass-spectrometric readout using a solid phase digestion (SP3) and multiplexing by TMT-labeling. This attempt was facilitated by an acidic elution step, which caused a further background reduction by separation of the TUBE protein from bound polyubiquitinated payloads. However, the detection of enriched MZ1 targets required proteasomal inhibition, which showed a drastic influence on the cellular polyubiquitome. As a consequence, the next application case of TUBE-MS did not use this additive in order to benchmark the method's sensitivity towards subtle polyubiquitome changes. The investigation of three literature-reported deubiquitinase inhibitors targeting USP7, USP10/13, and USP14 revealed the compound-related alteration of several literature-reported, but also novel potential targets of the inhibited DUBs. Among the latter, USP7 inhibition led to the increased polyubiquitination of UBE3A. The stable global levels of UBE3A over a duration of 48 h of USP7 inhibitor treatment indicated a non-degradative nature of the underlying polyubiquitin signaling. The ability to detect even small changes in protein polyubiquitination displayed the potency of TUBE-MS to work reliably for enrichments from native cell states with intact proteasome. Nevertheless, the intact turnover of ubiquitin signals in this context required the considerations of both enriched and less abundant proteins from compound-treated conditions. This depends on the respective kinetics of the polyubiquitination as well as its conjugated protein. In further application cases on mostly uncharacterized research compounds, TUBE-MS proved its capability to indicate altered protein polyubiquitination already after short treatment times, where proteome profiling is not able to display broader changes in protein abundances yet. Still, the characterization of members of a potential newly established proteasome cluster in the phenotypic cell painting assay did not give

clear indication of a common target of these substances, if there is one. In the analysis of 12 members of derivatives of an IDO1 degrader library with proven inactivity against the parental target, TUBE-MS gave several hit proteins, of which some altered polyubiquitinations revealed to be real effects, even though they were not of a degradative nature and thus indicated the exquisite selectivity of the IDO1 degrader chemotype.

The limitations of TUBE-MS include its restricted ability to exclusively enrich polyubiquitinated proteins, as a certain fraction of unmodified or Ub-binding proteins were always copurified, which is natural, given the low site-occupancy of Ub in the whole proteome. Furthermore, the turnover of the polyubiquitin signal limits the detectability of compound-induced effects on the polyubiquitome with intact or inhibited proteasome. Thus, TUBE-MS should always be accompanied by orthogonal validation experiments (e.g. diGly proteomics) to confirm the observed effects. Compared to other mass-spectrometric methods in the field of therapeutic targeting of the ubiquitin system, TUBE-MS is a valuable addition to the assay portfolio. TUBE-MS unites the unbiased detection and broad coverage of a proteome profiling with the direct detection of ubiquitination given by an DiGly enrichment. With this, it provides a suitable platform for systematically screening uncharacterized research compounds in a discovery setup and for characterizing cellular polyubiquitin alterations resulting from inhibitor treatment in-depth.

In the future, it might be fruitful to automate the protocol, enabling for increased throughput and miniaturization in screening setups, while reducing sample variability. Together with recent milestones in the proteomics hardware, as well as software development, TUBE-MS will facilitate the studying of under-investigated effects of ubiquitination and their potential therapeutic applications, such as the non-degradative polyubiquitination of UBE3A upon USP7 inhibition.

As the field of therapeutic targeting of the ubiquitin system is just emerging and keeps steadily growing, TUBE-MS will be benchmarked against novel MoAs and approaches in this context, such as the induced polyubiquitination of small molecules themselves instead of proteins[172]. To meet these ever-changing needs, it will remain important to utilize TUBE-MS in combination with suitable follow-up methods, which allow for the orthogonal validation of the observed compound-induced effects in the proteomics assay, whether through established assays to show target engagement or genetic strategies to validate connected cellular signaling.

With this in hand, I am convinced that TUBE-MS will be a powerful tool for studying compound-induced changes in polyubiquitination and will find fruitful application in researching chemical biology in the context of the ubiquitin system.

7. Experimental Part

7.1 Material

7.1.1 Mammalian cell lines

Table 2: Mammalian cell lines and their culturing conditions used within this thesis.

Name	Supplier/Source	Prod. Number	Organism and tissue	Culture medium
HEK 293T	ATCC	CRL-1268	Human embryonic kidney	DMEM +10 % FBS (v/v), 1 % MEM NEAA (v/v), 1% Sodium Pyruvate (v/v)
Jurkat	CLS Cell Lines Service GmbH	302147	Human acute T-cell Leukemia cell line	RPMI 1640 +10 % FBS (v/v)
MM.1S	ATCC	CRL-2974	Human B lymphoblast myeloma	RPMI 1640 +10 % FBS (v/v)

7.1.2 Bacterial strains

Table 3: Bacterial strains used for cloning and protein expression within this thesis.

Name	Organism	Supplier
BL21(DE3)	*Escherichia coli*	Merck KGaA (Darmstadt, Germany)
Top10F’	*Escherichia coli*	Invitrogen™ / Thermo Fisher Scientific (Waltham, MA, USA)

7.1.3 Buffers

Table 4: Name and composition of buffers used within this thesis.

Name	Composition
2YT medium	1.6 % (w/v) Bacto tryptone, 1.0 % (w/v) Bacto yeast extract, 85 mM NaCl, pH 7.4
Cell lysis buffer	50 mM TRIS, 150 mM NaCl, 1% NP-40, 2 mM EDTA, 5% Glycerol, 20 mM NEM, protease inhibitor cocktail, pH 7.5
CETSA lysis buffer	PBS containing 0.5 % NP-40 alternative
Co-IP lysis buffer	20 mM Tris, 100 mM NaCl, 0.1 mM EDTA, 0.5 % NP-40 alternative, protease inhibitor cocktail, pH 7.5
Co-IP washing buffer	50 mM Tris, 150 mM NaCl, 1 mM EDTA, 0.05% NP40 alternative, protease inhibitor cocktail, pH7.4
Dilution buffer	10 mM TRIS, 150 mM NaCl, 1 mM EDTA, pH 7.5
High imidazole buffer	50 mM H_2NaPO_4, 300 mM NaCl, 500 mM imidazole, 4 mM beta-mercaptoethanol, pH 8.0
LB agar plates	LB Medium, 1.5 % Bacto agar
Low imidazole buffer	50 mM H_2NaPO_4, 300 mM NaCl, 20 mM imidazole, 4 mM beta-mercaptoethanol, pH 8.0
Lysogeny broth medium (LB)	1 % (w/v) Bacto tryptone, 0.5 % (w/v) Bacto yeast extract, 171 mM NaCl, pH 7.4
PBS-T	Phosphate-buffered Saline, pH 7.4, 0.1 % Tween-20
Phosphate buffered Saline (PBS) 10x	2.7 mM KCl, 1.5 mM KH_2PO_4, 136.9 mM NaCl, 8.1 mM Na_2HPO_4, pH 7.4
Proteomics denaturing buffer (4X)	240 mM HEPES, 4 % SDS, 40 mM TCEP, 160 mM CAA, pH 8.0
Proteomics digestion mix	100 mM TEAB, pH 8.5, 12 µg/mL Trypsin/LysC mix

Pulldown elution buffer (for proteomics)	100 mM glycine, pH 2.5
Pulldown elution buffer (for western blots)	25 mM Biotin, 10 mM TRIS, 150 mM NaCl, 1 mM EDTA, pH 7.5
Pulldown lysis buffer	4 M urea, 50 mM TRIS, 150 mM NaCl, 1% NP-40, 2 mM EDTA, 5% Glycerol, 20 mM NEM, protease inhibitor cocktail, pH 7.5
Pulldown washing buffer 1	10 mM TRIS, 150 mM NaCl, 0.1% Tween20, 1 mM EDTA, pH 7.5
Pulldown washing buffer 2	4 M urea 10 mM TRIS, 150 mM NaCl, 0.1% Tween20, 1 mM EDTA, pH 7.5
ResQ high salt buffer	25 mM TRIS, 500 mM NaCl, 4 mM DTT, pH 8.5
ResQ low salt buffer	25 mM TRIS, 50 mM NaCl, 4 mM DTT, pH 8.5
SEC buffer	20 mM TRIS, 100 mM NaCl, 5 mM EDTA, 4 mM TCEP, pH 8.5
Stage Tip Buffer A	0.1 % formic acid in MilliQ H_2O
Stage Tip Buffer B	0.1% formic acid in 80% Acetonitrile in H_2O
TAE buffer (50x)	2 M Tris, 1 M acetic acid, 50 mM EDTA, pH 8.5
Towbin transfer buffer	25 mM Tris, 192 mM glycine, 20% (v/v) methanol, pH 8.3

7.1.4 Antibodies

Table 5: Primary and secondary antibodies for immunoblotting used within this thesis.

Antigen	Source organism	Supplier	Prod number	Used dilution in WB	Blocking conditions
BRD2 (D89B4)	Rabbit	Cell Signaling Technology (Danvers, Massachusetts, USA)	5848S	1:1000	Intercept® Blocking Buffer PBS
COX7A2	Rabbit	ABclonal Germany GmbH (Düsseldorf, Germany)	A8406	1:1000	Intercept® Blocking Buffer PBS
DIABLO	Rabbit	Proteintech Group, Inc (Rosemont, Illinois, USA)	10434-1-AP	1:2000	Intercept® Blocking Buffer PBS
EMC7	Rabbit	Proteintech Group, Inc (Rosemont, Illinois, USA)	27550-1-AP	1:2500 - 1:1000	Intercept® Blocking Buffer PBS
Flag	Rabbit	Millipore™/ Merck KGaA (Darmstadt, Germany)	F7425	1 µg per 25 µL protein G magnetic beads	
GAPDH	Mouse	Invitrogen™ / Thermo Fisher Scientific (Waltham Massachusetts, USA)	AM4300	1:10000	Intercept® Blocking Buffer PBS

IKZF3	Rabbit	ABclonal Germany GmbH (Düsseldorf, Germany)	A8614	1:1000	Intercept® Blocking Buffer PBS
Mouse IgG Secondary Antibody IRDye® 680RD	Goat	Li-Cor Biosciences (Lincoln, Nebraska, USA)	926-68070	1:1000	none
Mouse IgG Secondary Antibody IRDye® 800CW	Goat	Li-Cor Biosciences (Lincoln, Nebraska, USA)	926-32210	1:1000	none
Mouse IgG, HRP-linked Antibody	Sheep	Amersham Cytiva Lice Sciences (Marlborough, Massachusetts, USA)	NXA931V	1:1000	none
MYO5A	Rabbit	Cell Signaling Technology (Danvers, Massachusetts, USA)	3402	1:1000-1:500	Intercept® Blocking Buffer PBS
NINJ2	Rabbit	Abcam (Cambridge, UK)	AB172627	1:1000	Intercept® Blocking Buffer PBS
pan-Ras (Ras10)	Mouse	Invitrogen™ / Thermo Fisher Scientific (Waltham Massachusetts, USA)	MA1-012	1:1000	Intercept® Blocking Buffer PBS

PDE6D	Rabbit	Invitrogen™ / Thermo Fisher Scientific (Waltham Massachusetts, USA)	PA5-22008	1:1000	Intercept® Blocking Buffer PBS
POR	Rabbit	Abcam (Cambridge, UK)	AB180597	1:1000	Intercept® Blocking Buffer PBS
Rabbit IgG Secondary Antibody IRDye® 800CW	Donkey	Li-Cor Biosciences (Lincoln, Nebraska, USA)	926-32213	1:1000	none
Rabbit IgG, HRP-linked Antibody	Goat	Cell Signaling Technology (Danvers, Massachusetts, USA)	7074S	1:1000	none
RBM14	Rabbit	Proteintech Group, Inc (Rosemont, Illinois, USA)	10196-1-AP	1:1000	Intercept® Blocking Buffer PBS
RPL23A	Mouse	Abnova Corporation (Taipei, Taiwan)	H00006147-M10	1:1000	Intercept® Blocking Buffer PBS
STK3	Rabbit	Proteintech Group, Inc (Rosemont, Illinois, USA)	12097-1-AP	1:500	Intercept® Blocking Buffer PBS
STX18	Rabbit	Proteintech Group, Inc (Rosemont, Illinois, USA)	16013-1-AP	1:1000	Intercept® Blocking Buffer PBS

TAZ	Rabbit	Cell Signaling Technology (Danvers, Massachusetts, USA)	4883S	1:1000	Intercept® Blocking Buffer PBS
TEAD2	Rabbit	Proteintech Group, Inc (Rosemont, Illinois, USA)	21159-1-AP	1:1000	Intercept® Blocking Buffer PBS
TRIM14	Rabbit	Proteintech Group, Inc (Rosemont, Illinois, USA)	15742-1-AP	1:1000	Intercept® Blocking Buffer PBS
UBE3A	Rabbit	Proteintech Group, Inc (Rosemont, Illinois, USA)	10344-1-AP	1:1000	Intercept® Blocking Buffer PBS
UBE3A	Mouse	Sigma-Aldrich (Burlington, Massachusetts, USA)	SAB1404508	1:500	Intercept® Blocking Buffer PBS
Ubiquitin (FK2)	Mouse	Calbiochem® Sigma-Aldrich (Burlington, Massachusetts, USA)	ST1200	1:1000	Intercept® Blocking Buffer PBS
Ubiquitin (P4D1)	Mouse	Cell Signaling Technology (Danvers, Massachusetts, USA)	3936S	1:1000	Intercept® Blocking Buffer PBS
USE1	Rabbit	Proteintech Group, Inc (Rosemont, Illinois, USA)	25218-1-AP	1:500	Intercept® Blocking Buffer PBS

USP7	Mouse	Proteintech Group, Inc (Rosemont, Illinois, USA)	66514-1-Ig	1:5000	Intercept® Blocking Buffer PBS
USP7	Rabbit	Abcam (Cambridge, UK)	ab190183	1:2000	Intercept® Blocking Buffer PBS
Vinculin	Mouse	Sigma-Aldrich (Burlington, Massachusetts, USA)	V9131	1:1000	Intercept® Blocking Buffer PBS
β-actin	Rabbit	Abcam (Cambridge, UK)	ab8227	1:2000	Intercept® Blocking Buffer PBS

7.1.5 Plasmids and Primers

Table 6: Plasmids for protein expression used within this thesis.

Name	Backbone	Insert Protein	Resistance	Tags	Organism
Avi-TUBE3	pOpinE	Ubiquilin-1	Ampicillin	C-term His	Human
BirA-His6	pEt21a	BirA (1-361 linker His6)	Ampicillin	C-term His	*E. coli*
C-OtUBD	pOpinB	Cystein-OtUBD	Kanamycin	N-term His, 3C cleavage site	*Orientia tsutsugamushi*

Table 7: Primer used for the cloning of indicated plasmids used within this thesis.

Name	Protein	Plasmid Name	Supplier	Sequence
Cys-OtUBD-pOpinB-fw	Cystein-OtUBD	C-OtUBD	Sigma-Aldrich (Burlington, MA, USA)	AAGTTCTGTTTCAGG GCCCGTGTGGAGGA TACCCATACGGAGG

Cys-OtUBD-pOpinB-rev	Cystein-OtUBD	C-OtUBD	Sigma-Aldrich (Burlington, MA, USA)	ATGGTCTAGAAAGCTTTAGGTTCTTCATTTGTTGAACTTCTCATTCAGCAAC

7.1.6 Kits

Table 8: Commercial kits used within this thesis.

Name	Supplier	Prod. Number
DC assay	Bio-Rad Laboratories Inc. (Hercules, CA, USA)	5000116
High pH Reversed-Phase Peptide Fractionation Kit	Pierce™ / Thermo Fisher Scientific (Waltham Massachusetts, USA)	84868
In-Fusion HD Cloning Kit (100 rxns)	Takara Bio Europe SAS (Saint-Germain-en-Lay, France)	639650
Micro BCA™ Protein Assay Kit	Pierce™ / Thermo Fisher Scientific (Waltham Massachusetts, USA)	23235
QIAprep Spin Miniprep Kit	Qiagen GmbH (Hilden, Germany)	27106
QIAquick Gel Extraction Kit	Qiagen GmbH (Hilden, Germany)	28704
Trans-Blot Turbo RTA Midi 0.2 µm Nitrocellulose Transfer Kit	Bio-Rad Laboratories Inc. (Hercules, CA, USA)	1704271

7.1.7 Mammalian cell culture media

Table 9: Mammalian cell culture media and their supplements used in this thesis

Name	Supplier	Prod. number	Supplements
Dulbecco's modified eagle medium (DMEM)	PAN-Biotech GmbH (Aidenbach, Germany)	P04-03550	+ 1 % NEAA, + 1 % Sodium Pyruvate, + 10 % FBS
Fetal bovine serum (FBS)	Gibco, Thermo Fisher Scientific (Waltham, MA, USA)	10270-106	-
MEM NEAA, non-essential Amino Acid Solution (100x)	PAN-Biotech GmbH (Aidenbach, Germany)	P08-32100	-
RPMI 1640	PAN-Biotech GmbH (Aidenbach, Germany)	P04-18047	10 % FBS
Sodium Pyruvate, 100 mM	PAN-Biotech GmbH (Aidenbach, Germany)	P04-43100	-
Trypsin/EDTA	PAN-Biotech GmbH (Aidenbach, Germany)	P10-023100	-

7.1.8 Chemicals and reagents

Table 10: Chemicals, reagents and commercial solutions used within this thesis.

Name	Supplier	Prod. number
2-(4-(2- hydroxyethyl)-1-piperazine ethane sulfonic acid (HEPES)	GERBU Biotechnik GmbH (Heidelberg, Germany)	1009.0250
2-chloroacetamide	Sigma-Aldrich (Burlington, MA, USA)	C0267

Acetonitrile (ACN), HPLC grade	VWR International GmbH (Darmstadt, Germany)	83640.290
Ampicillin sodium salt	Carl Roth (Karlsruhe, Germany)	K029.4
Biocytin	Sigma-Aldrich (Burlington, MA, USA)	B4261
Biotin	Carl Roth (Karlsruhe, Germany)	3822.1
Biotin-(PEO)3-iodoacetamide	abcr GmbH (Karlsruhe, Germany)	AB572497
Carfilzomib	MedChemExpress/Hycultec GmbH (Beutelsbach, Germany)	HY-10455
cOmplete™, EDTA-free protease inhibitor cocktail	Roche Diagnostics GmbH	4693132001
Dimethyl sulfoxide (DMSO)	Sigma-Aldrich (Burlington, MA, USA)	41639
Dithiothreitol (DTT)	GERBU Biotechnik GmbH (Heidelberg, Germany)	1008
DNase I	AppliChem GmbH (Darmstadt, Germany)	A3778
Ethanol, absolute	VWR International GmbH (Darmstadt, Germany)	153386F
Ethylenediaminetetraacetic acid (EDTA)	GERBU Biotechnik GmbH (Heidelberg, Germany)	1034
FPFT-2216	MedChemExpress/Hycultec GmbH (Beutelsbach, Germany)	HY-145319
FT671	MedChemExpress/Hycultec GmbH (Beutelsbach, Germany)	HY-107985
Glycerol	Carl Roth (Karlsruhe, Germany)	783.1
Glycine	Carl Roth (Karlsruhe, Germany)	3790.2
GNE-6640	MedChemExpress/Hycultec GmbH (Beutelsbach, Germany)	HY-112937

Hydrochloric acid (HCl)	VWR International GmbH (Darmstadt, Germany)	30024.29
Hydroxylamine 50 wt.% in H2O	Sigma-Aldrich (Burlington, MA, USA)	467804
Indisulam	MedChemExpress/Hycultec GmbH (Beutelsbach, Germany)	HY-13650
InstantBlue® Coomassie Protein Stain (ISB1L)	Abcam (Cambridge, UK)	ab119211
Intercept® Blocking Buffer PBS	LI-COR Biosciences (Lincoln, USA)	927-70001
Intercept® T20 (PBS) Antibody Diluent	LI-COR Biosciences (Lincoln, USA)	927-75001
IPTG min. 99 %, for biochemistry	Carl Roth (Karlsruhe, Germany)	CN08.3
IU1-47	MedChemExpress/Hycultec GmbH (Beutelsbach, Germany)	HY-122243
Kanamycin	Carl Roth (Karlsruhe, Germany)	T832.2
Lysozyme	Sigma-Aldrich (Burlington, MA, USA)	L6876
Methanol (MeOH)	Honeywell International Inc. (Charlotte, NC, USA)	32213
MZ1	Abcam (Cambridge, UK)	AB230371
N-Ethylmaleimide (NEM)	TCI Deutschland GmbH (Eschborn, Germany)	E0136
NMS-873	Sigma-Aldrich (Burlington, MA, USA)	SML1128
Nonyl phenoxypolyethoxylethanol (NP-40) alternative	Merck KGaA (Darmstadt, Germany)	492016
NuPAGE™ LDS Sample Buffer (4X)	Invitrogen™ / Thermo Fisher Scientific (Waltham, MA, USA)	NP0007
NuPAGE™ MES SDS Running Buffer (20X)	Invitrogen™ / Thermo Fisher Scientific (Waltham, MA, USA)	NP0002

Phenanthroline monohydrate	VWR International GmbH (Darmstadt, Germany)	26227.101
Phusion High-Fidelity DNA Polymerase	New England Biolabs GmbH (Frankfurt a. M., Germany)	M0530L
Pomalidomide	Thermo Scientific™ / Thermo Fisher Scientific (Waltham MA, USA)	465702500
Ponceau S solution for electrophoresis (0.2 %)	Serva Electrophoresis GmbH (Heidelberg, Germany)	33427.01
PR-619	MedChemExpress/Hycultec GmbH (Beutelsbach, Germany)	HY-13814
Quick Start Bovine Serum Albumin Std	Bio-Rad Laboratories Inc. (Hercules, CA, USA)	5000206
Re-Blot Plus Strong Solution (10x)	Millipore™/ Merck KGaA (Darmstadt, Germany)	2504
SeeBlue Plus2 Prestained Protein Standard	Invitrogen™ / Thermo Fisher Scientific (Waltham MA, USA)	LC5925
Sodium chloride (NaCl)	VWR International GmbH (Darmstadt, Germany)	27810.295
Spautin-1	TCI Deutschland GmbH (Eschborn, Germany)	P2613
SuperSignal™ West Dura Extended Duration Substrat	Invitrogen™ / Thermo Fisher Scientific (Waltham, MA, USA)	34076
SuperSignal™ West Femto Maximum Sensitivity Substrat	Invitrogen™ / Thermo Fisher Scientific (Waltham, MA, USA)	34095
TCEP HCl	Thermo Scientific™ / Thermo Fisher Scientific (Waltham MA, USA)	20491
TMT10plex™ Isobaric Label Reagent Sets	Thermo Scientific™ / Thermo Fisher Scientific (Waltham MA, USA)	90110

TMTpro™ 16plex Label Reagent Set	Thermo Scientific™ / Thermo Fisher Scientific (Waltham MA, USA)	A44522
Trans-Blot Turbo 5x Transfer Buffer	Bio-Rad Laboratories Inc. (Hercules, CA, USA)	#1704271
Triethylammonium bicarbonate buffer (TEAB), 1 M, pH 8.5	Sigma-Aldrich (Burlington, MA, USA)	T7408
Tris(hydroxymethyl)aminomethane (TRIS)	Carl Roth (Karlsruhe, Germany)	4855.2
Trypan Blue stain 0.4 %	Invitrogen™ / Thermo Fisher Scientific (Waltham MA, USA)	T10282
Trypsin/LysC MIX, Mass Spec Grade	Promega Corporation (Madison, WI, USA)	V5073
Tween-20	Sigma-Aldrich (Burlington, MA, USA)	P2287
Urea	J. T. Baker (Munich, Germany)	0345
USP7-797	MedChemExpress/Hycultec GmbH (Beutelsbach, Germany)	HY-136910

7.1.9 Consumables

Table 11: Consumables used within this thesis.

Name	Prod. number	Supplier
10 µL Filter TIP "E" low binding natural	770020	Biozym Scientific GmbH (Oldendorf,Germany)
100 µL Filter Tip low binding natural	770100	Biozym Scientific GmbH (Oldendorf,Germany)
1000 µL Filter Tip "XL" (Capacity 1250 µL)	770600	Biozym Scientific GmbH (Oldendorf,Germany)

200 µL Filter TIP "NX" low binding natural	770210	Biozym Scientific GmbH (Oldendorf,Germany)
Amicon® Ultra-15 Centrifugal Filter Unit	UFC901096	Merck KGaA (Darmstadt, Germany)
Bis-Tris gradient gels 4-12%	NP0323BOX	Invitrogen™ / Thermo Fisher Scientific (Waltham MA, USA)
Blotting Pad, 707	732-0594	VWR International GmbH (Darmstadt, Germany)
Cell culture flask 175 cm2	83.3912.002	SARSTEDT AG & Co. KG (Nümbrecht, Germany)
Cell culture flask 25 cm2	83.3910.002	SARSTEDT AG & Co. KG (Nümbrecht, Germany)
Cell culture flask 75 cm2	83.3911.002	SARSTEDT AG & Co. KG (Nümbrecht, Germany)
Cell Culture plate, 12-well	83.3921	SARSTEDT AG & Co. KG (Nümbrecht, Germany)
Cell Culture plate, 24-well	83.3922	SARSTEDT AG & Co. KG (Nümbrecht, Germany)
Cell Culture plate, 96-well	83.3924	SARSTEDT AG & Co. KG (Nümbrecht, Germany)
Countess™ Cell Counting Chamber Slides	C10283	Invitrogen™ / Thermo Fisher Scientific (Waltham MA, USA)
Dynabeads™ Protein G	10003D	Invitrogen™ / Thermo Fisher Scientific (Waltham MA, USA
Filtropur S 0.2	83.1826.001	SARSTEDT AG & Co. KG (Nümbrecht, Germany)
Gel loading tips 100 µL	10078930	Corning Inc. (corning, NY, USA)
Microplate, 96 well, conical bottom, clear	82.1583001	SARSTEDT AG & Co. KG (Nümbrecht, Germany)

Nitrocellulose membranes 0.2 µm	162-0146	Bio-Rad Laboratories Inc. (Hercules, CA, USA)
Pierce™ High Capacity Streptavidin Agarose Resin	20357	Thermo Fisher Scientific (Waltham, Massachusetts, USA)
Pierce™ Streptavidin Magnetic Beads	88817	Thermo Fisher Scientific (Waltham, Massachusetts, USA)
Polypropylene conical tubes 15 mL	62.554.502	SARSTEDT AG & Co. KG (Nümbrecht, Germany)
Polypropylene conical tubes 50 mL	62.547.254	SARSTEDT AG & Co. KG (Nümbrecht, Germany)
Protein LoBind tube 0,5 mL	022431064	Eppendorf SE (Hamburg, Germany)
Protein LoBind tube 1,5 mL	0030108442	Eppendorf SE (Hamburg, Germany)
Protein LoBind tube 2,0 mL	022431102	Eppendorf SE (Hamburg, Germany)
SafeSeal reaction tube, 0.5 ml, PP	72.706	SARSTEDT AG & Co. KG (Nümbrecht, Germany)
SafeSeal reaction tube, 1.5 ml, PP	72.704	SARSTEDT AG & Co. KG (Nümbrecht, Germany)
SafeSeal reaction tube, 2.0 ml, PP	72.695.500	SARSTEDT AG & Co. KG (Nümbrecht, Germany)
Sera-Mag™ SpeedBeads Carboxylate-Modified Magnetic particles - hydrophilic	45152105050250	Cytiva (Marlborough, MA, USA)
Sera-Mag™ SpeedBeads Carboxylate-Modified Magnetic particles - hydrophobic	65152105050250	Cytiva (Marlborough, MA, USA)
Serological pipette, with tip, plugged, 1 ml, sterile, 1 piece(s)/blister	86.1251.001	SARSTEDT AG & Co. KG (Nümbrecht, Germany)

Serological pipette, with tip, plugged, 10 ml, sterile, 1 piece(s)/blister	86.1254.001	SARSTEDT AG & Co. KG (Nümbrecht, Germany)
Serological pipette, with tip, plugged, 25 ml, sterile, 1 piece(s)/blister	86.1685.001	SARSTEDT AG & Co. KG (Nümbrecht, Germany)
Serological pipette, with tip, plugged, 5 ml, sterile, 1 piece(s)/blister	86.1253.001	SARSTEDT AG & Co. KG (Nümbrecht, Germany)
Serological pipette, with tip, plugged, 50 ml, sterile, 1 piece(s)/blister	86.1256.001	SARSTEDT AG & Co. KG (Nümbrecht, Germany)
SnakeSkin™ Dialysis tubing, 22 mm ID, 3.5 kDa MWCO	68035	Thermo Fisher Scientific (Waltham, Massachusetts, USA)
Trans-Blot Turbo Midi-size transfer Stacks	1704159	Bio-Rad Laboratories Inc. (Hercules, CA, USA)
Tyvek® 500 Armstulpe Modell PS32LA	TYPS32SWHLA	DuPont de Nemours, Inc. (Wilmington, DE, USA)

7.1.10 Instruments

Table 12: Instruments used within this thesis.

Name	Description	Manufacturer
5418 R	Centrifuge	Eppendorf SE (Hamburg, Germany)
ChemiDoc MP	Imaging System for Western blots	Bio-Rad Laboratories Inc. (Hercules, CA, USA)
Concentrator Plus	Vacuum concentrator	Eppendorf SE (Hamburg, Germany)

Countess® II FL	Automated Cell Counter	Invitrogen™ / Thermo Fisher Scientific (Waltham, MA, USA)
DynaMag-2	Magnetic rack	Invitrogen™ / Thermo Fisher Scientific (Waltham, Massachusetts, USA)
Eppendorf™ Research™ plus	(Multi-channel) pipettes	Eppendorf SE (Hamburg, Germany)
Fluorescence Spark®	Multifunction microplate reader	Tecan (Wiesbaden, Germany)
Labgard Nuaire ES Class II Type A2	Biological safety cabinet	NuAire, Inc. (Plymouth, MN, USA)
MagRack 6	Magnetic rack	GE Healthcare (Chicago, Illinois, USA)
MasterCycler X50s	PCR cycler	Eppendorf SE (Hamburg, Germany)
MCO-50AIC-PE	CO_2-incubator	PHC Holdings Corporation (Tokyo, Japan)
Mini Trans-Blot® Cell	Wet tank blotting System	Bio-Rad Laboratories Inc. (Hercules, CA, USA)
Mini-PROTEAN Tetra Cell	Polyacrylamide gel electrophoresis system	Bio-Rad Laboratories Inc. (Hercules, CA, USA)
Orbitrap Fusion Lumos	Mass spectrometer	Thermo Scientific™ / Thermo Fisher Scientific (Waltham MA, USA)
PowerPac™ Basic	Power supply for electrophoresis	Bio-Rad Laboratories Inc. (Hercules, CA, USA)
Q Exactive HF Hybrid Quadrupole-Orbitrap	Mass spectrometer	Thermo Scientific™ / Thermo Fisher Scientific (Waltham MA, USA)

Sonorex RK 100 H	Sonicator bath	BANDELIN electronic GmbH & Co. KG (Berlin, Germany)
SSM3	Rocking platform	Stuart (Paris, France)
Themomixer comfort	Temperature-controlled reaction tube mixer	Eppendorf SE (Hamburg, Germany)
TRM 50	Multi-Angle Rotating Mixer	IDL GmbH & Co. KG (Hanau, Germany)
Vacuboy and Vacusip with Battery	Hand pipetting operator	Integra Biosciences AG (Zizers, Switzerland)
Vortex Genie 2	Vortex mixer	Scientific Industries, Inc. (Bohemia, NY, USA)
XCell SureLock Mini-Cell Electrophoresis System	Protein Gel Electrophoresis Chamber System	Invitrogen™ / Thermo Fisher Scientific (Waltham, Massachusetts, USA)

7.1.11 Software

Table 13: Software used within this thesis.

Software	Version	Supplier	Description
Adobe Illustrator	2023	Adobe Inc.	Illustration of figures and schemes, depiction of immunoblot and proteomics results
DeepL Write	2025	DeepL SE, subscription plan of the Max Planck Society	Checking grammar, spelling and sentence building of self-written sentences in parts of this thesis. No full original texts were generated with this software

FragPipe	V20.0, V21.1, V22.0	Nesvizhskii lab, University of Michigan Medical School	Processing of proteomics data, protein identification and quantification
FragPipe Analyst	V1.9	Nesvizhskii lab, University of Michigan Medical School	Evaluation of FragPipe results
GraphPad Prism	9.5.1	GraphPad Software, Inc.	Statistical analysis and depiction of quantified immunoblotting and mass spetrometry results
Image Lab	6.0.1	Bio-Rad Laboratories Inc. (Hercules, CA, USA)	Visualization and quantification of immunoblot bands
MSConvertGUI (64-bit) in ProteoWizard	3.0.23170-df762d9	ProteoWizard (open source)	Conversion of proteomics raw files to mzML format
Venn diagram generator	n/a	https://bioinformatics.psb.ugent.be/webtools/Venn/	Generation of Venn diagrams and their data export in text format

7.2 Methods

Parts of this section were published in the following publications:

S. Führer, K. Gallant, F. Kaschani, M. Kaiser, P. Janning, H. Waldmann, M. Gersch. Small Molecule-Induced Alterations of Protein Polyubiquitination Revealed by Mass-Spectrometric Ubiquitome Analysis. *Angew. Chem. Int. Ed.* 2025, 64, e202508916. https://doi.org/10.1002/anie.202508916[1]

K. Wendrich, K. Gallant, S. Recknagel, S. Petroulia, N. H. Kazi, J. A. Hane, **S. Führer**, K. Bezstarosti, R. O'Dea, J. Demmers, M. Gersch. Discovery and mechanism of K63-linkage-directed deubiquitinase activity in USP53. *Nat Chem Biol* (2024). https://doi.org/10.1038/s41589-024-01777-0[2]

Wherever a text passage was taken from the respective publication as a quote, it is indicated with a citation at the end of the chapter.

7.2.1 Plasmid cloning

The plasmid cloned within this thesis were obtained by In-Fusion cloning, using the In-Fusion HD Cloning Kit. Plasmid backbones were selected as given in Table 6. Primers were designed with fixed plasmid backbone overhangs and used for insert amplification using PCR (see Table 7). PCR products were separated in 1 % agarose in TAE buffer, correct inserts were cut out of the gel and purified using a gel extraction kit. Purified inserts were combined using an In-Fusion polymerase and transformed into chemically competent TOP10F' bacteria. Transformed bacteria were plated onto an LB-medium agar plate, supplied with suitable selection antibiotics. Successfully amplified colonies were picked the next day and clones were amplified in LB medium overnight. The next day, plasmid DNA was isolated from bacteria using a mini-prep kit according to the manufacturer's protocol.

7.2.2 Protein Expression and Purification

Purified plasmids coding for desired proteins (Table 6) were transformed into chemically competent protein expression *E. coli* strain BL21(DE3) using a 30 second heat shock (42 °C), followed by 1 h of incubation in 400 µL LB medium at 37 °C. Afterwards, the bacterial suspension was spread onto LB agar plates, equipped with the respective selection antibiotic and incubated overnight at 37 °C. Colonies were picked by streaking from the plate, inoculated into 30 to 100 mL

of LB medium containing selection antibiotics and incubated with shaking overnight at 37°C. The next day, bacteria cultures were inoculated 1:100 in 2YT medium containing the respective selection antibiotic and incubated at 37 °C with shaking until an optical density (O.D.) value of 0.8 to 1.2 was reached. Bacterial cultures were cooled to 18 °C and protein expression was induced by addition of IPTG to a final concentration of 0.5 mM. Cells were incubated overnight at 18°C and afterwards harvested by centrifugation at 20,000 xg for 10 min. Cell pellets were stored at -80°C until further use. Bacteria were lysed in ice-cooled low imidazole buffer to which was added lysozyme and DNAse. The lysate was sonicated with ice cooling. Lysate was cleared by centrifugation at 22000 rpm at 4 °C for 30 to 40 min and afterwards filtered with 45 µM syringe filters. Protein purification was carried out on a Äkta pure system (GE healthcare). His-tagged proteins were isolated using a 5 mL HisTrap column and eluted with high imidazole buffer. Eluates were dialyzed into the respective next chromatography buffer. Bir A was further purified by size exclusion chromatography in PBS. Avi-TUBEs were purified by ion exchange chromatography using a ResQ column in low salt buffer with a gradient elution to high salt buffer. Protein purity and identity were investigated using SDS-PAGE and LC-MS. Protein concentration was determined either by Nanodrop (Thermo Fisher Scientific) or DC assay (BioRad).

7.2.3 Protein Biotinylation using BirA

Proteins containing an Avi-tag in ResQ high salt buffer (1 equiv.) were mixed with $MgCl_2$ to a final concentration of 4.5 mM (50 equiv.), Biotin (1 mM, 11 equiv.), BirA to a final concentration of 0.005 mM (0.06 equiv.) and ATP (1.8 mM, 20 equiv.). The resulting mixture was stirred at 4 °C overnight. To monitor the completeness of biotinylation, an intact protein LC-MS analysis was performed. To prepare the protein mixture for further ion exchange chromatography, it was dialyzed overnight into ResQ low salt buffer before being subjected to anion exchange purification. The identity of the protein was confirmed by LC-MS measurement. The protein concentration was assessed by DC-assay.

7.2.4 Protein Biotinylation using Biotin-$(PEO)_3$-Iodoacetamide

C-OtUBD (15.0 mg, 1.00 equiv. in SEC buffer) was reduced by the addition of TCEP (0.366 mg, 1.00 equiv.) to the buffered mixture and gentle shaking for 30 minutes. Subsequently, Biotin-$(PEO)_3$-iodoacetamide (7.00 mg, 10.0 equiv.) was added to the solution, and the reaction mixture was subjected to gentle shaking at 22 °C for a period of 4 hours. Upon completion of the reaction, the protein was purified by a 5-step sequential dialysis into 20 mM TRIS, 100 mM NaCl, 5% glycerol buffer at pH 8.0. The protein concentration was determined by DC assay, giving a yield

of 60%. Protein purity and identity were further validated by LC-MS. The purified protein was aliquoted into 1-mL portions and stored at -80°C.

7.2.5 Mammalian cell culture methods

7.2.5.1 Cell cultivation and subculturing

All cell lines were cultured at 37 °C in 5 % CO_2 atmosphere with humidification using the respective complete media as given in Table 9. Suspension cell lines were subcultured every two to three days. Adherent cell lines were subcultured as soon as 70 to 90 % of confluency were reached. For subculturing of suspension cells, cells in medium were transferred into a 50 mL falcon tube and centrifuged at 130 xg for 7 min to pellet cells. Supernatant medium was removed, cells were resuspended in 10 mL of fresh complete medium and counted using a Countess II cell counting system (Invitrogen). 4 to 6 Mio cells were seeded into 20 to 30 mL of fresh complete medium and incubated at 37 °C.

For subculturing of adherent cells, the respective growth medium was carefully removed from the cell layer and cells were rinsed with 10 mL of PBS. Afterwards, 2 mL of Trypsin/EDTA solution were added and cells were incubated at 37 °C until completely detached from the flask bottom. Afterwards, 8 mL of fresh complete medium were added and cells were resuspended. The resulting 10 mL of suspension were centrifuged at 300 xg for 3 to 4 min to pellet cells. Supernatant medium was removed, cells were resuspended in 10 mL of fresh complete medium and either diluted 1:10 in 10 to 20 mL of fresh growth medium or counted using a Countess II cell counting system (Invitrogen). After counting, 300,000 to 500,000 cells were seeded into 10 to 20 mL of complete growth medium.

7.2.5.2 Cryopreservation of mammalian cell cultures

For cryopreservation, confluent cell cultures from a T175 flask were detached or resuspended respectively and pelleted. Supernatant medium was removed and cell pellets were resuspended in 10 mL of complete growth medium supplemented with 10 % of DMSO. Cell suspension was aliquoted in 1 mL portions in cryo-vials and slowly cooled to -80 °C in a freezing container. The next day, cells were moved to the vapor phase of a liquid nitrogen tank for long-term storage.

7.2.5.3 Small molecule treatment of mammalian cell lines

Compounds for treatment of mammalian cells were dissolved in DMSO to 1000 x the desired final concentration in cell culture (e.g. for 1 µM final concentration for cell treatment, a 1 mM stock solution in DMSO was created). If proteasomal inhibition was required for cellular treatment, Carfilzomib in a 1000 x concentration was added to cells 1 h prior to the addition of remaining

small molecules, reaching a final concentration of 500 nM, if not stated otherwise. If not indicated differently, the final DMSO concentration in medium did not exceed 0.5 % (v/v). For suspension cells, compounds in DMSO were either added directly to the medium containing cells, followed by mixing on a plate shaker or predispensed into a cell culture plate with the cell suspension being added on top. For semi-adherent cells, compounds were added directly to the medium containing cells. After the intended incubation time, suspension cells were transferred into an Eppendorf tube, pelleted by centrifugation and washed with PBS once, before being lysed or stored at -80 °C until further use and downstream processing. For semi-adherent cells (MM1.S), the adherent part of the cells was scraped off the dish into the medium containing the suspension cell fraction and fully detached cells were transferred into an appropriate container before being pelleted by centrifugation. Pellets were washed using PBS and lysed or stored at -80 °C until further use and downstream processing.

If not stated otherwise, in section 7.2.6, cell pellets were lysed by resuspension in cell lysis buffer, followed by incubation on ice for 1 h. Afterwards, lysates were sonicated three to five times in 30 sec intervals in an ice-cooled water bath and centrifuged at 4 °C and 17,000 xg for 10 min to remove debris. The supernatants were transferred into a fresh tube and protein concentration was determined by means of the DC assay. Lysates were boiled with 4 x LDS containing 2 µL of 1 M DTT solution per 10 µL.

7.2.6 Cell-based assays

7.2.6.1 Cellular thermal shift assay (CETSA)

Jurkat cells from a confluent T175 flask were harvested and lysed using CETSA lysis buffer and incubated on ice for 1 h. Afterwards, lysates were centrifuged at 20,000 xg for 10 min to remove debris. The protein concentration was determined using the DC assay kit according to the manufacturer's protocol and the protein concentration was adjusted to 2.0 mg/mL. The lysate was split into two fractions of 500 µL each. One fraction was treated with 20 µL of FT671, while the other one was treated with the respective volume of DMSO. Both fractions were incubated at RT for 15 min. Each sample was subsequently equally split into ten fractions in PCR tubes and subjected to heat treatment for 3 min in a PCR cycler ranging from 36.8 °C to 65.4 °C. Afterwards, heat-treated fractions were centrifuged at 20,000 xg and 4 °C for 25 min to remove aggregated proteins. Supernatant fractions were transferred into fresh PCR tubes and boiled with 4x LDS at 95 °C for 5 min. Samples were analyzed by immunoblotting against USP7 and UBE3A as described in section 7.2.7.4. The protein intensities were quantified in the Biorad Image Lab

software and normalized to the 36.8 °C value of the respective compound- or DMSO-treated sample. Melting curves were analyzed in GraphPad Prism in a non-linear regression curve.

7.2.6.2 Co-Immunoprecipitation (CoIP) of UBE3A

Jurkat cells were seeded with a density of 3.5 Mio cells per mL in 2 mL medium (7 Mio cells per well) in a 12 well plate and incubated with FT671 (1 µM) or DMSO for 4 hours before being harvested. The pellets were washed with PBS once and frozen at -80 °C until further use.

Pellets were resuspended in 250 µL Co-IP lysis buffer and lysed by 4 freeze thaw cycles. Debris were removed by centrifugation at 17,000 xg for 15 min at 4 °C and protein concentration was determined by DC assay. 125 µL Dynabeads protein G were equilibrated using CoIP washing buffer and pelleted using a magnetic rack. 50 µL beads were each precoated with 2 µg anti UBE3A (rabbit) or anti Flag antibody and inverted at 4 °C for 2 h. Beads were washed twice with Co-IP washing buffer and each split into two tubes, so the equivalent of 25 µL beads were present in each tube. 500 µg of complete lysate in 500 µL solution per condition were transferred onto the beads, whereby the lysate of FT671-treated cells was supplemented additionally with 1 µM FT671 5 min prior to the lysate addition onto the beads. Beads were inverted overnight at 4 °C. The next day, beads were pelleted and supernatant was removed, while taking a sample for supernatant analysis. Beads were carefully washed 3x with CoIP washing buffer and 3x with PBS. The bound proteins were eluted twice using 15 µL of 2x LDS and 2 µL of 1 M DTT. Eluates were analyzed by WB against UBE3A and USP7, using the antibodies produced in mice according to Table 5.

7.2.6.3 TUBE pulldown

“Cells were lysed under denaturing conditions and incubated on ice for 30 min, followed by sonication in an ice-cooled sonicator bath for 4 x 30 s with 30 s breaks between intervals. Cell debris were removed by centrifugation at 17,000 to 20,000 xg for at least 10 min at 4 °C. Supernatants were transferred into fresh tubes and protein concentrations were determined with a DC assay using a BSA calibration curve. 30 µL of streptavidin magnetic beads per sample were transferred into a low-binding tube, were washed twice with washing buffer 1 and resuspended in 100 µL of washing buffer 1 per sample. Afterwards, 10 µL of Biotin-TUBE (0.6 nmol) per sample were added and the mixture was inverted for at least 1 h at 4 °C. Beads were then washed to remove excess Biotin-TUBE and the equivalent of 30 µL of equilibrated beads were added into a fresh low-binding tube. Beads were pelleted and 1 mg of protein from lysates in 500 µL in lysis buffer was transferred to each tube. The mixture was inverted overnight at 4 °C. Afterwards, beads were pelleted, and the supernatants were discarded. Beads were washed once using 1 mL

of washing buffer 2, once with washing buffer 1 and two times with PBS, each time followed by gentle bead resuspension, pelleting of the beads and discarding of the supernatant.

For downstream immunoblot analysis, bound proteins were eluted from the beads using 20 µL of a 25 mM biotin solution in dilution buffer (saturated at 95°C) followed by heating and mixing of the samples for 5 min at 95°C. Beads were pelleted, the eluates were transferred into a fresh tube and elution was repeated as described before using 10 µL of 4x LDS. Finally, beads were pelleted, eluates were united (further concentrated through evaporation […]) and the eluted protein fractions were analyzed by western blot.

For proteomics analysis and to allow for separate elution of ubiquitinated proteins and the TUBE reagent, bound proteins were eluted twice by incubating the beads with 20 µL of a 100 mM glycine solution, pH 2.5, for 5 min at 37 °C, followed by bead separation. Both eluates were pooled and then neutralized with 3.6 µL of 1 M HEPES solution at pH 8.0. Subsequently, SP3 on-bead digest was performed [as described in section 7.2.8.1]. For [western blotting] experiments […], an additional boiling step with 4x LDS was performed as described above to elute TUBE reagent off the beads."[1]

7.2.6.4 TUBE pulldown under different urea concentrations

"Jurkat cells were lysed in 3 mL of 1.5x lysis buffer without urea for 1.5 hours at 4 °C. Following this, the cells were sonicated in an ice-cooled water bath for 5x30 seconds, with 30-second breaks between intervals. Debris were removed by centrifugation at 17,000 xg for 40 minutes at 4 °C. The protein concentration was determined by DC assay. 240 µL of streptavidin magnetic beads were equilibrated with 80 µL of Biotin-TUBE3, as previously described, and subsequently washed and split into seven low-binding tubes. For each condition, 1 mg of cell lysate was diluted into 500 µL of 1x lysis buffer containing increasing concentrations of urea from 0 to 12 M. Lysate mixtures were added onto the TUBE-beads and inverted overnight at 4 °C. The next day, the beads were pelleted and washed two times with washing buffer without urea and two times with PBS. The elution of bound proteins from the beads was accomplished by subjecting them to boiling in 20 µL of a 25 mM biotin solution for five minutes, followed by bead separation and the transfer of the supernatant into a fresh tube. This procedure was repeated using 10 µL of 2x LDS sample buffer. The eluates were subsequently united, dried overnight in a speedvac, redissolved into 10 µL of MilliQ water, and analyzed by immunoblot against ubiquitin and beta actin."[1]

7.2.6.5 TUBE pulldown under native conditions using streptavidin agarose resin

MM1.S cells were either treated with 1 µM Carfilzomib or DMSO and incubated at 37°C for 4 h, before being scraped off the dish into medium, centrifuged down (7 min 130 rcf) and washed with PBS. Cells were transferred into a 2 mL tube, pelleted again and supernatant was removed. Cells were lysed in 600 µL cell lysis buffer supplemented with 2 mM Phenanthroline and 1.5 nmol Biotin-TUBE3 and incubated on ice for 30 min before being sonicated in an ice cooled water bath for 3x30 sec. Debris were removed by centrifugation for 10 min at 4 °C and 17,000 g and the supernatant was transferred to a fresh tube. 240 µL of agarose high capacity streptavidin beads were washed and equilibrated with dilution buffer and the equivalent of 40 µL bead slurry was transferred into a low binding tube. Protein concentrations of the cell lysates were determined using a microBCA assay. 2 mg of total protein in 800 µL lysis buffer were added each onto the beads and the mixture was inverted overnight at 4 °C. Pulldown samples were centrifuged for 2 min at 500 g to spin down the agarose beads. Supernatant was removed and 20 µL were kept for further analysis. The beads were washed three times using 1 mL of pulldown washing buffer 1 followed by centrifugation for 2 min at 500 xg and 4 °C. Bound proteins were eluted from beads by mixing 1:1 15 µL of 25 mM Biotin solution and 5x LDS sample buffer with DTT, adding the mixture to the beads and boiling the samples for 5 min at 95°C. Agarose beads were spun down and supernatant was analyzed by western blot.

7.2.7 Biochemical and molecular biology-based methods

7.2.7.1 *In vitro* pulldown of tetraUb chains

“A total of 360 µL of streptavidin magnetic beads (NEB, #S1421S) were suspended in 0.9 mL of dilution buffer (10 mM Tris, 150 mM NaCl, 1 mM EDTA, pH 7.5). The beads were then subjected to magnetic separation, followed by two washes with dilution buffer. Thereafter, the beads were resuspended in the original volume. The equivalent of 40 µL of bead suspension (160 µg) was transferred into fresh tubes and subjected to bead pulling using a magnet. The supernatant was removed and 80 µL of Biotin-TUBE solution (64 pmol, 1 equiv.) or biocytin control (64 pmol, 1 equiv.) were added onto the beads. Subsequently, 80 µL of dilution buffer were added, the tubes were incubated for 1 h, and the beads were washed. Thereafter, 80 µL of differently linked tetraUb chains (M1, K63, K48, 48 pmol, 0.75 equiv.) in solution and 80 µL of dilution buffer were added. The tubes were inverted overnight at 4 °C. The bead supernatant was then removed. The beads were then washed thrice by suspending them in 500 µL of washing buffer (10 mM Tris, 150 mM NaCl, 0.1% (v/v) NP-40, 1 mM EDTA, pH 7.5). This was followed by a magnet-based removal of the beads and aspiration of the remaining solution. Finally, bound proteins were eluted from the

beads by adding 20 µL of a 25 mM solution of biotin in washing buffer at 90 °C and boiling at 95 °C for 5 min. The eluted fractions and the supernatants were then subjected to SDS-PAGE followed by Coomassie staining for analysis."[1]

7.2.7.2 Titration of lysis buffer additives for DUB inhibition in lysates

"HEK293 cells were lysed in a standard lysis buffer (50 mM Tris, 150 mM NaCl, 1% (v/v) NP-40, 1 mM EDTA, 5% (v/v) glycerol, protease inhibitor cocktail, pH 7.5). The lysate was then subjected to centrifugation for 10 min at 4 °C and 17,000 xg to remove any debris. The protein concentration was adjusted to 2 mg/mL. The lysate was split into the respective number of samples containing 100 µL each, and N-ethylmaleimide (NEM) in concentrations from 0 to 20 mM or different additives for DUB inhibition were added. NEM was predissolved in 20x the desired concentration in EtOH and added immediately before lysis to the respective buffer solution. Subsequently, K63-linked triUb chains (8.4 mg/mL, 329 µM, 1 µL) were spiked into the lysates, and the mixtures were incubated at 4 °C for 1 h. Four-fold LDS sample buffer (NuPAGE, Thermo Fisher Scientific, #NP0008) was added, and the samples were boiled at 95 °C for 5 min. Subsequently, the samples were subjected to immunoblotting against ubiquitin, as outlined below, to ascertain the extent of cleaved Ub chains."[1]

7.2.7.3 SDS PAGE

For immunoblotting of cell-lysate-derived or ubiquitin-chain samples, protein solutions were boiled with LDS as indicated in the respective method section and applied onto 4-12% Bis-Tris gradient gels (Invitrogen) in 1x MES running buffer. Gels were run at 80-100 V constant for 5 to 10 min before the voltage was increased to 120-130 V for up to 90 min. Afterwards, gels were either stained with Coomassie blue stain according to the manufacturer's protocol or further processed by immunoblotting, as indicated.

7.2.7.4 Immunoblotting

Gels from SDS PAGE, Whatman paper and nitrocellulose membranes were equilibrated in either Towbin transfer buffer (for overnight transfer) or Trans Blot Turbo transfer buffer (for fast transfer) for at least 5 min. For overnight transfer, the blotting stack was assembled in Towbin transfer buffer, transferred into the buffer container and run overnight at either 30 V constant or 90 mA constant at 4 °C. For fast transfer, the blotting stack was assembled in the respective transfer buffer and run in the transfer cassette for 12 min in the respective membrane size program.

After completion of the transfer, membranes were stained with Ponceau S stain for 1 min and washed three times with ultrapure water before imaging. Afterwards, membranes were blocked

with blocking buffer as indicated in Table 6 for 1 h at room temperature before primary antibodies were added onto the membrane in the respective dilution (see Table 6), followed by incubation overnight at 4 °C. The next day, membranes were washed three times for at least five minutes and incubated with host-compatible secondary antibodies for detection for either 1 h at room temperature or overnight at 4 °C. Finally, membranes were washed three times with PBS-T for at least five minutes, Luminol detection reagent was applied onto membranes, which were incubated with HRP-coupled secondary antibodies, and signal readout was performed in a Chemidoc system.

7.2.7.5 Stripping and reprobing of immunoblotting membranes

For the analysis of an already analyzed nitrocellulose membrane, immunoblots were incubated with 1x Re-blot plus strong solution in water for 15 min with careful tilting. Afterwards, the stripping solution was discarded and the membrane was washed three times using PBS-T. Membranes were blocked again for 15 to 20 min using Licor PBS blocking buffer, followed by the addition and incubation with the respective new primary antibody overnight at 4 °C. All remaining steps for the detection of the desired antigen were conducted as described in section 7.2.7.4.

7.2.8 Mass spectrometry-based methods

7.2.8.1 SP3 on-bead digest

This method was performed according to the previously published protocol from *C.S. Hughes* and colleagues[132]. Previously eluted proteins from TUBE-pulldowns or 15 µg of whole cell lysate were adjusted to a volume of 40 µL and 13 µL of 4x proteomics denaturing buffer were added before samples were incubated at 95 °C for 5 min for reduction and alkylation of proteins. Subsequently, 3 µL of equilibrated SP3 bead mixture (1:1 hydrophilic/hydrophobic, 50 µg/µL) were added to each protein solution and samples were briefly mixed. Protein precipitation was induced by addition of 60 µL of absolute EtOH to the mixture, followed by mixing at 24 °C for 20 min. Beads were separated with a magnetic rack and supernatant was discarded. Beads were washed three times using 180 µL of 80 % EtOH in water by resuspension and subsequent bead separation. Finally, protein digestion was performed by adding 100 µL of proteomics digestion mix onto each bead pellet, resuspension and incubation for 14 - 18 h at 37 °C with shaking at 1400 RPM. Beads were separated and supernatants were transferred into a fresh tube for subsequent TMT-labeling.

7.2.8.2 TMT-labeling

TMT-labeling was performed according to the manufacturer's protocol (TMTpro 16plex Label Reagent Set / TMT10plex Isobaric Label Reagent Set, see Table 10). Modifications were made as follows: 0.5 mg (TMTpro 16plex) or 0.8 mg (TMT10plex) of each label were dissolved in 42 µL

of anhydrous ACN at room temperature for 5 min. 20 µL of each label were transferred to 100 µL of digested protein sample in 100 mM TEAB, pH 8.5. The labeling mixtures were incubated at RT for 2 h, before the reaction was quenched with 8 µL of a 5 % hydroxylamine solution followed by 15 min of incubation. 100 – 120 µL of each labeled peptide solution were pooled and solvents were evaporated in a vacuum centrifuge until dryness. TMT-labeled peptides were fractionated at high pH using the respective kit (see Table 8) according to the manufacturer's protocol. Solvents were evaporated and sample were subjected to nanoHPLC-MS/MS analysis.

7.2.8.3 Mass spectrometric analysis of pulldown eluates

"For nanoHPLC-MS/MS analysis samples were dissolved in 10 µL (TMT10plex) or 20 µL (TMTpro16plex) of 0.1% TFA in water and 10 µL (TMT10plex) or 3 µL (TMTpro16plex) were injected onto an UltiMate 3000 RSLCnano system (Thermo Fisher Scientific, Germany) online coupled to a Q Exactive HF Hybrid Quadrupole-Orbitrap mass spectrometer equipped with a nanospray source (Nanospray Flex Ion Source, Thermo Scientific). All solvents were LC-MS grade. For desalting, the samples were injected onto a pre-column cartridge (5 µm, 100 Å, 300 µm ID x 5 mm, Dionex, Germany) using 0.1% TFA in water as eluent with a flow rate of 30 µL/min. Desalting was performed for 5 min with eluent flow to waste followed by back-flushing of the sample during the whole analysis from the pre-column to the PepMap100 RSLC C18 nanoHPLC column (2 µm, 100 Å, 75 µm ID x 50 cm, nanoViper, Dionex, Germany) using a linear gradient starting with 95% solvent A (water containing 0.1 % formic acid) / 5% solvent B (acetonitrile containing 0.1% formic acid) and increasing to 40% (TMT10plex) or 28% (TMTpro16plex) solvent B within 120 min (TMT10plex) or 100 min (TMTpro16plex), respectively, using a flow rate of 300 nL/min. Afterwards, the column was washed (reaching 95% solvent B) and re-equilibrated to starting conditions. Spectra were recorded in data-dependent mode. For TMT10plex, a mass range of m/z 300 to 1650 was acquired with a resolution of 60000 for full scans, followed by up to 15 high energy collision dissociation (HCD) MS / MS scans of the most intense at least doubly charged ions using a resolution of 30000 and an NCE energy of 35%. For TMTpro16plex, a mass range of m/z 375 to 1500 was acquired with a resolution of 120000 for full scan, followed by up to 15 high energy collision dissociation (HCD) MS / MS scans of the most intense at least doubly charged ions using a resolution of 60000 and an NCE energy of 32%. For samples corresponding to the data shown in […] [Figure 19D-H], the TMTpro16plex-labeled samples were measured as described for TMT10plex-labeled samples with the injection volume being changed to 5 µL.

For samples corresponding to the data shown in […] [Supplementary Figure 2], LC-MS/MS analyses of peptide samples were performed on an Orbitrap Fusion Lumos mass spectrometer

(Thermo Scientific, Waltham, MA, USA) coupled to a Vanquish Neo ultra high-performance liquid chromatography (UHPLC) system (Thermo Scientific, Waltham, MA, USA) that was operated in the one-column mode. The analytical column was a fused silica capillary (inner diameter 75 µm, outer diameter 360 µm, length 46 cm; CoAnn Technologies, Richland, WA, USA) with an integrated sintered frit packed in-house with Kinetex 1.7 µm XB-C18 core shell material (Phenomenex, Aschaffenburg, Germany). The analytical column was encased by a PRSO-V2 column oven (Sonation, Biberach, Germany) and attached to a nanospray flex ion source (Thermo Scientific, Waltham, MA, USA). The column oven temperature was set to 50 °C during sample loading and data acquisition. The LC was equipped with two mobile phases: solvent A (2% ACN and 0.2% FA, in water) and solvent B (80% ACN and 0.2% FA, in water). All solvents were of UHPLC grade (Honeywell, Charlotte, NC, USA). Peptides were directly loaded onto the analytical column with a maximum flow rate that would not exceed the set pressure limit of 950 bar (usually around 0.5 – 0.6 µl min–1) and separated on the analytical column by running a 120 min gradient of solvent A and solvent B at a flow rate of 250 nL/min (start with 3% (v/v) B, gradient 3% to 9% (v/v) B for 5 min, gradient 9% to 28% (v/v) B for 87 min, gradient 28% to 100% (v/v) B for 16 min, 100% (v/v) B for 12 min).

The mass spectrometer was controlled by the Orbitrap Fusion Lumos Tune Application (v4.1.4244) and operated using the Xcalibur software (v4.7.69.37). For the experiment shown in Fig. S5, the mass spectrometer was set to: dynamic exclusion enabled (exclude after n times = 1; exclusion duration (s) = 60; mass tolerance = ± 10 ppm), intensity threshold: 5000, ion transfer tube temp.: 250 °C, and ion source voltage: 2500 V. In MS1, the analyzer was set to Fourier Transform (Orbitrap), max. Resolution at 200 m/z = 120000, scan range: 400 – 1400 m/z, absolute automatic gain control = 400,000, max. ion acquisition time = 50 ms, RF Lens 30 % and data dependent mode (cycle time in seconds = 3 sec). In MS^2, the analyzer was set to OT, max. resolution at 200 m/z = 120000, scan range: start 110 m/z, automatic gain control = 200%, absolute automatic gain control = 100000, max. ion acquisition time = auto, charge states used for fragmentation: +2 to +7, Isolation mode: Quadrupole, Isolation window = 0.7 m/z, fragmentation method: higher-energy collisional dissociation and normalized collision energy = 35."[1]

7.2.8.4 Analysis of proteomics data

"Raw files from proteomics analysis were converted using the MSConvertGUI (64bit) package in ProteoWizard into mzML format , with applying the filter peakPicking vendor msLevel = 1- [173]. Protein identification search and quantification of TMT-labeled samples were performed using

FragPipe V20.0 and V21.1 and V22.0 with MSFragger search engine, MSBooster and Percolator PSM rescoring, Philosopher FDR filtering and TMTintegrator quantification, using the default workflows for TMT10plex and TMT16plex analysis provided by the program authors with specifying the used digestion enzymes as Trypsin and LysC[174-179]. Data visualization was performed using FragPipe-Analyst (v0.35) and MSstasShiny[180]. For data shown in […] [Figure 20], annotation of known DUB and p97 targets was performed using BioGRID4.4. Therefore, hit proteins from proteomics experiments were searched within the respective subchapter of the deubiquitinase or p97. For data shown in […] [Supplementary Figure 2C], protein assignment was performed using the Panther classification system. Additional sources for target annotation are cited in the respective section of this publication."[1]

8. References

1 Führer, S. *et al.* Small Molecule-Induced Alterations of Protein Polyubiquitination Revealed by Mass-Spectrometric Ubiquitome Analysis. *Angew. Chem. Int. Ed.* **64**, e202508916 (2025). https://doi.org/10.1002/anie.202508916

2 Wendrich, K. *et al.* Discovery and mechanism of K63-linkage-directed deubiquitinase activity in USP53. *Nat Chem Biol* (2024). https://doi.org/10.1038/s41589-024-01777-0

3 Mullard, A. 2024 FDA approvals. *Nat Rev Drug Discov* **24**, 75-82 (2025). https://doi.org/10.1038/d41573-025-00001-5

4 Southey, M. W. Y. & Brunavs, M. Introduction to small molecule drug discovery and preclinical development. *Frontiers in Drug Discovery* **3** (2023). https://doi.org/10.3389/fddsv.2023.1314077

5 Moffat, J. G., Rudolph, J. & Bailey, D. Phenotypic screening in cancer drug discovery - past, present and future. *Nat Rev Drug Discov* **13**, 588-602 (2014). https://doi.org/10.1038/nrd4366

6 Sadri, A. Is Target-Based Drug Discovery Efficient? Discovery and "Off-Target" Mechanisms of All Drugs. *J Med Chem* **66**, 12651-12677 (2023). https://doi.org/10.1021/acs.jmedchem.2c01737

7 Roberts, A. W. & Huang, D. Targeting BCL2 With BH3 Mimetics: Basic Science and Clinical Application of Venetoclax in Chronic Lymphocytic Leukemia and Related B Cell Malignancies. *Clin Pharmacol Ther* **101**, 89-98 (2017). https://doi.org/10.1002/cpt.553

8 Boike, L., Henning, N. J. & Nomura, D. K. Advances in covalent drug discovery. *Nat Rev Drug Discov* **21**, 881-898 (2022). https://doi.org/10.1038/s41573-022-00542-z

9 Dong, G., Ding, Y., He, S. & Sheng, C. Molecular Glues for Targeted Protein Degradation: From Serendipity to Rational Discovery. *J Med Chem* **64**, 10606-10620 (2021). https://doi.org/10.1021/acs.jmedchem.1c00895

10 Bondeson, D. P. & Crews, C. M. Targeted Protein Degradation by Small Molecules. *Annu Rev Pharmacol Toxicol* **57**, 107-123 (2017). https://doi.org/10.1146/annurev-pharmtox-010715-103507

11 Clague, M. J., Heride, C. & Urbe, S. The demographics of the ubiquitin system. *Trends Cell Biol* **25**, 417-426 (2015). https://doi.org/10.1016/j.tcb.2015.03.002

12 Komander, D. & Rape, M. The ubiquitin code. *Annu Rev Biochem* **81**, 203-229 (2012). https://doi.org/10.1146/annurev-biochem-060310-170328

13 Swatek, K. N. & Komander, D. Ubiquitin modifications. *Cell Res* **26**, 399-422 (2016). https://doi.org/10.1038/cr.2016.39

14 Schulman, B. A. & Harper, J. W. Ubiquitin-like protein activation by E1 enzymes: the apex for downstream signalling pathways. *Nat Rev Mol Cell Biol* **10**, 319-331 (2009). https://doi.org/10.1038/nrm2673

15 Ye, Y. & Rape, M. Building ubiquitin chains: E2 enzymes at work. *Nat Rev Mol Cell Biol* **10**, 755-764 (2009). https://doi.org/10.1038/nrm2780

16 Deshaies, R. J. & Joazeiro, C. A. RING domain E3 ubiquitin ligases. *Annu Rev Biochem* **78**, 399-434 (2009). https://doi.org/10.1146/annurev.biochem.78.101807.093809

17 Perez Berrocal, D. A., Witting, K. F., Ovaa, H. & Mulder, M. P. C. Hybrid Chains: A Collaboration of Ubiquitin and Ubiquitin-Like Modifiers Introducing Cross-Functionality to the Ubiquitin Code. *Front Chem* **7**, 931 (2019). https://doi.org/10.3389/fchem.2019.00931

18 Glickman, M. H. & Ciechanover, A. The ubiquitin-proteasome proteolytic pathway: destruction for the sake of construction. *Physiol Rev* **82**, 373-428 (2002). https://doi.org/10.1152/physrev.00027.2001

19 Rahman, S. & Wolberger, C. Breaking the K48-chain: linking ubiquitin beyond protein degradation. *Nat Struct Mol Biol* **31**, 216-218 (2024). https://doi.org/10.1038/s41594-024-01221-w
20 Hoeller, D. *et al.* Regulation of ubiquitin-binding proteins by monoubiquitination. *Nat Cell Biol* **8**, 163-169 (2006). https://doi.org/10.1038/ncb1354
21 Fiil, B. K. & Gyrd-Hansen, M. The Met1-linked ubiquitin machinery in inflammation and infection. *Cell Death Differ* **28**, 557-569 (2021). https://doi.org/10.1038/s41418-020-00702-x
22 Yu, Y. *et al.* K29-linked ubiquitin signaling regulates proteotoxic stress response and cell cycle. *Nat Chem Biol* **17**, 896-905 (2021). https://doi.org/10.1038/s41589-021-00823-5
23 Liu, P. *et al.* K63-linked polyubiquitin chains bind to DNA to facilitate DNA damage repair. *Sci Signal* **11**, eaar8133 (2018). https://doi.org/10.1126/scisignal.aar8133
24 Husnjak, K. & Dikic, I. Ubiquitin-binding proteins: decoders of ubiquitin-mediated cellular functions. *Annu Rev Biochem* **81**, 291-322 (2012). https://doi.org/10.1146/annurev-biochem-051810-094654
25 Hurley, J. H., Lee, S. & Prag, G. Ubiquitin-binding domains. *Biochem J* **399**, 361-372 (2006). https://doi.org/10.1042/BJ20061138
26 Kirkin, V. & Dikic, I. Role of ubiquitin- and Ubl-binding proteins in cell signaling. *Curr Opin Cell Biol* **19**, 199-205 (2007). https://doi.org/10.1016/j.ceb.2007.02.002
27 Hoeller, D. *et al.* E3-independent monoubiquitination of ubiquitin-binding proteins. *Mol Cell* **26**, 891-898 (2007). https://doi.org/10.1016/j.molcel.2007.05.014
28 Haapasalo, A. *et al.* Emerging role of Alzheimer's disease-associated ubiquilin-1 in protein aggregation. *Biochem Soc T* **38**, 150-155 (2010). https://doi.org/10.1042/Bst0380150
29 Harman, C. A. & Monteiro, M. J. The specificity of ubiquitin binding to ubiquilin-1 is regulated by sequences besides its UBA domain. *Bba-Gen Subjects* **1863**, 1568-1574 (2019). https://doi.org/10.1016/j.bbagen.2019.06.002
30 Komander, D., Clague, M. J. & Urbe, S. Breaking the chains: structure and function of the deubiquitinases. *Nat Rev Mol Cell Biol* **10**, 550-563 (2009). https://doi.org/10.1038/nrm2731
31 Clague, M. J., Urbe, S. & Komander, D. Breaking the chains: deubiquitylating enzyme specificity begets function. *Nat Rev Mol Cell Biol* **20**, 338-352 (2019). https://doi.org/10.1038/s41580-019-0099-1
32 Lange, S. M., Armstrong, L. A. & Kulathu, Y. Deubiquitinases: From mechanisms to their inhibition by small molecules. *Mol Cell* **82**, 15-29 (2022). https://doi.org/10.1016/j.molcel.2021.10.027
33 Lee, B. H. *et al.* USP14 deubiquitinates proteasome-bound substrates that are ubiquitinated at multiple sites. *Nature* **532**, 398-401 (2016). https://doi.org/10.1038/nature17433
34 Patel, K. *et al.* Discovering proteasomal deubiquitinating enzyme inhibitors for cancer therapy: lessons from rational design, nature and old drug reposition. *Future Med Chem* **10**, 2087-2108 (2018). https://doi.org/10.4155/fmc-2018-0091
35 Cavadini, S. *et al.* Cullin-RING ubiquitin E3 ligase regulation by the COP9 signalosome. *Nature* **531**, 598-603 (2016). https://doi.org/10.1038/nature17416
36 Dewson, G., Eichhorn, P. J. A. & Komander, D. Deubiquitinases in cancer. *Nat Rev Cancer* **23**, 842-862 (2023). https://doi.org/10.1038/s41568-023-00633-y
37 Xian, Y. *et al.* Deubiquitinases as novel therapeutic targets for diseases. *MedComm (2020)* **5**, e70036 (2024). https://doi.org/10.1002/mco2.70036
38 Testa, J. R. *et al.* Germline BAP1 mutations predispose to malignant mesothelioma. *Nat Genet* **43**, 1022-1025 (2011). https://doi.org/10.1038/ng.912
39 Harbour, J. W. *et al.* Frequent mutation of BAP1 in metastasizing uveal melanomas. *Science* **330**, 1410-1413 (2010). https://doi.org/10.1126/science.1194472

40 Lu, L. *et al.* FSTL1-USP10-Notch1 Signaling Axis Protects Against Cardiac Dysfunction Through Inhibition of Myocardial Fibrosis in Diabetic Mice. *Front Cell Dev Biol* **9**, 757068 (2021). https://doi.org/10.3389/fcell.2021.757068
41 Shin, D. *et al.* Bacterial OTU deubiquitinases regulate substrate ubiquitination upon Legionella infection. *Elife* **9**, e58277 (2020). https://doi.org/10.7554/eLife.58277
42 Kubori, T., Kitao, T. & Nagai, H. Emerging insights into bacterial deubiquitinases. *Curr Opin Microbiol* **47**, 14-19 (2019). https://doi.org/10.1016/j.mib.2018.10.001
43 Kumar, P., Kumar, P., Mandal, D. & Velayutham, R. The emerging role of Deubiquitinases (DUBs) in parasites: A foresight review. *Front Cell Infect Microbiol* **12**, 985178 (2022). https://doi.org/10.3389/fcimb.2022.985178
44 Yap, T. A. *et al.* First-in-human phase I trial of the oral first-in-class ubiquitin specific peptidase 1 (USP1) inhibitor KSQ-4279 (KSQi), given as single agent (SA) and in combination with olaparib (OLA) or carboplatin (CARBO) in patients (pts) with advanced solid tumors, enriched for deleterious homologous recombination repair (HRR) mutations. *Journal of Clinical Oncology* **42**, 3005-3005 (2024). https://doi.org/10.1200/JCO.2024.42.16_suppl.3005
45 Xu, J. Y. *et al.* Preclinical Study of a Novel USP28 Inhibitor for the Treatment of Burkitt Lymphoma. *Blood* **144**, 5838-5839 (2024). https://doi.org/10.1182/blood-2024-209311
46 Therapeutics, M. *Mission Therapeutics announces US FDA approval to initiate Phase II clinical trial of its lead asset MTX652 in Acute Kidney Injury*, <https://missiontherapeutics.com/mission-therapeutics-announces-us-fda-approval-to-initiate-phase-ii-clinical-trial-of-its-lead-asset-mtx652-in-acute-kidney-injury/> (2023).
47 Hoeller, D. & Dikic, I. Targeting the ubiquitin system in cancer therapy. *Nature* **458**, 438-444 (2009). https://doi.org/10.1038/nature07960
48 Wu, H. Q., Baker, D. & Ovaa, H. Small molecules that target the ubiquitin system. *Biochem Soc Trans* **48**, 479-497 (2020). https://doi.org/10.1042/BST20190535
49 Manasanch, E. E. & Orlowski, R. Z. Proteasome inhibitors in cancer therapy. *Nat Rev Clin Oncol* **14**, 417-433 (2017). https://doi.org/10.1038/nrclinonc.2016.206
50 Kim, J., So, D., Shin, H. W., Chun, Y. S. & Park, J. W. HIF-1α Upregulation due to Depletion of the Free Ubiquitin Pool. *J Korean Med Sci* **30**, 1388-1395 (2015). https://doi.org/10.3346/jkms.2015.30.10.1388
51 Robak, T. *et al.* Bortezomib-based therapy for newly diagnosed mantle-cell lymphoma. *N Engl J Med* **372**, 944-953 (2015). https://doi.org/10.1056/NEJMoa1412096
52 Kim, K. B. & Crews, C. M. From epoxomicin to carfilzomib: chemistry, biology, and medical outcomes. *Nat Prod Rep* **30**, 600-604 (2013). https://doi.org/10.1039/c3np20126k
53 Kisselev, A. F. & Goldberg, A. L. Proteasome inhibitors: from research tools to drug candidates. *Chem Biol* **8**, 739-758 (2001). https://doi.org/10.1016/s1074-5521(01)00056-4
54 Maio, G. [On the history of the Contergan (thalidomide) catastrophe in the light of drug legislation]. *Dtsch Med Wochenschr* **126**, 1183-1186 (2001). https://doi.org/10.1055/s-2001-17888
55 McBride, W. G. Thalidomide and congenital abnormalities. *Lancet* **2**, 90927-90928 (1961).
56 Lenz, W., Pfeiffer, R. A., Kosenow, W. & Hayman, D. J. Thalidomide and Congenital Abnormalities. *The Lancet* **279**, 45-46 (1962). https://doi.org/10.1016/s0140-6736(62)92665-x
57 Kronke, J. *et al.* Lenalidomide causes selective degradation of IKZF1 and IKZF3 in multiple myeloma cells. *Science* **343**, 301-305 (2014). https://doi.org/10.1126/science.1244851
58 Ito, T. *et al.* Identification of a primary target of thalidomide teratogenicity. *Science* **327**, 1345-1350 (2010). https://doi.org/10.1126/science.1177319

59 Fischer, E. S. *et al.* Structure of the DDB1-CRBN E3 ubiquitin ligase in complex with thalidomide. *Nature* **512**, 49-53 (2014). https://doi.org/10.1038/nature13527
60 Sievers, Q. L., Gasser, J. A., Cowley, G. S., Fischer, E. S. & Ebert, B. L. Genome-wide screen identifies cullin-RING ligase machinery required for lenalidomide-dependent CRL4(CRBN) activity. *Blood* **132**, 1293-1303 (2018). https://doi.org/10.1182/blood-2018-01-821769
61 Tan, X. *et al.* Mechanism of auxin perception by the TIR1 ubiquitin ligase. *Nature* **446**, 640-645 (2007). https://doi.org/10.1038/nature05731
62 Tsai, J. M., Nowak, R. P., Ebert, B. L. & Fischer, E. S. Targeted protein degradation: from mechanisms to clinic. *Nat Rev Mol Cell Biol* **25**, 740-757 (2024). https://doi.org/10.1038/s41580-024-00729-9
63 Dimitrova, Y. N., Gutierrez, J. A. & Huard, K. It's ok to be outnumbered - sub-stoichiometric modulation of homomeric protein complexes. *RSC Med Chem* **14**, 22-46 (2023). https://doi.org/10.1039/d2md00212d
64 Han, T. *et al.* Anticancer sulfonamides target splicing by inducing RBM39 degradation via recruitment to DCAF15. *Science* **356** (2017). https://doi.org/10.1126/science.aal3755
65 Uehara, T. *et al.* Selective degradation of splicing factor CAPERalpha by anticancer sulfonamides. *Nat Chem Biol* **13**, 675-680 (2017). https://doi.org/10.1038/nchembio.2363
66 Oleinikovas, V., Gainza, P., Ryckmans, T., Fasching, B. & Thoma, N. H. From Thalidomide to Rational Molecular Glue Design for Targeted Protein Degradation. *Annu Rev Pharmacol Toxicol* **64**, 291-312 (2024). https://doi.org/10.1146/annurev-pharmtox-022123-104147
67 Teng, M. *et al.* Development of PDE6D and CK1alpha Degraders through Chemical Derivatization of FPFT-2216. *J Med Chem* **65**, 747-756 (2022). https://doi.org/10.1021/acs.jmedchem.1c01832
68 Sakamoto, K. M. *et al.* Protacs: chimeric molecules that target proteins to the Skp1-Cullin-F box complex for ubiquitination and degradation. *Proc Natl Acad Sci U S A* **98**, 8554-8559 (2001). https://doi.org/10.1073/pnas.141230798
69 Schneekloth, A. R., Pucheault, M., Tae, H. S. & Crews, C. M. Targeted intracellular protein degradation induced by a small molecule: En route to chemical proteomics. *Bioorg Med Chem Lett* **18**, 5904-5908 (2008). https://doi.org/10.1016/j.bmcl.2008.07.114
70 Ishida, T. & Ciulli, A. E3 Ligase Ligands for PROTACs: How They Were Found and How to Discover New Ones. *SLAS Discov* **26**, 484-502 (2021). https://doi.org/10.1177/2472555220965528
71 Zengerle, M., Chan, K. H. & Ciulli, A. Selective Small Molecule Induced Degradation of the BET Bromodomain Protein BRD4. *ACS Chem Biol* **10**, 1770-1777 (2015). https://doi.org/10.1021/acschembio.5b00216
72 Winter, G. E. *et al.* DRUG DEVELOPMENT. Phthalimide conjugation as a strategy for in vivo target protein degradation. *Science* **348**, 1376-1381 (2015). https://doi.org/10.1126/science.aab1433
73 Jevtic, P., Haakonsen, D. L. & Rape, M. An E3 ligase guide to the galaxy of small-molecule-induced protein degradation. *Cell Chem Biol* **28**, 1000-1013 (2021). https://doi.org/10.1016/j.chembiol.2021.04.002
74 Burslem, G. M. & Crews, C. M. Proteolysis-Targeting Chimeras as Therapeutics and Tools for Biological Discovery. *Cell* **181**, 102-114 (2020). https://doi.org/10.1016/j.cell.2019.11.031
75 Bemis, T. A., La Clair, J. J. & Burkart, M. D. Unraveling the Role of Linker Design in Proteolysis Targeting Chimeras. *J Med Chem* **64**, 8042-8052 (2021). https://doi.org/10.1021/acs.jmedchem.1c00482

76 Kannt, A. & Dikic, I. Expanding the arsenal of E3 ubiquitin ligases for proximity-induced protein degradation. *Cell Chem Biol* **28**, 1014-1031 (2021). https://doi.org/10.1016/j.chembiol.2021.04.007
77 Chan, W. C. *et al.* Accelerating inhibitor discovery for deubiquitinating enzymes. *Nat Commun* **14**, 686 (2023). https://doi.org/10.1038/s41467-023-36246-0
78 Altun, M. *et al.* Activity-based chemical proteomics accelerates inhibitor development for deubiquitylating enzymes. *Chem Biol* **18**, 1401-1412 (2011). https://doi.org/10.1016/j.chembiol.2011.08.018
79 Wrigley, J. D. *et al.* Identification and Characterization of Dual Inhibitors of the USP25/28 Deubiquitinating Enzyme Subfamily. *ACS Chem Biol* **12**, 3113-3125 (2017). https://doi.org/10.1021/acschembio.7b00334
80 Di Lello, P. *et al.* Discovery of Small-Molecule Inhibitors of Ubiquitin Specific Protease 7 (USP7) Using Integrated NMR and in Silico Techniques. *J Med Chem* **60**, 10056-10070 (2017). https://doi.org/10.1021/acs.jmedchem.7b01293
81 Kluge, A. F. *et al.* Novel highly selective inhibitors of ubiquitin specific protease 30 (USP30) accelerate mitophagy. *Bioorg Med Chem Lett* **28**, 2655-2659 (2018). https://doi.org/10.1016/j.bmcl.2018.05.013
82 Chan, W. C. *et al.* Accelerating inhibitor discovery for deubiquitinating enzymes. *Nature Communications* **14**, 686 (2023). https://doi.org/10.1038/s41467-023-36246-0
83 Gavory, G. *et al.* Discovery and characterization of highly potent and selective allosteric USP7 inhibitors. *Nat Chem Biol* **14**, 118-125 (2018). https://doi.org/10.1038/nchembio.2528
84 Varca, A. C. *et al.* Identification and validation of selective deubiquitinase inhibitors. *Cell Chem Biol* **28**, 1758-1771 e1713 (2021). https://doi.org/10.1016/j.chembiol.2021.05.012
85 Goricke, F. *et al.* Discovery and Characterization of BAY-805, a Potent and Selective Inhibitor of Ubiquitin-Specific Protease USP21. *J Med Chem* **66**, 3431-3447 (2023). https://doi.org/10.1021/acs.jmedchem.2c01933
86 Turnbull, A. P. *et al.* Molecular basis of USP7 inhibition by selective small-molecule inhibitors. *Nature* **550**, 481-486 (2017). https://doi.org/10.1038/nature24451
87 Lee, B. H. *et al.* Enhancement of proteasome activity by a small-molecule inhibitor of USP14. *Nature* **467**, 179-184 (2010). https://doi.org/10.1038/nature09299
88 Boselli, M. *et al.* An inhibitor of the proteasomal deubiquitinating enzyme USP14 induces tau elimination in cultured neurons. *J Biol Chem* **292**, 19209-19225 (2017). https://doi.org/10.1074/jbc.M117.815126
89 Grethe, C. *et al.* Structural basis for specific inhibition of the deubiquitinase UCHL1. *Nat Commun* **13**, 5950 (2022). https://doi.org/10.1038/s41467-022-33559-4
90 Schmidt, M. *et al.* N-Cyanopiperazines as Specific Covalent Inhibitors of the Deubiquitinating Enzyme UCHL1. *Angew Chem Int Ed Engl* **63**, e202318849 (2024). https://doi.org/10.1002/anie.202318849
91 Murgai, A. *et al.* Targeting the deubiquitinase USP7 for degradation with PROTACs. *Chem Commun (Camb)* **58**, 8858-8861 (2022). https://doi.org/10.1039/d2cc02094g
92 Henning, N. J. *et al.* Deubiquitinase-targeting chimeras for targeted protein stabilization. *Nat Chem Biol* **18**, 412-421 (2022). https://doi.org/10.1038/s41589-022-00971-2
93 Ma, Z., Zhou, M., Chen, H., Shen, Q. & Zhou, J. Deubiquitinase-Targeting Chimeras (DUBTACs) as a Potential Paradigm-Shifting Drug Discovery Approach. *J Med Chem* **68**, 6897-6915 (2025). https://doi.org/10.1021/acs.jmedchem.4c02975
94 Langlois, C. R. *et al.* A GID E3 ligase assembly ubiquitinates an Rsp5 E3 adaptor and regulates plasma membrane transporters. *EMBO Rep* **23**, e53835 (2022). https://doi.org/10.15252/embr.202153835

95 Duda, D. M. *et al.* Structural insights into NEDD8 activation of cullin-RING ligases: conformational control of conjugation. *Cell* **134**, 995-1006 (2008). https://doi.org/10.1016/j.cell.2008.07.022
96 Huang, H. T. *et al.* Ubiquitin-specific proximity labeling for the identification of E3 ligase substrates. *Nat Chem Biol* **20**, 1227-1236 (2024). https://doi.org/10.1038/s41589-024-01590-9
97 van Tilburg, G. B., Elhebieshy, A. F. & Ovaa, H. Synthetic and semi-synthetic strategies to study ubiquitin signaling. *Curr Opin Struct Biol* **38**, 92-101 (2016). https://doi.org/10.1016/j.sbi.2016.05.022
98 Leestemaker, Y. & Ovaa, H. Tools to investigate the ubiquitin proteasome system. *Drug Discov Today Technol* **26**, 25-31 (2017). https://doi.org/10.1016/j.ddtec.2017.11.006
99 Sui, X. *et al.* Development and application of ubiquitin-based chemical probes. *Chem Sci* **11**, 12633-12646 (2020). https://doi.org/10.1039/d0sc03295f
100 Zhao, Z., O'Dea, R., Wendrich, K., Kazi, N. & Gersch, M. Native Semisynthesis of Isopeptide-Linked Substrates for Specificity Analysis of Deubiquitinases and Ubl Proteases. *J Am Chem Soc* **145**, 20801-20812 (2023). https://doi.org/10.1021/jacs.3c04062
101 Verma, R. *et al.* Role of Rpn11 metalloprotease in deubiquitination and degradation by the 26S proteasome. *Science* **298**, 611-615 (2002). https://doi.org/10.1126/science.1075898
102 Prus, G., Satpathy, S., Weinert, B. T., Narita, T. & Choudhary, C. Global, site-resolved analysis of ubiquitylation occupancy and turnover rate reveals systems properties. *Cell* **187**, 2875-2892 e2821 (2024). https://doi.org/10.1016/j.cell.2024.03.024
103 Mattern, M., Sutherland, J., Kadimisetty, K., Barrio, R. & Rodriguez, M. S. Using Ubiquitin Binders to Decipher the Ubiquitin Code. *Trends Biochem Sci* **44**, 599-615 (2019). https://doi.org/10.1016/j.tibs.2019.01.011
104 Sun, M. & Zhang, X. Current methodologies in protein ubiquitination characterization: from ubiquitinated protein to ubiquitin chain architecture. *Cell Biosci* **12**, 126 (2022). https://doi.org/10.1186/s13578-022-00870-y
105 Fulzele, A. & Bennett, E. J. in *The Ubiquitin Proteasome System: Methods and Protocols* (eds Thibault Mayor & Gary Kleiger) 363-384 (Springer New York, 2018).
106 Stes, E. *et al.* A COFRADIC protocol to study protein ubiquitination. *J Proteome Res* **13**, 3107-3113 (2014). https://doi.org/10.1021/pr4012443
107 Berk, J. M. *et al.* A deubiquitylase with an unusually high-affinity ubiquitin-binding domain from the scrub typhus pathogen Orientia tsutsugamushi. *Nat Commun* **11**, 2343 (2020). https://doi.org/10.1038/s41467-020-15985-4
108 Zhang, M., Berk, J. M., Mehrtash, A. B., Kanyo, J. & Hochstrasser, M. A versatile new tool derived from a bacterial deubiquitylase to detect and purify ubiquitylated substrates and their interacting proteins. *PLoS Biol* **20**, e3001501 (2022). https://doi.org/10.1371/journal.pbio.3001501
109 Yoshida, Y. *et al.* A comprehensive method for detecting ubiquitinated substrates using TR-TUBE. *Proc Natl Acad Sci U S A* **112**, 4630-4635 (2015). https://doi.org/10.1073/pnas.1422313112
110 Hjerpe, R. *et al.* Efficient protection and isolation of ubiquitylated proteins using tandem ubiquitin-binding entities. *EMBO Rep* **10**, 1250-1258 (2009). https://doi.org/10.1038/embor.2009.192
111 Sato, Y. *et al.* Structural basis for specific recognition of Lys 63-linked polyubiquitin chains by tandem UIMs of RAP80. *EMBO J* **28**, 2461-2468 (2009). https://doi.org/10.1038/emboj.2009.160

112 Kristariyanto, Y. A., Abdul Rehman, S. A., Weidlich, S., Knebel, A. & Kulathu, Y. A single MIU motif of MINDY-1 recognizes K48-linked polyubiquitin chains. *EMBO Rep* **18**, 392-402 (2017). https://doi.org/10.15252/embr.201643205
113 Tsuchiya, H. *et al.* Ub-ProT reveals global length and composition of protein ubiquitylation in cells. *Nat Commun* **9**, 524 (2018). https://doi.org/10.1038/s41467-018-02869-x
114 Scholes, N. S., Mayor-Ruiz, C. & Winter, G. E. Identification and selectivity profiling of small-molecule degraders via multi-omics approaches. *Cell Chem Biol* **28**, 1048-1060 (2021). https://doi.org/10.1016/j.chembiol.2021.03.007
115 Mayor-Ruiz, C. *et al.* Rational discovery of molecular glue degraders via scalable chemical profiling. *Nat Chem Biol* **16**, 1199-1207 (2020). https://doi.org/10.1038/s41589-020-0594-x
116 Vendrell-Navarro, G., Brockmeyer, A., Waldmann, H., Janning, P. & Ziegler, S. in *Chemical Biology: Methods and Protocols* (eds Jonathan E. Hempel, Charles H. Williams, & Charles C. Hong) 263-286 (Springer New York, 2015).
117 Winzker, M. *et al.* Development of a PDEdelta-Targeting PROTACs that Impair Lipid Metabolism. *Angew Chem Int Ed Engl* **59**, 5595-5601 (2020). https://doi.org/10.1002/anie.201913904
118 Jochem, M. *et al.* Degradome analysis to identify direct protein substrates of small-molecule degraders. *Cell Chem Biol* **32**, 192-200 e196 (2025). https://doi.org/10.1016/j.chembiol.2024.10.007
119 Kawamura, T. *et al.* Discovery of small-molecule modulator of heterotrimeric G(i)-protein by integrated phenotypic profiling and chemical proteomics. *Biosci Biotechnol Biochem* **84**, 2484-2490 (2020). https://doi.org/10.1080/09168451.2020.1812375
120 Wolf-Levy, H. *et al.* Revealing the cellular degradome by mass spectrometry analysis of proteasome-cleaved peptides. *Nat Biotechnol* **36**, 1110-1116 (2018). https://doi.org/10.1038/nbt.4279
121 Johnson, A. & Vert, G. Unraveling K63 Polyubiquitination Networks by Sensor-Based Proteomics. *Plant Physiol* **171**, 1808-1820 (2016). https://doi.org/10.1104/pp.16.00619
122 Gao, Y. *et al.* Enhanced Purification of Ubiquitinated Proteins by Engineered Tandem Hybrid Ubiquitin-binding Domains (ThUBDs). *Mol Cell Proteomics* **15**, 1381-1396 (2016). https://doi.org/10.1074/mcp.o115.051839
123 Silva, G. M., Finley, D. & Vogel, C. K63 polyubiquitination is a new modulator of the oxidative stress response. *Nat Struct Mol Biol* **22**, 116-123 (2015). https://doi.org/10.1038/nsmb.2955
124 Mata-Cantero, L. *et al.* New insights into host-parasite ubiquitin proteome dynamics in P. falciparum infected red blood cells using a TUBEs-MS approach. *J Proteomics* **139**, 45-59 (2016). https://doi.org/10.1016/j.jprot.2016.03.004
125 Shi, Y. *et al.* A data set of human endogenous protein ubiquitination sites. *Mol Cell Proteomics* **10**, M110 002089 (2011). https://doi.org/10.1074/mcp.M110.002089
126 Quinet, G. *et al.* Constitutive Activation of p62/Sequestosome-1-Mediated Proteaphagy Regulates Proteolysis and Impairs Cell Death in Bortezomib-Resistant Mantle Cell Lymphoma. *Cancers (Basel)* **14** (2022). https://doi.org/10.3390/cancers14040923
127 Kadimisetty, K., Sheets, K. J., Gross, P. H., Zerr, M. J. & Ouazia, D. Tandem Ubiquitin Binding Entities (TUBEs) as Tools to Explore Ubiquitin-Proteasome System and PROTAC Drug Discovery. *Methods Mol Biol* **2365**, 185-202 (2021). https://doi.org/10.1007/978-1-0716-1665-9_10
128 Kandan, S., Thiagaraj, D. & Devi, R. R. in *Methods for Fragments Screening Using Surface Plasmon Resonance* (eds Sameer Mahmood Zaheer & Ramachandraiah Gosu) Ch. Chapter 4, 23-31 (Springer Singapore, 2021).
129 Keilhauer, E. C., Hein, M. Y. & Mann, M. Accurate protein complex retrieval by affinity enrichment mass spectrometry (AE-MS) rather than affinity purification mass

spectrometry (AP-MS). *Mol Cell Proteomics* **14**, 120-135 (2015). https://doi.org/10.1074/mcp.M114.041012

130 Meyer, H. & Weihl, C. C. The VCP/p97 system at a glance: connecting cellular function to disease pathogenesis. *J Cell Sci* **127**, 3877-3883 (2014). https://doi.org/10.1242/jcs.093831

131 Magnaghi, P. *et al.* Covalent and allosteric inhibitors of the ATPase VCP/p97 induce cancer cell death. *Nat Chem Biol* **9**, 548-556 (2013). https://doi.org/10.1038/nchembio.1313

132 Hughes, C. S. *et al.* Single-pot, solid-phase-enhanced sample preparation for proteomics experiments. *Nat Protoc* **14**, 68-85 (2019). https://doi.org/10.1038/s41596-018-0082-x

133 Yi, J. *et al.* Spautin-1 promotes PINK1-PRKN-dependent mitophagy and improves associative learning capability in an alzheimer disease animal model. *Autophagy* **20**, 2655-2676 (2024). https://doi.org/10.1080/15548627.2024.2383145

134 Meyer, C., Garzia, A., Morozov, P., Molina, H. & Tuschl, T. The G3BP1-Family-USP10 Deubiquitinase Complex Rescues Ubiquitinated 40S Subunits of Ribosomes Stalled in Translation from Lysosomal Degradation. *Mol Cell* **77**, 1193-1205 e1195 (2020). https://doi.org/10.1016/j.molcel.2019.12.024

135 Zhao, C. *et al.* A self-amplifying USP14-TAZ loop drives the progression and liver metastasis of pancreatic ductal adenocarcinoma. *Cell Death Differ* **30**, 1-15 (2023). https://doi.org/10.1038/s41418-022-01040-w

136 Li, C. *et al.* Nuclear receptor coactivator 4-mediated ferritinophagy contributes to cerebral ischemia-induced ferroptosis in ischemic stroke. *Pharmacol Res* **174**, 105933 (2021). https://doi.org/10.1016/j.phrs.2021.105933

137 Guo, Y. *et al.* Oncogenic KRAS effector USP13 promotes metastasis in non-small cell lung cancer through deubiquitinating beta-catenin. *Cell Rep* **42**, 113511 (2023). https://doi.org/10.1016/j.celrep.2023.113511

138 Sowa, M. E., Bennett, E. J., Gygi, S. P. & Harper, J. W. Defining the human deubiquitinating enzyme interaction landscape. *Cell* **138**, 389-403 (2009). https://doi.org/10.1016/j.cell.2009.04.042

139 Bushman, J. W. *et al.* Proteomics-Based Identification of DUB Substrates Using Selective Inhibitors. *Cell Chem Biol* **28**, 78-87 e73 (2021). https://doi.org/10.1016/j.chembiol.2020.09.005

140 Steger, M. *et al.* Time-resolved in vivo ubiquitinome profiling by DIA-MS reveals USP7 targets on a proteome-wide scale. *Nat Commun* **12**, 5399 (2021). https://doi.org/10.1038/s41467-021-25454-1

141 Scheffner, M., Werness, B. A., Huibregtse, J. M., Levine, A. J. & Howley, P. M. The E6 oncoprotein encoded by human papillomavirus types 16 and 18 promotes the degradation of p53. *Cell* **63**, 1129-1136 (1990). https://doi.org/10.1016/0092-8674(90)90409-8

142 Hennes, E. *et al.* Identification of a Monovalent Pseudo-Natural Product Degrader Class Supercharging Degradation of IDO1 by its native E3 KLHDC3. *bioRxiv*, 2024.2007.2010.602857 (2025). https://doi.org/10.1101/2024.07.10.602857

143 Homan, R. A., Jadhav, A. M., Conway, L. P. & Parker, C. G. A Chemical Proteomic Map of Heme-Protein Interactions. *J Am Chem Soc* **144**, 15013-15019 (2022). https://doi.org/10.1021/jacs.2c06104

144 Li, X. *et al.* Emerging discoveries on the role of TRIM14: from diseases to immune regulation. *Cell Death Discov* **10**, 513 (2024). https://doi.org/10.1038/s41420-024-02276-w

145 Zou, Y. *et al.* Cytochrome P450 oxidoreductase contributes to phospholipid peroxidation in ferroptosis. *Nat Chem Biol* **16**, 302-309 (2020). https://doi.org/10.1038/s41589-020-0472-6

146 Jahn, R. & Scheller, R. H. SNAREs--engines for membrane fusion. *Nat Rev Mol Cell Biol* **7**, 631-643 (2006). https://doi.org/10.1038/nrm2002
147 Jang, Y. *et al.* Intrinsically disordered protein RBM14 plays a role in generation of RNA:DNA hybrids at double-strand break sites. *Proc Natl Acad Sci U S A* **117**, 5329-5338 (2020). https://doi.org/10.1073/pnas.1913280117
148 Deng, S. *et al.* Overexpression of COX7A2 is associated with a good prognosis in patients with glioma. *J Neurooncol* **136**, 41-50 (2018). https://doi.org/10.1007/s11060-017-2637-z
149 Zhang, J. *et al.* Ninjurin 2 Modulates Tumorigenesis, Inflammation, and Metabolism via Pyroptosis. *Am J Pathol* **194**, 849-860 (2024). https://doi.org/10.1016/j.ajpath.2024.01.013
150 Zhou, R., Pan, J., Zhang, W. B. & Li, X. D. Myosin-5a facilitates stress granule formation by interacting with G3BP1. *Cell Mol Life Sci* **81**, 430 (2024). https://doi.org/10.1007/s00018-024-05468-w
151 Guna, A., Volkmar, N., Christianson, J. C. & Hegde, R. S. The ER membrane protein complex is a transmembrane domain insertase. *Science* **359**, 470-473 (2018). https://doi.org/10.1126/science.aao3099
152 Yuan, Z. *et al.* ATG14 targets lipid droplets and acts as an autophagic receptor for syntaxin18-regulated lipid droplet turnover. *Nat Commun* **15**, 631 (2024). https://doi.org/10.1038/s41467-024-44978-w
153 Guven, A. *et al.* Diablo ubiquitination analysis by sandwich immunoassay. *J Pharm Biomed Anal* **173**, 40-46 (2019). https://doi.org/10.1016/j.jpba.2019.05.005
154 Akbarzadeh, M. *et al.* Morphological profiling by means of the Cell Painting assay enables identification of tubulin-targeting compounds. *Cell Chem Biol* **29**, 1053-1064 e1053 (2022). https://doi.org/10.1016/j.chembiol.2021.12.009
155 Schneidewind, T. *et al.* Combined morphological and proteome profiling reveals target-independent impairment of cholesterol homeostasis. *Cell Chem Biol* **28**, 1780-1794 e1785 (2021). https://doi.org/10.1016/j.chembiol.2021.06.003
156 Porras-Yakushi, T. R., Reitsma, J. M., Sweredoski, M. J., Deshaies, R. J. & Hess, S. In-depth proteomic analysis of proteasome inhibitors bortezomib, carfilzomib and MG132 reveals that mortality factor 4-like 1 (MORF4L1) protein ubiquitylation is negatively impacted. *J Proteomics* **241**, 104197 (2021). https://doi.org/10.1016/j.jprot.2021.104197
157 Herline-Killian, K. *et al.* Modulation of CREB3L2-ATF4 heterodimerization via proteasome inhibition and HRI activation in Alzheimer's disease pathology. *Cell Death Dis* **16**, 225 (2025). https://doi.org/10.1038/s41419-025-07586-0
158 Townson, S. M. *et al.* SAFB2, a new scaffold attachment factor homolog and estrogen receptor corepressor. *J Biol Chem* **278**, 20059-20068 (2003). https://doi.org/10.1074/jbc.M212988200
159 Coates, H. W., Capell-Hattam, I. M. & Brown, A. J. The mammalian cholesterol synthesis enzyme squalene monooxygenase is proteasomally truncated to a constitutively active form. *J Biol Chem* **296**, 100731 (2021). https://doi.org/10.1016/j.jbc.2021.100731
160 Yang, E. *et al.* Elucidation of TRIM25 ubiquitination targets involved in diverse cellular and antiviral processes. *PLoS Pathog* **18**, e1010743 (2022). https://doi.org/10.1371/journal.ppat.1010743
161 Mast, S. W. *et al.* Human EDEM2, a novel homolog of family 47 glycosidases, is involved in ER-associated degradation of glycoproteins. *Glycobiology* **15**, 421-436 (2005). https://doi.org/10.1093/glycob/cwi014
162 Christianson, J. C. & Carvalho, P. Order through destruction: how ER-associated protein degradation contributes to organelle homeostasis. *EMBO J* **41**, e109845 (2022). https://doi.org/10.15252/embj.2021109845

163 Abdul Rehman, S. A. *et al.* MINDY-1 Is a Member of an Evolutionarily Conserved and Structurally Distinct New Family of Deubiquitinating Enzymes. *Mol Cell* **63**, 146-155 (2016). https://doi.org/10.1016/j.molcel.2016.05.009
164 Abdul Rehman, S. A. *et al.* Mechanism of activation and regulation of deubiquitinase activity in MINDY1 and MINDY2. *Mol Cell* **81**, 4176-4190 e4176 (2021). https://doi.org/10.1016/j.molcel.2021.08.024
165 Tang, J., Luo, Y., Long, G. & Zhou, L. MINDY1 promotes breast cancer cell proliferation by stabilizing estrogen receptor alpha. *Cell Death Dis* **12**, 937 (2021). https://doi.org/10.1038/s41419-021-04244-z
166 Kim, J., So, D., Shin, H. W., Chun, Y. S. & Park, J. W. HIF-1alpha Upregulation due to Depletion of the Free Ubiquitin Pool. *J Korean Med Sci* **30**, 1388-1395 (2015). https://doi.org/10.3346/jkms.2015.30.10.1388
167 Ciechanover, A. Proteolysis: from the lysosome to ubiquitin and the proteasome. *Nat Rev Mol Cell Biol* **6**, 79-87 (2005). https://doi.org/10.1038/nrm1552
168 Mauvezin, C. & Neufeld, T. P. Bafilomycin A1 disrupts autophagic flux by inhibiting both V-ATPase-dependent acidification and Ca-P60A/SERCA-dependent autophagosome-lysosome fusion. *Autophagy* **11**, 1437-1438 (2015). https://doi.org/10.1080/15548627.2015.1066957
169 Hospenthal, M. K., Mevissen, T. E. T. & Komander, D. Deubiquitinase-based analysis of ubiquitin chain architecture using Ubiquitin Chain Restriction (UbiCRest). *Nat Protoc* **10**, 349-361 (2015). https://doi.org/10.1038/nprot.2015.018
170 Davies, C. *et al.* Identification of a Novel Pseudo-Natural Product Type IV IDO1 Inhibitor Chemotype. *Angew Chem Int Ed Engl* **61**, e202209374 (2022). https://doi.org/10.1002/anie.202209374
171 Kelsall, I. R. Non-lysine ubiquitylation: Doing things differently. *Front Mol Biosci* **9**, 1008175 (2022). https://doi.org/10.3389/fmolb.2022.1008175
172 Li, W. *et al.* Highly specific intracellular ubiquitination of a small molecule. *Nat Chem Biol* (2025). https://doi.org/10.1038/s41589-025-02011-1
173 Holman, J. D., Tabb, D. L. & Mallick, P. Employing ProteoWizard to Convert Raw Mass Spectrometry Data. *Curr Protoc Bioinformatics* **46**, 13 24 11-13 24 19 (2014). https://doi.org/10.1002/0471250953.bi1324s46
174 da Veiga Leprevost, F. *et al.* Philosopher: a versatile toolkit for shotgun proteomics data analysis. *Nat Methods* **17**, 869-870 (2020). https://doi.org/10.1038/s41592-020-0912-y
175 Nesvizhskii, A. I., Keller, A., Kolker, E. & Aebersold, R. A statistical model for identifying proteins by tandem mass spectrometry. *Anal Chem* **75**, 4646-4658 (2003). https://doi.org/10.1021/ac0341261
176 Teo, G. C., Polasky, D. A., Yu, F. & Nesvizhskii, A. I. Fast Deisotoping Algorithm and Its Implementation in the MSFragger Search Engine. *J Proteome Res* **20**, 498-505 (2021). https://doi.org/10.1021/acs.jproteome.0c00544
177 Kong, A. T., Leprevost, F. V., Avtonomov, D. M., Mellacheruvu, D. & Nesvizhskii, A. I. MSFragger: ultrafast and comprehensive peptide identification in mass spectrometry-based proteomics. *Nat Methods* **14**, 513-520 (2017). https://doi.org/10.1038/nmeth.4256
178 Kall, L., Canterbury, J. D., Weston, J., Noble, W. S. & MacCoss, M. J. Semi-supervised learning for peptide identification from shotgun proteomics datasets. *Nat Methods* **4**, 923-925 (2007). https://doi.org/10.1038/nmeth1113
179 Yang, K. L. *et al.* MSBooster: improving peptide identification rates using deep learning-based features. *Nat Commun* **14**, 4539 (2023). https://doi.org/10.1038/s41467-023-40129-9
180 Kohler, D. *et al.* MSstatsShiny: A GUI for Versatile, Scalable, and Reproducible Statistical Analyses of Quantitative Proteomic Experiments. *J Proteome Res* **22**, 551-556 (2023). https://doi.org/10.1021/acs.jproteome.2c00603

9. Appendix

9.1 Supplementary Figures

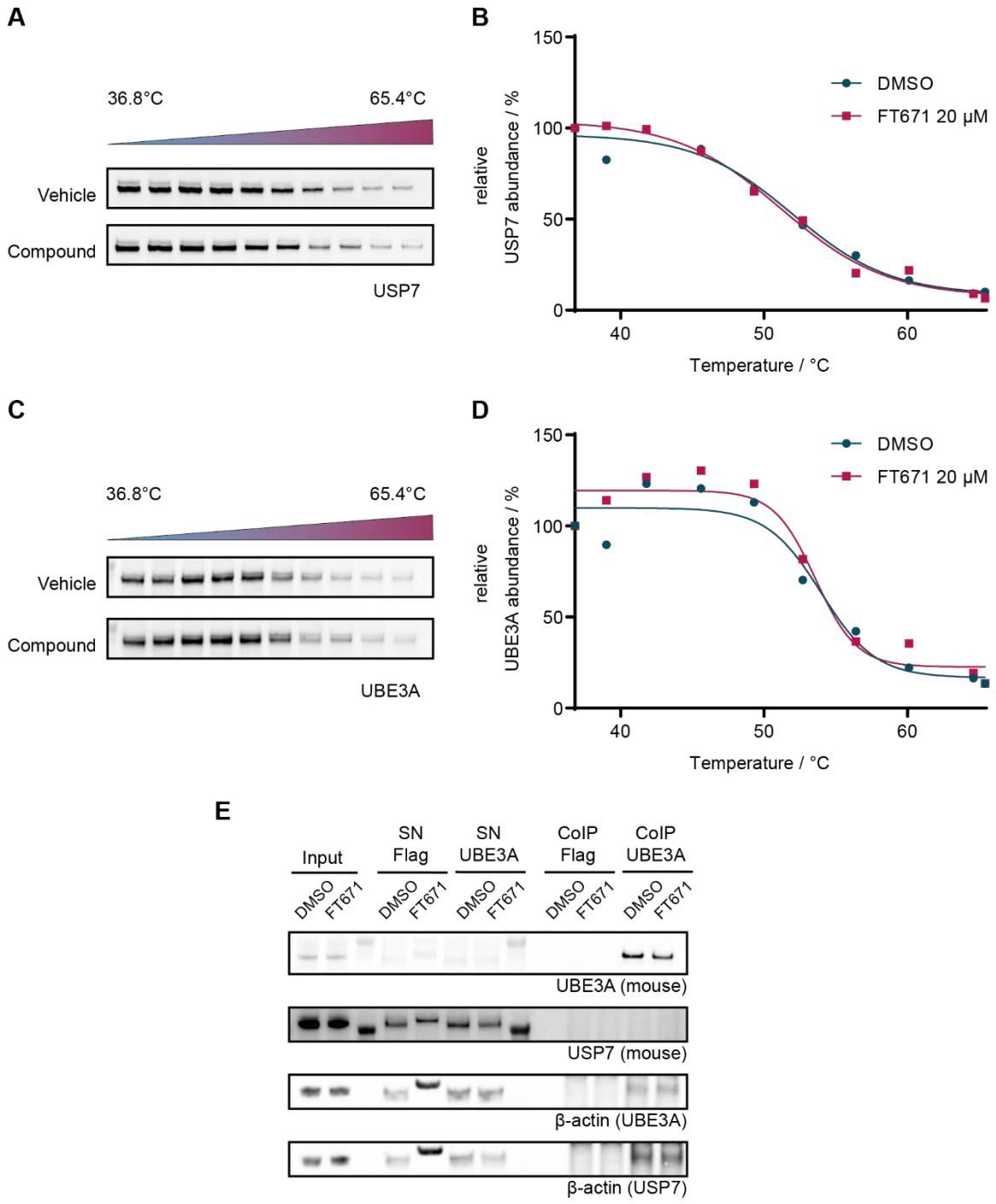

***Supplementary Figure 1**: Cellular thermal shift assay and CoIP of UBE3A and USP7 under FT671 treatment. **A**. Immunoblot of CETSA lysates after heat treatment, as indicated, against USP7 comparing vehicle (DMSO) with compound-treated (20 µM FT671) lysate. **B**. Nonlinear fit melting curve of USP7 protein abundance at different temperatures normalized to the 36.8 °C value for the indicated treatment. **C**. Immunoblot of CETSA lysates after heat*

treatment as indicated against UBE3A comparing vehicle (DMSO) with compound-treated (20 µM FT671) lysate. ***D****. Nonlinear fit melting curve of UBE3A protein abundance at different temperatures normalized to the 36.8 °C value for the indicated treatment.* ***E****. Immunoblotting analysis against UBE3A, USP7 and β-actin of CoIP input, supernatant (SN) and eluate fractions from FT671 or DMSO-treated samples comparing the eluates from anti-UBE3A-coated with anti-Flag-coated protein G beads. The experiments shown in this figure were performed in one replicate.*

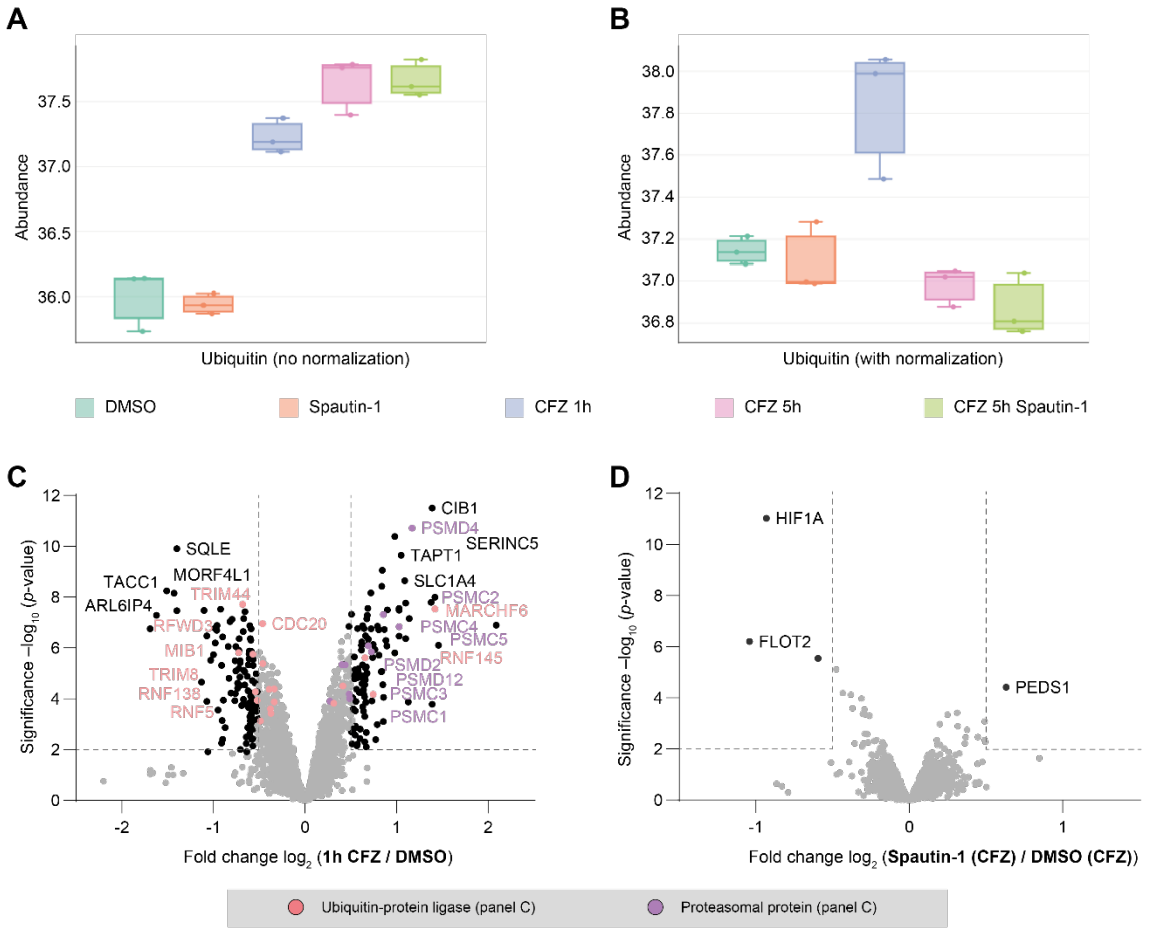

Supplementary Figure 2*: TUBE-MS analysis of Jurkat cells being treated with Spautin-1 (10 µM) for 4 h, CFZ (0.5 µM) for 1 h or 5 h, or DMSO, as indicated.* ***A****.-****B****. Boxplots comparing the individual abundances of Ubiquitin across replicates in the respective conditions, as indicated, from the experiment shown in panel C and D without normalization (panel* ***A****) and with normalization (panel* ***B****).* ***C****. Volcano plot of the TUBE-MS results comparing the polyubiquitome of Jurkat cells treated with CFZ for 1 h with the DMSO control. Ubiquitin ligating proteins and proteasomal proteins are highlighted respectively.* ***D****. Volcano plot of the TUBE-MS results comparing the polyubiquitome of Jurkat cells treated with CFZ for 5 h and Spautin-1 for 4 h with cells treated with CFZ for 5 h and DMSO for 4 h. This figure was taken from Führer, S. et al. Small Molecule-Induced Alterations of Protein Polyubiquitination Revealed by Mass-Spectrometric Ubiquitome Analysis. Angew. Chem. Int. Ed. 64, e202508916 (2025) under a CC-BY 4.0 license.*

9.2 Abbreviations

Abbreviation	Meaning
ABP	Activity-based probe
ACN	Acetonitrile
ATF4	Activating transcription factor 4
ATP	Adenosine triphosphate
BAP1	BRCA1-associated protein 1
Boc	*Tert*-butyloxycarbonyl
BRD2	Bromodomain-containing protein 2
CAA	2-chloroacetamide
CETSA	Cellular thermal shift assay
CFZ	Carfilzomib
Cmp	Compound
COFRADIC	Combined fractional diagonal chromatography
CoIP	Co-immunoprecipitation
CPA	Cell painting analysis
CRBN	Cereblon
CRISPR	Clustered regularly interspaced short palindromic repeats
DMSO	Dimethyl sulfoxide
DTT	Dithiothreitol
DUB	Deubiquitinase
DUBTAC	Deubiquitinase targeting chimera
ER	Endoplasmic reticulum
ERAD	ER-associated degradation
ERα	Estrogen receptor α
EtOH	Ethanol
FC	Fold change
GFP	Green fluorescent protein
GLRX3	Glutaredoxin-3

GST	Glutathione S-transferase
h	Hours
IB	Immunoblot
iDeg	IDO1 degrader
IDO1	Indoleamine-2,3-dioxygenase 1
IMiDs	Immunomodulatory imide drugs
IP	Immunoprecipitation
KD	Knockdown
KO	Knockout
Kyn	Kynurenine
LFQ	Label-free quantification
MGD	Molecular glue degrader
MIU	Motif interacting with Ub
MoA	Mode of action
MORF4L1	Mortality factor 4-like 1
MW	Molecular weight
NCOA4	Nuclear receptor coactivator 4
NEM	N-ethylmaleimide
OTU	Ovarian tumor proteases
PAGE	Polyacrylamide gel electrophoresis
PD	Pulldown
PDD	Phenotypic drug discovery
PEG	Polyethylene glycol
PEO	Polyethylene oxide
POI	Protein of interest
polyUb	Polyubiquitin
PP	Proteome profiling
pseudoNP	Pseudo-natural product
PROTAC	Proteolysis targeting chimera

RT	Room temperature
SARM	Selective androgen receptor modulator
SDS	Sodium dodecyl sulfate
SILAC	Stable isotope labeling by amino acids in cell culture
SN	Supernatant
STX18	Syntaxin 18
TCEP	Tris(2-carboxyethyl)phosphine
TDD	Target-based drug discovery
TEAB	Triethylammonium bicarbonate buffer
TMT	Tandem mass tag
TPD	Targeted protein degradation
TPS	Targeted protein stabilization
TUBE	Tandem ubiquitin binding entity
Ub	Ubiquitin
UBD	Ubiquitin binding domain
UBE3A	Ubiquitin-protein ligase E3A
UbiCRest	Ubiquitin chain restriction
UBL	Ubiquitin-like modifier
UCH	Ubiquitin C-terminal hydrolases
UIM	Ubiquitin-interacting motif
UPS	Ubiquitin-proteasome-system
USP	Ubiquitin-specific protease
VHL	Von Hippel-Lindau
VS	Vinyl-sulfone
WB	Washing buffer
WCL	Whole cell lysate

9.3 Acknowledgements

Although I am the only author of this thesis, it was only possible to conduct it with the help of many people, who I want to thank at this point.

First and foremost, I want to thank my supervisors, Prof. Dr. Dr. h.c. Herbert Waldmann and Dr. Malte Gersch, for the opportunity to obtain my PhD degree in such a high-level and inspiring environment, for helping me to grow in it, and for the invaluable support and guidance during this journey. I feel grateful for the chance to conduct my PhD in two groups with different expertises and at different career stages. With this, I not only obtained scientific knowledge in two complementary but synergistic fields, I gained experience in working in different environments with different requirements at the same time. While it was sometimes a challenge for me to work in multiple labs and two buildings at once, it never felt like 50/50, but always like 200 % in the best way possible, which I highly appreciate.

I want to express my deepest gratitude to Dr. Slava Ziegler for her supervision and guidance in the Biogroup. When I started my PhD, I had almost no idea what working in the field of small molecule drug discovery from the biology perspective meant, but her knowledge and support helped me to adapt to the new field and allowed me to learn continuously.

I want to thank Dr. Petra Janning, Andreas Brockmeyer, Malte Metz and all members of the HR-MS facility Dortmund for making my PhD project not only possible at all, but also putting a lot of effort into the measurement optimization and supporting the assay trouble-shooting. I also would like to express my sincere gratitude to Dr. Farnusch Kaschani for measuring LC-MS/MS samples and for bringing his expertise and advice into the project.

The results presented in this thesis were not exclusively my own. I want to thank my fantastic Bachelor student Sarah Ballmann for her contributions to the iDeg derivative validations, Celine Da Cruz Lopes Guita for her work on the proteasome cluster compounds and Daria Bezbakh for her support in the DUB inhibitor hit validation.

I would like to thank the IMPRS for Living Matter, especially Christa Hornemann and Dr. Lucia Sironi, for the financial support in attending conferences and workshops, hosting seminars, organizing retreats and social evenings, and for always being willing to lend a listening ear whenever help is needed. They truly breathe life into the PhD community at our institute.

Furthermore, I want to thank Prof. Dr. Petra Beli for her valuable contributions as a member of my thesis advisory committee.

Working in two groups at the same time also means having the privilege to work with twice as many inspiring scientists. I had the honor to receive so much support from my colleagues in both the Gersch and the Waldmann group, for which I am particularly grateful. Dr. Kai Gallant and Dr. Kim Wendrich, who not only warmly welcomed me to the lab, but taught me how to work with cloning, bacteria and ubiquitin in general. Dr. Aylin Binici and Dr. Lara Dötsch, who helped me to slowly transform from a sometimes-hasty chemist to a chemical biologist, who values accuracy even more. I want to thank Jana Bonowski, Celine Da Cruz Lopes Guita, Sandra Koska, Dr. Belén Lucas, Dr. Yasemin Akbulut and Daira Mirel Oropeza Benitez for their scientific expertise and their continuous support in the Biogroup during my PhD. I want to thank all past and current members of the Gersch group, particularly Jan Hane, Dr. Christian Hölzel, Dr. Nafizul Haque Kazi, Gian Kipka, Nikolas Klink, Dr. Rachel O'Dea, Dr. Mirko Schmidt, and Dr. Zhou Zhao for their help and scientific expertise, for welcoming me so warmly to the group and for inviting me to any (science-) coffee, even though I was always in another building. At the same time, all these people supported me not only professionally but also personally and I have the pleasure to call several of them not only colleagues but friends.

At the end of the day, my academic journey leading to my PhD would not have been possible without the support of my family and friends. A big thank you to Celine, Jana and Tobi for many lovely game and quiz nights. I want to thank Jana, my person, who has always been there for me for more than ten years now. Thank you to the people who took the same way studying in Mainz (for a longer or shorter period of time) and made this time against all odds enjoyable. Jenny, Alina, Nino, Franjo, Julius, Seb, Moritz, Simone, Jannis and Diana. They stayed true friends that I don't want to miss out on, even though they all live at least three hours away by car. No matter if it was festivals, online game nights, city trips, or unfortunately, hospital visits, we always stayed in touch and that is fairly not easy during a PhD!

Schließlich möchte ich meiner Familie danken. Meinen Eltern, Großeltern und Geschwistern, die mich seit meiner Kindheit stets ermutigt haben, meinen Traum, Forscherin zu werden, tatsächlich in die Tat umzusetzen, und mich auf diesem Weg immer unterstützt haben. Außerdem danke ich Natalie, Konstantin, Philipp und Denise – Vielen Dank, dass ich Teil eurer Familie werden durfte und sein darf. Zu guter Letzt danke ich meinem Partner, dessen bedingungslose Unterstützung, Verständnis und Geduld mir die Welt bedeuten. - Thank you! Vielen Dank!